

Project no.: 231608

Project acronym: OCTOPUS

Project full title: Novel Design Principles and Technologies for a New Generation of High Dexterity Soft-bodied Robots Inspired by the Morphology and Behavior of the Octopus

Large-Scale Integrating Project

SEVENTH FRAMEWORK PROGRAMME

THEME: ICT-2007.8.5

Future and Emerging Technologies (FET), Embodied Intelligence

Deliverable Number: D3.1

Fundamentals of robotic technologies relevant to octopus biology

Due date: April 30, 2009

Actual submission date: April 30, 2009

Start date of the project: February 1, 2009

Duration: 48 months

UZH - University of Zurich

Project co-funded by the European Commission within the Seventh Framework Programme (2007-2013)		
Dissemination Level		
PU	Public	<input checked="" type="checkbox"/>
PP	Restricted to other programme participants (including the Commission Services)	<input type="checkbox"/>
RE	Restricted to a group specified by the consortium (including the Commission Services)	<input type="checkbox"/>
CO	Confidential, only for members of the consortium (including the Commission Services)	<input type="checkbox"/>

Table of Content

Table of Content.....	i
1. Introduction (UZH).....	1
2. Survey of Sensing and Actuation Technologies (SSSA, UZH, IIT, FORTH).....	2
2.1 Sensing Technologies	2
2.1.1 Introduction (SSSA).....	2
2.1.2 Inertial Sensors (SSSA).....	12
2.1.3 Haptics (UZH).....	24
2.1.4 Proprioception (IIT).....	28
2.1.5. Vision Sensors (FORTH).....	32
2.2 Actuation Technologies	40
2.2.1 Introduction (SSSA).....	40
2.2.2 Hydraulic Actuators (IIT).....	45
2.2.3 Pneumatic Actuators (IIT).....	47
2.2.4 Piezoelectric Actuators (UZH).....	50
2.2.5 Shape Memory Alloy Actuators (IIT).....	51
2.2.6 Electro Active Polymer Actuators (SSSA).....	52
3. Survey of Bio-inspired Soft Robots and Control Schemes (IIT, FORTH).....	61
3.1 Introduction	61
3.2 Soft and Hyper Redundant Robots - Analysis and Control Challenges.	61
3.3 Octopus Arm Control	62
3.4 Soft and Hyper Redundant Robots Design	63
3.5 Soft and Hyper Redundant Robot Control.....	66
3.6 Evolutionary Design of Bio-inspired Systems (FORTH).....	72
4. Survey of Behavioral/Sensory-motor Control Architectures (UZH)	83
4.1. What is a Behavioural architecture?	83
4.2. Classification of Architectures	85
4.2.1. Biological vs. robotic.....	85
4.2.2. Model-based vs. reactive.....	86
4.2.3. Cognitivist , Emergent/ Connectionist, Enactive	89
4.3. The “Substrate” underlying the architectures	90
4.4. Examples of architectures	91
4.4.1. Extended Braitenberg Architecture.....	92
4.4.2. Subsumption architecture and behavior based methods	93
4.4.3. Dynamical systems	94
4.4.4. MOSAIC.....	95
4.4.5 Probabilistic Models.....	96
4.4.6. iCub modular bio-inspired motor architecture.....	97
4.4.7. Exploiting Body Dynamics.....	98

4.4.8. WalkNET.....	98
5. Survey of Bio-inspired Soft Materials (UREAD)	100
5.1 Introduction	100
5.2 Artificial Muscle	100
5.3 Fibre orientation in soft materials from Nature.....	102
5.3.1 Hydrostats of Fixed Fibre Length.....	104
5.3.2 Pennate Muscles.....	106
5.3.3 Muscular Hydrostats as Antagonists and levers.....	107
5.4 Smart textile and tissue engineering.....	110
5.4.1 Carbon nanotube yarns.....	110
5.4.2 Textile as sensors and monitors	110
5.4.3 Other Smart textiles.....	111
5.4.4 Technologies for biomimetic skins.....	112
5.4.5 Application of Silk in Stem cell-based Tissue engineering.....	115
5.5 Examples of Biomimetic Sensors	116
5.5.1 Biomimetic fin.....	116
5.5.2 Biomimetic Fingerprinted Sensors.....	117
5.5.3 Biomimetic Sensor for a Crawling Minirobot.....	117
5.6 Conclusions	118
6. References.....	120

1. Introduction (UZH)

The octopus is a marine invertebrate with amazing motor capabilities and intelligent behavior. Its body has no rigid structures and has interesting characteristics, from an engineering viewpoint: infinite number of degrees of freedom (DOFs), bending in many different directions, variable and controllable stiffness, high dexterity, fine manipulation, highly distributed control. The octopus represents a biological demonstration of how effective behavior in the real world is tightly related to the morphology of the body.

The grand challenge of the OCTOPUS IP is investigating and understanding the principles that give rise to the octopus sensory-motor capabilities and at incorporating them in new design approaches and ICT and robotics technologies to build an embodied artifact, based broadly on the anatomy of the 8-arm body of an octopus, and with similar performance in water, in terms of dexterity, speed, control, flexibility, and applicability.

The new technologies expected to result from the IP concern actuation (soft actuators), sensing (distributed flexible tactile sensors), control and robot architectures (distributed control, coordination of many DOF, materials (variable stiffness), mechanisms (soft-bodied hydrostat structures), kinematics models. The final robotic octopus prototype is aimed to be capable of locomotion on different substrates, of squeezing into small apertures, of dexterous manipulation by coordinating the eight arms, of anchoring in order to exert forces on external environment; of controlling a flexible structure with virtually infinite DOFs. This IP is expected to achieve new science and new technology, demonstrated by joint publications and patents, through a truly interdisciplinary research work programme, by a consortium of engineering and biology groups, each involving diverse disciplines and all experienced in bio-mimetics, possessing, as a consortium, the best expertise available in Europe for pursuing the objectives of the IP.

The report presents the results of the first task to be undertaken, which is a comprehensive review in the area of robotics and ICT technologies that could possibly be applied in the design and development of a robotic octopus. This survey includes the state of art in current technologies in sensing, actuation, soft materials, bio-inspired sensory-motor control and is intended to be a comprehensive tutorial on the larger field of bio-mimetic and bio-inspired robotics, and in particular, the technologies pertinent to the Octopus Project.

With due consideration to the multidisciplinary expertise of the consortium, as well as the specializations of the partners involved, this survey has individual sections dealt with in detail by the respective research groups specializing in those areas. The survey thus represents a balanced analysis of the various technical challenges involved, providing a strong foundation for the design and development phases to follow. It is also hoped that it provides a broad introductory overview of the area for the partner research groups specializing in biology, thus enabling an equitable sharing of knowledge thereby further aiding the subsequent tasks. The survey also cites some of the best known published literature in the various research areas dealt with.

This report has been organised as follows. The Section 2 has a detailed survey of sensing and actuation technologies coordinated by the Scuola Superiore Sant'Anna (SSSA) and with contributions from Italian Institute of Technology (IIT), University of Zürich (UZH) and the Foundation of Research and Technology, Hellas (FORTH). Section 3, on Bio-inspired control is has been coordinated by IIT, with contributions from FORTH. A survey of Behavior/Sensory Motor Control Architectures from the UZH comprises section 4. The final section is on Bio-inspired Soft materials carried out by the University of Reading (UREAD) followed by the References organised section-wise.

2. Survey of Sensing and Actuation Technologies (SSSA, UZH, IIT, FORTH)

2.1 Sensing Technologies

2.1.1 Introduction (SSSA)

Artificial sensors, similar to natural sensing receptors, are the devices that a robotic system, or a biological organism, uses to interface with the environment and to perceive itself.

Artificial sensing contributes to the lack of information due to the unstructured characteristics of real world, providing data about the state of the environment itself and the state of the robotic system as basis for control, decision making, and interaction with other agents in the environment, such biological system do with sensing receptors and organs.

Robotic systems use the so-called *exteroceptive sensors* (similar to the biological exteroceptive receptors) to obtain information on the environmental conditions and on the interaction with external agents (i.e. touch, temperature or vision sensors), and *proprioceptive sensors* (similar to the biological proprioceptive receptors) to perceive the internal state of each own component (i.e. stretch, force, body parts position and velocities sensors).

As definition, a sensor is a part of a measurement system, that responds to a change of the physical phenomena (*stimulus* or *measurand*) that has to be measured, and converts the physical quantity into an electric signal, which can be read by the other components of the measurement system.

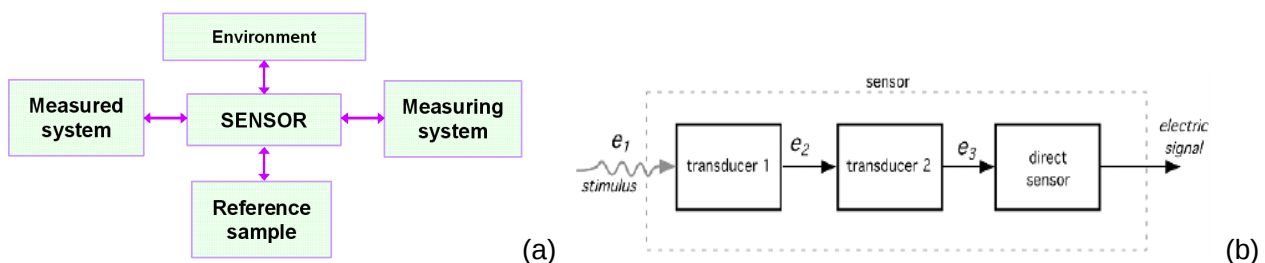


Figure 2. 1 Functional schemes for a general sensor: the interfaces are towards the system of the physical variable that has to be measured, the environment and a sample of the measured variable, as reference for the measurement itself and the transduction in signal for the measuring system (a); a sensor is a system that can use more then one transducer to translate the external stimulus to the final electric signal.

Sensing can be view as a process of information transferring, based on an energy flow to transform the physical stimulus (force, pressure, temperature, light intensity, distance) into a representation for the robotic system, that subsequently elaborates and process and finally responds in an adequate manner.

Transducer in general are different from sensors because are “simply” energy converter, not necessary for a measurement aim: in this sense, a sensor can be composed by more then one transducer (Figure 2. 1) and a transducer with an electric output may be defined as a sensor.

Sensors can be classified in a large variety of ways, more or less complex, on the base on:

Technology or physical work principle (resistive, capacitive, hall effect..);

Type of measured variable (temperature, displacement, velocity, light...);

Application field (automation, environmental, biomedical...);

Energetic behavior (“active sensors” require an external energy source, or excitation signal, to obtain the measure; “passive sensors” operate without external energy sources, and directly translate the input energy stimulus into the output signal);

Output response mode (analog sensors have a continuous response for a defined range of inputs; digital sensors have a discrete form of output, see Figure 2. 2).

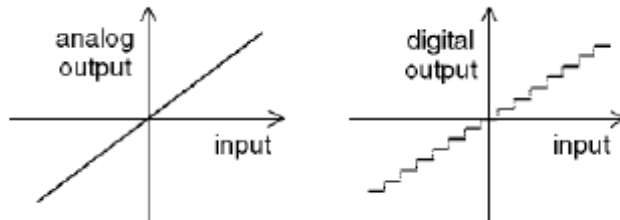


Figure 2. 2 Analog and digital sensor outputs.

Sensors need one or more steps to translate the physical phenomena into an electric signal. Several characteristic parameters and functions can be used to define the behavior of a sensor, its nature and the performances or steps required to the conversion. Some of the **fundamental characteristics** and properties used to define the performances and to compare sensors are briefly described.

Transfer function

The transfer function of a sensor is the relationship between the input stimulus and its output response. Each sensor is theoretically based on an ideally stimulus-output relationship (Figure 2. 3): this function establishes the dependence between the electrical signal S produced by the sensor and the stimulus s : $S = f(s)$.



Figure 2. 3 Relationship scheme between an input stimulus (s) and the output response (S) of a sensor characterized by a theoretical transfer function (f)

The transfer function can be linear or nonlinear (exponential, logarithmic, power function...), or can vary the linearity/nonlinearity characteristic for different work range. In general the transfer function is one-dimensional (one stimuli-one output), but can also be multi-dimensional, when the sensor output depends on more than one stimuli.

Range (or span)

The dynamic range of a sensor is the difference between the minimum and maximum inputs that will give a valid output, without causing an unacceptably large inaccuracy. The full scale value represent the maximum input value.

Resolution

The resolution of a sensor is the smallest increment of input that can give an output. In other words is the minimal variation of the stimulus value that can be measured.

Usually analog sensors have a resolution limited only by low-level electrical noise, and often much better than equivalent digital sensors.

Sensitivity

Is the ratio between the change in the output signal and the change in the input stimulus: $\left(\frac{\Delta out}{\Delta in} \right)$

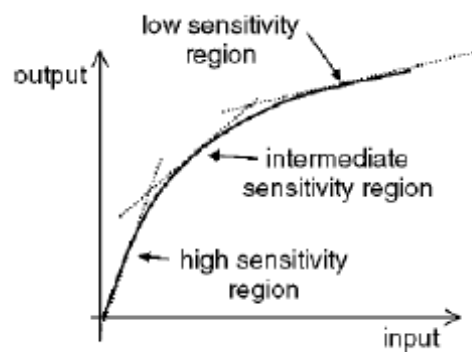


Figure 2. 4 Sensor sensitivity

For a digital sensor the sensitivity usually is strictly related to the resolution, whereas for an analog the sensitivity corresponds to the slope of the output versus the input line (Figure 2. 4)

Calibration

The calibration process is used to know the actual relationship between an output value and its corresponding input value, considering the entire circuit of the measuring system.

In the calibrating cycle the output values have to be measured for known values of the input, considering the complete range of work of the sensor, and both for increasing and decreasing input values.

Hysteresis

Sensors usually show different behavior if are measuring increasing or decreasing stimuli.

The hysteresis loop is the curve delineated during the calibrating cycle and represents the relationship between the output values generated by increasing input values and the output values for decreasing input values.

The hysteresis is the maximal difference between the two tracts (curve of increasing values and curve of decreasing values) of the hysteresis loop, and is usually measured in term of full scale (FS) percentage (Figure 2. 5).

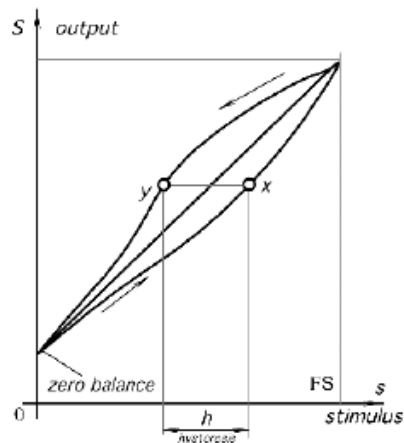


Figure 2. 5 Example of transfer function with hysteresis.

Error

Error is the difference between a measured value and the true input value.

An error can be systematic (bias) or random (precision) type. Random errors can be minimized with a statistical approach, whereas systematic errors not. The systematic error is present in all the measurements made with a sensor and can be:

- calibration errors (a zero or null point error is a common type of bias error created by a non-zero-output value when the input is zero);
- loading errors (adding the sensor to the measured system changes the system);
- errors due to sensor sensitivity to variables other than the desired one (e.g., temperature effects on strain gages).

Linearity

The linearity correspond to the maximal difference between the hysteresis loop and the ideal straight line of linearity (expressed in percentage of full scale).

Repeatability

The repeatability, or reproducibility, describes the sensor's capacity of responding with the same output to identical input values given, under the stated conditions. The repeatability error, due for example by thermal noise or material plasticity, is expressed as the maximum difference between output readings as determined by two calibrating cycles, as percentage of full scale:

$$\delta_{rep} = \frac{\Delta_{max}}{FS} \cdot 100$$

Accuracy

The accuracy defines the sensor's maximal deviation value from the output value and the true value of the stimulus. Accuracy is a measure of the conformity of the measured values in respect to the defined reference standard.

Accuracy is different from repeatability: a sensor can have a good repeatability characteristic, but no accuracy (see Figure 2. 6).

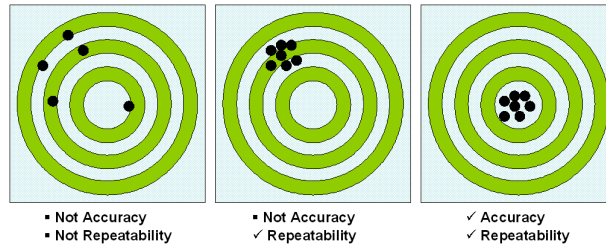


Figure 2. 6 Graphical difference between the characteristic of accuracy and repeatability.

Reliability

The reliability is the capacity of a sensor to perform in a defined manner and know modality, under stated condition and for a stated period. Reliability is an important feature for a sensor, but not always specified probably for the absence of a commonly accepted measure: usually it is expressed in statistically terms as a probability that the device will function without failure over a specified time or for a number of uses.

Saturation

Every sensor has an input level limit, after that a further increase in stimulus doesn't generate an noticeable signal in output. That means the saturation of the sensor, graphically represented by a plateau tract in the transfer function curve (Figure 2. 7).

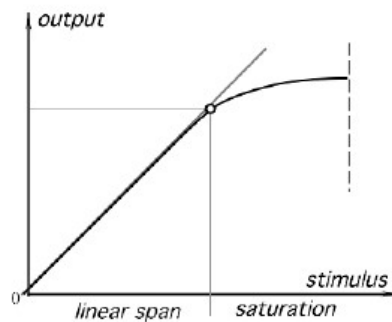


Figure 2. 7 Saturation region of a sensor is the plateau tract in the transfer function curve.

Dead Band

A sensor can have an insensitivity range inside the total input signal range, where the output signal approximately has the same value (usually near zero) for the entire dead band zone.

Dynamic characteristics

Sensor can respond to input stimuli that change with time and can be so considered dynamic system. However a sensor cannot respond instantly to a stimulus and that's the reason why is necessary to describe some of its characteristic also in a time-dependent form, considering the presence of a dynamic error due to the delay in response itself or to external factor that modify some of the sensor characteristics during its performance. An example is the *zero-shift error* that is the shift of the origin of the linear characteristic from the zero to another value; another dynamic error is the *sensibility drift*, that is the shift of the sensibility of the sensor during its operate. An example of dynamic characteristic is the *warm-up time*, that is the time between an input is applied and the moment when the sensor operates within its specific accuracy.

Application characteristics and special properties

As consequence of the application area characteristics, the choice between different sensor is affected also by the design, the dimension, the weight and in general all the packaging features. Besides, the application field, as the technology or physical principle used by the sensor may introduce specific detail (for example the spectral response in some light detectors with a limited optical bandwidth).

To operate as energy converter and generate the electric signal for the acquisition system, sensors essentially work on physical or chemical principles.

There are several physical effects which result in the direct generation of the appropriate electric signal in response to a nonelectrical stimulus, that the so called "direct" sensors exploit. Many other stimuli cannot be directly converted into electricity, thus "complex" sensors have multiple conversion steps.

Here are briefly described some of the mainly physical principles usable for a direct conversion of stimuli into electric signal and employed in many sensing technology.

Piezoresistive Effect

The electrical resistance (R , measured in ohms [Ω]) of an object is a measure of its opposition to the passage of an electric current and determines the amount of current (I , measured in amperes [A]) through the object for a given potential difference (V , measured in volts [V]) across the object (Ohm's law):

$$R = \frac{V}{I}$$

Resistance is given by the electrical resistivity (ρ , measured in volt-metres per ampere, [Vm/A] or ohm-metres, [Ω m]) of the material (that is an intrinsic property of the material, depending on temperature) and its geometric dimension (length, ℓ and cross-sectional area, A , respectively measured in metres [m] and square metres [m^2]):

$$R = \rho(T) \frac{\ell}{A}$$

The piezoresistive effect describes the changing electrical resistance of a material (metal or semiconductor) due to applied mechanical stress.

The piezoresistive effect can be employed in sensors which are responsive to mechanical stress σ :

$$\sigma = \frac{F}{A} = E \frac{d\ell}{\ell}$$

that is the ratio between the applied force (F) and the area (A) where the force is applied. A mechanical stress is also equal to the product of the Young's modulus of the material (E) and the *strain* ($\varepsilon = d\ell/\ell$), which is the normalized deformation of the material due to the applied force.

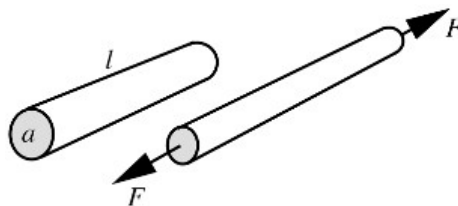


Figure 2. 8 Strain changes the geometry of a conductor and its resistance.

Considering a cylindrical conductor (a wire, as shown in Figure 2. 8), with constant volume v , the resistance is:

$$R = \rho(T) \frac{\ell^2}{v}$$

and differentiating we can define sensitivity of resistance with respect to wire elongation:

$$\frac{dR}{d\ell} = 2\rho(T) \frac{\ell}{v}$$

It follows that the sensitivity becomes higher for the longer and thinner wires with a high specific resistance. Normalized incremental resistance of the strained wire is a linear function of strain:

$$\frac{dR}{R} = G \frac{d\ell}{\ell}$$

where G is the *gauge factor* that characterize the sensitivity of a piezoresistive device ($G = 2-6$ for metal; $G = 50-200$ for semiconductors).

Materials with high gauge factor show large changes of resistance even for small deformations.

Piezoresistive effect of metal sensors is only due to the change of the sensor geometry resulting from applied mechanical stress. This geometrical piezoresistive effect results in gauge factor:

$$G = 1 - 2\nu$$

where ν is the Poisson's ratio. Piezoresistors, i.e. strain gages, are successfully used in a wide range of applications

Piezoelectric Effect

Piezoelectricity is a property of some crystalline materials to generate electric charge upon subjecting them to stress. The effect is present in natural crystal, as quartz (SiO_2), or artificially polarized ceramics or some polymers (for example, as polyvinylidene fluoride, PVDF), and it is appreciable also in the modelling and remodelling phenomena of bones.

The piezoelectric effect is a reversible physical phenomenon. That means that applying voltage across the crystal produces mechanical strain. By placing several electrodes on the crystal, it is possible to use one pair of electrodes to deliver voltage to the crystal and the other pair of electrodes to pick up charge resulting from developed strain. This method is used quite extensively in various piezoelectric transducers.

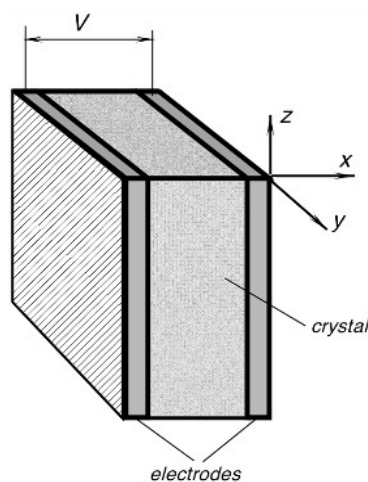


Figure 2. 9 General arrangement for a piezoelectric sensor, where electrodes are applied to a poled crystalline material.

In a piezoelectric crystal the piezoelectric property has usually no homogenous distribution, meaning that the response along one axis can be different in respect to the response of another one.

Hence, the magnitude of the piezoelectric effect can be represented with a matrix relationship between the polarization vector (P) and the stress matrix (σ), in which the components are correlated by different piezoelectric coefficients (d):

$$P = d\sigma$$

$$\begin{bmatrix} P_{xx} \\ P_{yy} \\ P_{zz} \end{bmatrix} = \begin{bmatrix} d_{11}\sigma_{xx} + d_{12}\sigma_{yy} + d_{13}\sigma_{zz} \\ d_{21}\sigma_{xx} + d_{22}\sigma_{yy} + d_{23}\sigma_{zz} \\ d_{31}\sigma_{xx} + d_{32}\sigma_{yy} + d_{33}\sigma_{zz} \end{bmatrix}$$

where the constants d_{mn} along the orthogonal axes of the crystal cut have dimensions of charge unit per unit force (coulomb/newton).

An additional coefficient is usually introduced for convenience to define the ratio between the coefficient d and the absolute dielectric constant of the material:

$$g = d\epsilon$$

which has dimension in volt-meter per newton-square meter: $\left(\frac{V}{m} / \frac{N}{m^2}\right)$.

In this manner the coefficient g represents a voltage gradient (electric field) generated by the crystal per unit applied pressure.

Another coefficient (h) is obtained by multiplying the g coefficient by the corresponding Young's moduli for the corresponding crystal axes.

Piezoelectric crystals are direct converters of mechanical energy into electrical. The efficiency of conversion can be determined from the so-called *coupling coefficient* k_{mn} :

$$k_{mn} = \sqrt{d_{mn}h_{mn}}$$

The k coefficient is an important characteristic for applications where energy efficiency is of a prime importance.

The charge generated by the piezoelectric crystal is proportional to applied force and depends on the direction, for example in the x direction the charge Q in response to the applied force F is:

$$Q_x = d_{11}F_x$$

Using the deposited electrodes and the piezoelectric crystal as a capacitor, with capacitance C , it is possible to measure the voltage V developed across the plates:

$$V = \frac{Q_x}{C} = \frac{d_{11}}{C} F_x$$

Hall Effect

Initially, the Hall effect had the mainly application as tool for studying electrical conduction in metals, semiconductors and other materials. Currently, Hall effect sensors are used to detect magnetic fields and position or displacement of objects.

The Hall effect is the production of a potential different (called *Hall voltage*) across an electrical conductor, transverse to an electric current in the conductor and a magnetic field perpendicular to the current.

The effect is based on the interaction between moving electric carriers and an external magnetic field. When an electron moves through a magnetic field, a sideways force (*Lorentz Force*) acts upon it:

$$F_L = qvB$$

where $q=1.6 \times 10^{-19} \text{C}$ is an electronic charge, v is the speed of an electron and \mathbf{B} is the intensity of the magnetic field, measured in Tesla = 1newton/(ampere-meter)= 10^4 gauss.

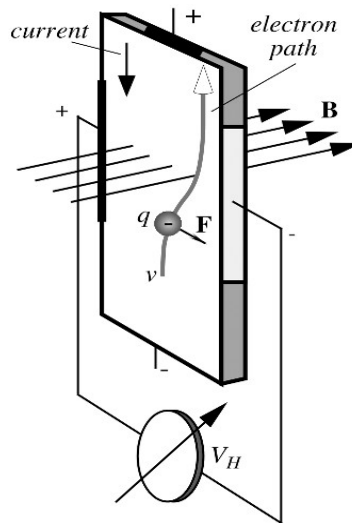


Figure 2. 10 Hall effect principle: a magnetic field deflects movement of electric charge.

If a magnetic field is applied perpendicular to a conductive strip, which is crossed by an electric current, the Lorentz force shifts moving electrons to one side of the strip (Figure 2. 10), which becomes more negative than the other, generating the so-called transverse Hall potential difference, V_H :

$$V_H = h i B \sin \alpha$$

where α is the angle between the magnetic field vector and the Hall plate, and h is the coefficient of overall sensitivity, depending on the plate material, its geometry (active area) and its temperature.

The overall sensitivity depends on the Hall coefficient, H , that is the transverse electric potential gradient per unit magnetic field intensity per unit current density and, according to the free-electron theory of metals is:

$$H = \frac{1}{N c q}$$

where N is the number of free electrons per unit volume and c is the speed of light.

Thermoelectric Effects: Seebeck and Peltier Effects

The thermoelectric effect is the direct conversion of temperature differences to electric voltage and vice versa: a thermoelectric device creates a voltage difference when there is a different temperature on each side. Conversely, an applied voltage generates a temperature difference.

The Joule effect, that is generated whenever a voltage is applied across a resistive material, is somewhat related, but it is not generally termed as thermoelectric effect because it is not reversible and it is usually regarded as being a loss mechanism, due to non-ideality in thermoelectric devices.

Thermoelectric effect can be used to generate electricity, to measure temperature, to cool or heat objects; thermoelectric devices are useful temperature controllers because the direction of heating and cooling is determined by the direction of the applied voltage.

If a conductor has one end into a cold place and the opposite into a warm place, thermal energy will flow from the warm to cold part. The intensity of the heat flow is proportional to the thermal conductivity of the conductor. In addition, the thermal gradient sets an electric field inside the conductor. The field results in incremental voltage that can be measured:

$$dV_a = (S_a - S_b) dT = \alpha_a dT$$

where dT is the temperature gradient across a small length, dx , and α_a is the absolute Seebeck coefficient of the material (difference between the two Seebeck coefficients, if two different material are jointed).

The measurement of the Seebeck voltage allows to measure the difference of temperature between the two different junctions.

The Peltier effect is the calorific effect of an electrical current at the junction of two different metals. When a current I is made to flow through the circuit, heat is evolved at the upper junction (at T_2), and absorbed at the lower junction (at T_1). The Peltier heat absorbed by the lower junction per unit time, dQ/dt , is:

$$\frac{dQ}{dt} = (P_a - P_b) I$$

where P_a and P_b are the Peltier coefficients, that represent how much heat current is carried per unit charge through the material.

The direction of heat transfer is controlled by the polarity of the current: reversing the polarity will change the direction of transfer and thus the sign of the heat absorbed/evolved (Figure 2. 11).

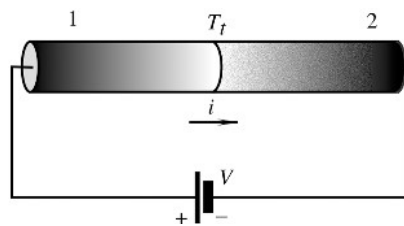


Figure 2. 11 Peltier effect: if an electric current passes from one substance (1) to another (2), then heat may be given or absorbed at the junction.

Photoelectric Effect

The photoelectric effect is a phenomenon in which electrons are emitted from material after the absorption of energy from electromagnetic radiation such as X-rays or visible light.

When a metallic surface is exposed to electromagnetic radiation above a certain threshold frequency (typically visible light), the light is absorbed and electrons are emitted.

The photons of a light beam have a characteristic energy determined by the frequency of the light. In general, photoelectric effect takes place with photons with energies of about a few electronvolts.

In the photoemission process, if an electron within some material absorbs the energy of one photon and thus has more energy than the work function (the electron binding energy) of the material, it is ejected. If the photon energy is too low, the electron is unable to escape the material. Increasing the intensity of the light beam increases the number of photons in the light beam, and thus increases the number of electrons emitted, but does not increase the energy that each electron possesses. Thus the energy of the emitted electrons does not depend on the intensity of the incoming light, but only on the energy of the individual photons.

Experimental characteristics:

For a given metal and frequency of incident radiation, the rate at which photoelectrons are ejected is directly proportional to the intensity of the incident light.

For a given metal, there exists a certain minimum frequency of incident radiation below which no photoelectrons can be emitted. This frequency is called the threshold frequency.

Above the threshold frequency, the maximum kinetic energy of the emitted photoelectron is independent of the intensity of the incident light but depends on the frequency of the incident light.

The time lag between the incidence of radiation and the emission of a photoelectron is very small, less than 10^{-9} second.

Photoelectric effect is used in photodiode, phototransistors, image sensors, photoelectron spectroscopy and so on.

2.1.2 Inertial Sensors (SSSA)

The *Octopus vulgaris* Vestibular System

Cephalopods and vertebrates have similar information requirements about their position in space: a swift-moving animal needs to know the direction of the gravity force and the angular acceleration that occurs when it changes path. Considering the lack of hard external or internal skeletons, octopuses are unable to have spatial information recording joints angle with hair plates or cuticular strain gauge. Therefore, they use similar orientation system to the one of vertebrates, that basically depends upon the deflection of "flaps" when the body moves relative to the fluids inside them.

The octopus vestibular system basically consists of gravity and angular acceleration detectors.

Octopus has a pair of statocysts embedded in a cartilage below and either side of the brain, filled with clear fluids that are ionically similar to the blood. Inside each statocyst there are: the gravity receptor, the macula, and the angular acceleration receptors, the flaps of the crista (arranged in three sets at right angles). In addition to the cells concentrated along the crista and in the macula, there are hair cells scattered all over the inner surface of the statocyst, contributing axons to a network of nerves that is particularly rich around the bulging posterior sac.

From behavioral observations the removal of one statocyst has very little effect on the movements of an octopus walking or swimming around its tank, whereas the removal of both statocysts get the animal noticeably unstable, though it can still walk right way up and can still make visually oriented detours to get food.

Orientation of the eye is strictly connected with statocyst function. At rest, the slit pupil of the eye runs horizontally, more or less regardless of the posture of the animal. If the removal of one statocyst has little effect on the compensatory counter-rolling, the removal of both eliminates totally this mechanism.

The maculae of the two statocyst lie at 90° to one another, with the hair cell fields set at 45° to vertical longitudinal plane of the body. Experimental works showed that, unlike crustaceans and vertebrates where the gravity receptors respond to magnitude as well as to the direction of a shear force, octopus receptors are affected to the direction changes, but not to changes of magnitude.

Somehow, the octopus system is organized to eliminate the effect of changing the magnitude of the shear force, while preserving information about its change of direction. This property is perhaps related to the very considerable accelerations that cephalopods can produce during jet propulsion movement: during prey hunting or danger escaping, octopuses yet need to preserve eyes orientation, since their system of forms recognition depends upon this.

Counter-rolling and vertical displacement of the eyes both depend upon changes in the direction of shear in the macula. The two sorts of movement should therefore, always occur together.

The elimination of shear magnitude as a property determining compensatory eye movements must be achieved centrally, since individual receptors (i.e. hair cells that are inside the two maculae) behave like the receptors of crustaceans and vertebrates, with the properties of quick adaptation and high sensibility to vibrations.

The crista is sensitive to rotation, with each of its section more responsive to deflection in one direction than the other. The strip of hair cells that forms the crista includes sensory elements of varying size, arrayed along a ridge, with a distinct single or double row of very large hair cells at the crest. The hair cell processes are embedded in an amorphous ground substance to form a series of flat plates, the cupulae. Each section of the crista bears three plates, sticking out at right angles into the endolymph. In the first plate of the transverse crista the hair cells lie in a double row, whereas in the second lie in a single row, and then alternately ending with a final double row in the last plate of the vertical crista. The differences of the anatomical paths have no explanations, at yet.

Electrophysiological experiments on the crista's nerve showed that crista are sensitive to low frequency vibration and they are able to differentiate between clockwise and counter-clockwise accelerations; the crista from the left statocyst responded best to the onset of counter-clockwise rotation, and to the cessation of clockwise movement. The longitudinal crista system clearly differentiates between rotations to the left and to the right, with results depending upon the position with respect to gravity at start of the run; the transverse crista system response to rotation around earth-transverse axes; the vertical crista system response to rotation around the vertical axes.

Inertial Sensors: accelerometers and gyroscopes

Accelerometers

Acceleration is a dynamic characteristic of an object with a certain mass m that, according to the Newton's second law, is subjected to a force F : $F = ma$. Position, velocity and acceleration of a certain mass are all related: velocity is the rate of change of position (first derivative of position) and acceleration is the rate of change of velocity (second derivative of position). Considering that, the acceleration of an object can be measured both in a direct way (usually applied in linear or circular motion) and in an indirect way, that is to derive the velocity (usually applied in curved motion). However, in a noisy environment the derivatives may result in extremely high errors, even if complex signal conditioning circuits are employed. For that reason, to measure velocity and acceleration is better to use special sensors, that directly measure the variable of interest.

A basic principle behind the transduction of velocity or acceleration is the measurement of the displacement of an object in respect to a reference system, which is usually integral part of the sensor itself. Otherwise, some velocity sensors or accelerometers don't use intermediate displacement transducer because they can directly convert the motion into electric signal.

Vibration is a dynamic mechanical phenomenon with a periodic oscillatory motion around a reference position. Accelerometers are basically mass-spring-damper devices, in which the mass (*seismic mass* or *proof mass*) oscillates around a reference position supported by the spring-like element in a frame structure with damping properties (Figure 2. 12).

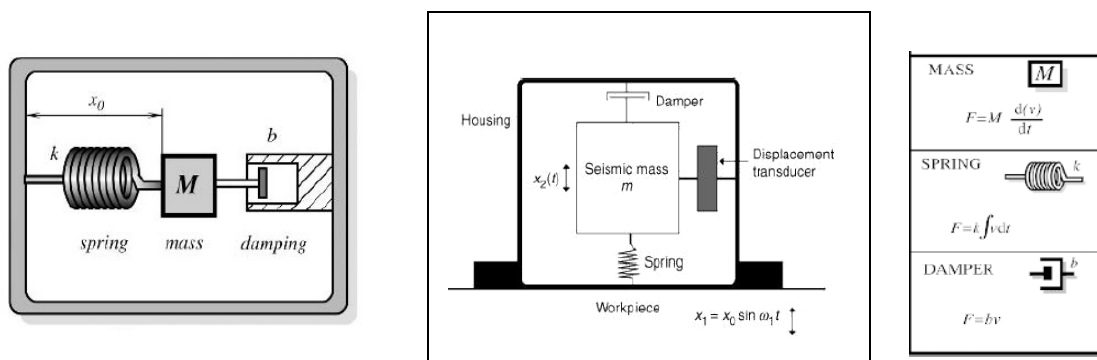


Figure 2. 12 General schemes for accelerometers and mathematical models for its fundamental elements: the seismic mass (M), connected to the spring (k) and the damper elements (b), can move around its reference position with a periodic oscillatory motion; the displacement can be detected by some kind of sensor and translated in a signal for the acquisition system.

Accelerometers are sensitive to external forces acting upon them (including gravity) and uses different mechanisms or physical properties to transduce these forces into a computer-readable signal.

A mathematical model that describe a single-degree-of-freedom accelerometer is represented in Eq (3), obtained applying the Newton's second law to the mass motion, Eq.(1), and considering the acceleration of the mass relative to the Earth, Eq. (2).

$$Mf = -kx - b \frac{dx}{dt} \quad (1)$$

$$f = \frac{d^2x}{dt^2} - \frac{d^2y}{dt^2} \quad (2)$$

$$M \frac{d^2x}{dt^2} + b \frac{dx}{dt} + kx = M \frac{d^2y}{dt^2} \quad (3)$$

where:

M = seismic mass;

f = acceleration of the mass relative to the Earth;

k = spring elastic constant;

b = damper coefficient;

x = displacement, dx/dt = velocity, d^2x/dt^2 = horizontal acceleration;

d^2y/dt^2 = input acceleration of the accelerometer body.

A correctly designed and calibrated accelerometer is characterized by a resonant (or natural) frequency and a flat frequency response within the most accurate measurement can be made and the output of the sensor correctly reflect the vibrating frequency changes (Figure 2. 13). Viscous damping can be used to improve the useful frequency range limiting the effects of the resonant. Silicone oil is often used as damping medium.

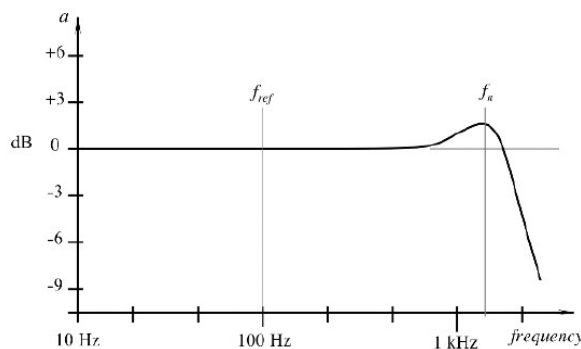


Figure 2. 13 A typical response of an accelerometer: f_n is a natural frequency and f_{ref} is the reference frequency.

Mechanical or Inertial Accelerometers

A mechanical accelerometer is essentially based on a spring-mass-damper system jointed to a mechanical system to transduce the displacement. Mechanical accelerometer can use potentiometer as sensor to measure the displacement of the mass and convert it into a signal for the acquisition system. In Figure 2. 14 is shown a possible configuration for a potentiometric accelerometer, where the seismic mass is jointed to two springs and it is connected to one of the potentiometer terminal; as damper element is often used a viscous liquid (such as silicon oil) at the base of the mass. The potentiometer reads the displacements as a variation of the resistance.

Typical Characteristics:

Low frequency range (<100 Hz);

Natural frequency: 12-89 Hz;

Damper coefficient: $\zeta = 0.5-0.8$;

Potentiometer Resistance: 1000-10000 with a corresponding resolution 0.45-0.25%fs;

Cross-axial sensibility $\leq \pm 1\%$;

Accuracy: $\pm 1\%$ fs ;

Dimension: 50mm³.

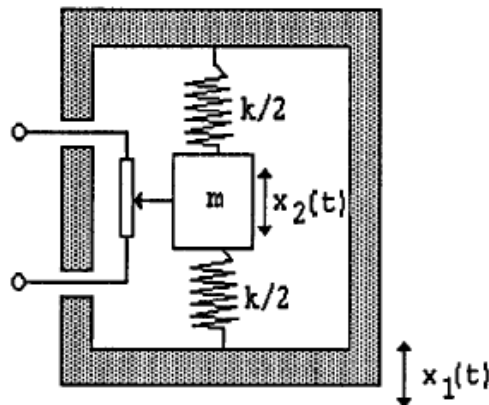


Figure 2. 14 General scheme for a potentiometric accelerometer: the seismic mass, m , is jointed to the housing by two springs and immersed in a viscous liquid with damping properties; a terminal of a potentiometer is connected to the mass to read the displacements as a variation of the resistance.

Piezoelectric Accelerometers

The piezoelectric effect showed in a crystalline material composed of electrical dipoles is a direct conversion of the mechanical energy into electrical energy, representing a natural application in sensing vibration and acceleration.

The seismic mass is directly connected to the piezoelectric crystal, that represents both the elastic element and the sensor. As an external force is applied on the system the mass moves on the crystal and the compression of the crystal produces a proportional electric signal (Figure 2. 15).

Quartz crystal are often used as piezoelectric element, but piezoelectric ceramics as barium titanate or zirconite titanate (PZT) are the most popular. For miniature piezoelectric accelerometer is usually employed a silicon structure, integrated with a thin deposited film of lead titanate to provide piezoelectric properties.

The piezoelectric signal is amplified by a charge-to-voltage or current-to-voltage converter, usually integrated on board into the same housing as the piezoelectric crystal, to have a good frequency characteristics.

Typical Characteristics:

Frequency range: 2Hz ÷ 5kHz;

Good off-axis noise rejection;

High linearity;

Wide operating temperature range (up to 120°).

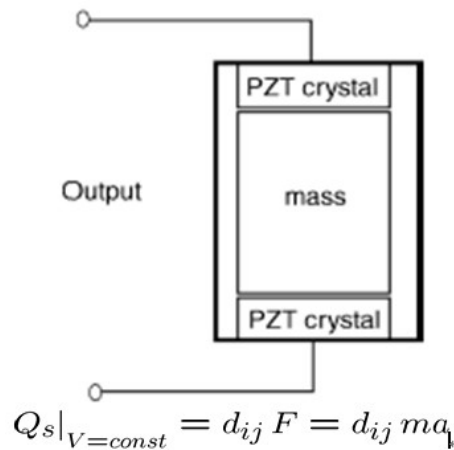


Figure 2. 15 General scheme for a piezoelectric accelerometer where the mass is enclosed between two piezoelectric crystals: the measured electric signal (Q) is equal to the force (F) applied on a crystal, due to the acceleration of the mass, multiplied for the piezoelectric coefficient (d_{ij}).

Piezoresistive Accelerometers

In piezoresistive accelerometers the seismic mass is supported by elastic elements, like spring, which incorporates strain-gauge as sensing elements. The strain-gauge can be fixed on both side of the elastic elements to measure the strain and directly converts in a electric signal. The measured strain is connected to the magnitude and rate of mass displacement and, subsequently, with the acceleration.

The damping medium is usually visco-elastic fluid (Figure 2. 16).

Typical Characteristics:

Broad frequency range: from dc up to 13 kHz;

Overshock up to 10000g, with a proper design;

Dynamic range: ± 1000g, with error less than 1%;

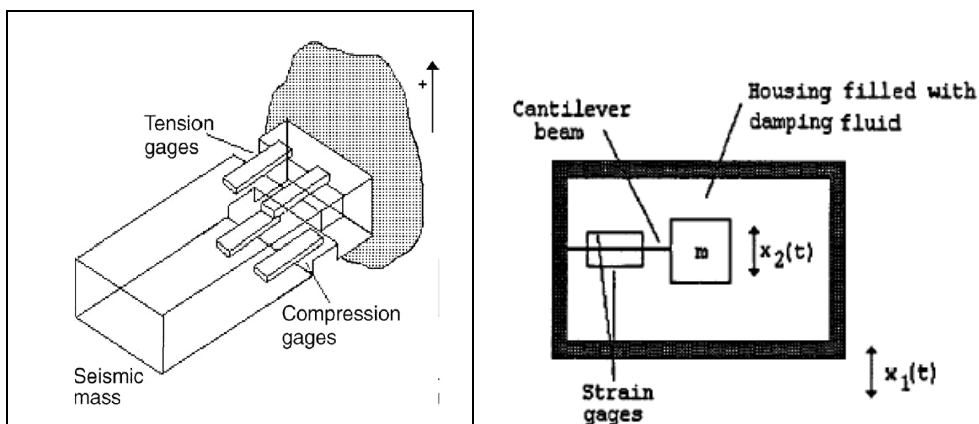


Figure 2. 16 Picture and general scheme for a piezoresistive accelerometer: the seismic mass is supported by an elastic element, that incorporates the strain gauges; the housing is filled with viscous fluid with damping properties

Capacitive Accelerometers

The capacitive displacement conversion is one of the proven and reliable methods to measure acceleration detecting the displacement of the mass with respect to the accelerometer housing.

In a capacitive accelerometers the seismic mass usually constitutes one of the plate of the capacitor and it is connected to an elastic support (usually a membrane). The other plate is connected to the housing of the accelerometer, constituting the reference position. In this manner the plates form a capacitor whose value is a function of a distance d between the plates and so it is modulated by the acceleration (Figure 2. 17). An appropriate circuit detects the capacitor value, generating an electric signal that is proportional to the displacement of the mass.

Some capacitive accelerometers show a differential configuration, with two plates fixed to the housing and a third plate, that is the seismic mass, that can moves from a side to the opposite. Then, an acceleration can be represented by a difference in values between the two capacitors.

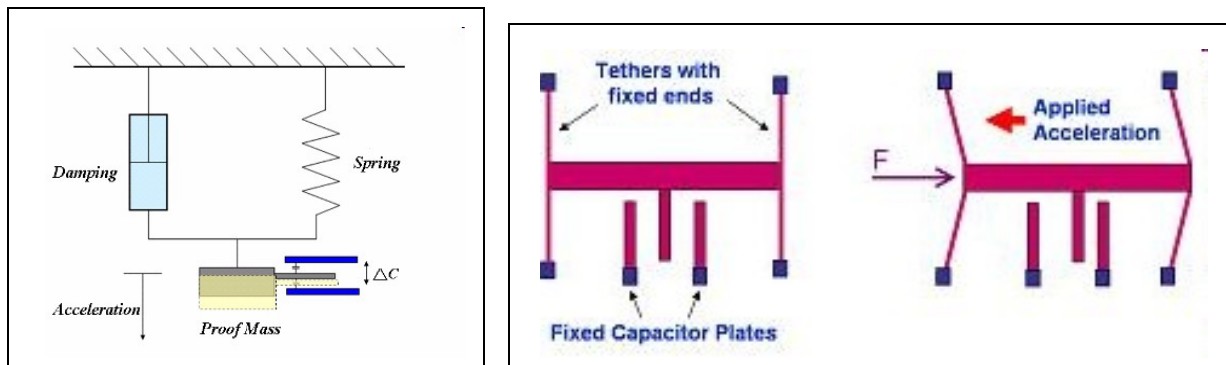


Figure 2. 17 On the left: functional scheme of a capacitive accelerometer, with a damping element and a spring in parallel, both connected with the seismic mass that can move between the two plates of a capacitor. On the right: movement of the seismic mass between the two fixed capacitor plates in response to a force generated by an applied acceleration.

Typical Characteristics:

A maximum displacement which is measured by the capacitive accelerometer rarely exceeds $20 \mu\text{m}$;

With a differential technique the resolution increase.

Inductive Accelerometers

Inductive accelerometers use a LVDT (Linear Variable Differential Transformer) to detect the displacement produced by acceleration.

The LVDT is a type of electrical transformer used to measure linear displacement (also in position sensors). The fundamental principle of the LVDT is the electromagnetic induction and the measurement of the variation of the mutual inductance.

The transformer has three solenoidal coils placed end-to-end around a tube. The centre coil is the primary, and the two outer coils are the secondaries. A cylindrical ferromagnetic core, attached to the object whose position is to be measured, slides along the axes of the tube.

An alternating current is driven through the primary, causing a voltage to be induced in each secondary proportional to its mutual inductance with the primary. The frequency is usually in the range 1 to 10 kHz. As the core moves, these mutual inductances change, causing the voltages induced in the

secondaries to change. The coils are connected in reverse series, so that the output voltage is the difference (hence "differential") between the two secondary voltages.

When the core is in its central position, equidistant between the two secondaries, equal but opposite voltages are induced in these two coils, so the output voltage is zero. When the core is displaced in one direction, the voltage in one coil increases as the other decreases, causing the output voltage to increase from zero to a maximum. This voltage is in phase with the primary voltage. When the core moves in the other direction, the output voltage also increases from zero to a maximum, but its phase is opposite to that of the primary. The magnitude of the output voltage is proportional to the distance moved by the core (up to its limit of travel), which is why the device is described as "linear". The phase of the voltage indicates the direction of the displacement. Because the sliding core does not touch the inside of the tube, it can move without friction, making the LVDT a highly reliable device. The absence of any sliding or rotating contacts allows the LVDT to be completely sealed against the environment. LVDTs are commonly used for position feedback in servomechanisms, and for automated measurement in machine tools and many other industrial and scientific applications.

In an inductive accelerometer the seismic mass is hanged between two springs, constituting the ferromagnetic core, and can move inside the channel where are the coils (Figure 2. 18). The displacement of the mass is measured with an appropriate circuit and transduced in a proportional electric signal.

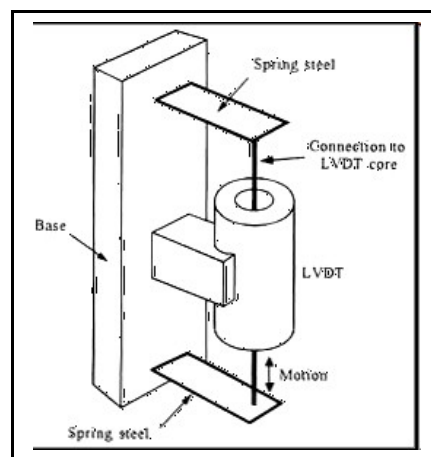


Figure 2. 18 Graphical scheme of an LVDT accelerometer: the seismic mass is hanged between two springs, constituting the ferromagnetic core, and can move inside the channel where are the coils.

Typical Characteristics:

High natural frequency = 35-620 Hz;

Higher resolution;

Lower resistance to motion;

Range: ± 2 - 700 g;

Non linearity $\sim 1\%$ fs;

FS output ~ 1 V with LVDT =10 V @ 2000 Hz

Damping ration = 0.6-0.7;

Residue zero voltage: 1%;

Hysteresis $< 1\%$ fs;

Dimension ~ 50 mm³.

Thermal Accelerometers

Thermal accelerometers use thermal convection principles and micro-machine technology to measure the movement of the seismic mass as convert the variation of thermal energy in an appropriate electric signal.

Thermal energy can be transferred in three ways: conduction, convection and radiation.

The thermal energy transfers with convection requires an intermediate agent (gas or liquid) that takes heat from a warmer body towards a cooler body, releases heat, and then may or may not return back to the warmer body to pick up another portion of heat.

$$H = \alpha A (T_1 - T_2)$$

where:

H = is the thermal flow, that is the heat lost or received by an object which has a different temperature in respect to the surrounding environment;

α = convective coefficient, depending on the fluid's specific heat, viscosity and rate of movement. The coefficient is dependent both on gravity force and temperature gradient;

A = is the exposed area;

T_1 and T_2 = are the temperatures of the object and the environment.

Convection may be natural (gravitational) or forced (produced by a mechanism). In the natural convection the difference of temperature between the solid and the fluid provokes local gradient of density that generates the fluid movement. In the forced convection, an external force imposes the movement of the fluid in respect to the solid surface.

There are two main type of thermal accelerometer: Heated-Plate or Heated-Gas, both with the structural components fabricated using micromachine technology.

In the heated-plate accelerometer the seismic mass is suspended by a thin cantilever, near one heat sink or between two heat sink, as shown in Figure 2. 19. The internal space is filled with a thermally conductive gas. The mass is heated by a surface or imbedded heater to a defined temperature. Under no-acceleration a thermal equilibrium is established between the mass and the heat sinks: the amounts of heat conducted through the gas is a function of distances between the mass itself and each sink. The temperature difference is a function of the variation of the distance from the support and the gaps at the heat sink, of the thermal conductivities of gas and silicon, of the cantilever beam's geometric dimensions and of the thermal power. A temperature sensor can be deposited on the beam to measure the temperature variation. Usually heated-plate accelerometers integrate silicon diodes into the beam or connecting thermocouples on the beam surface itself. In this way, the measure of the beam temperature is the measure of the acceleration.

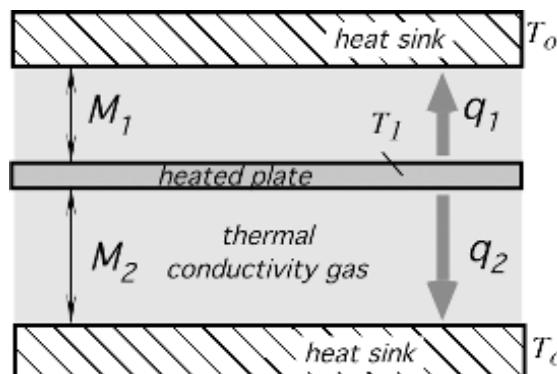


Figure 2. 19 Graphical scheme of a heated-plate accelerometer where the seismic mass is suspended by a thin cantilever between two heat sink; a thermal conductivity gas fill the internal space.

Typical Characteristics:

Sensitivity ~ 1% of change in the output signal per g; smaller than that of the capacitive or piezoelectric type

much less susceptible to such interferences as ambient temperature or electromagnetic and electrostatic noise.

In the heated-gas accelerometer (HGA) the seismic mass is represented by a gas. An example is the HGA developed by MEMSIC Corporation, that is microfabricated on a micromachined CMOS chip with a biaxial motion measurement system. In this case, the fundamental principle is forced thermal convection, where the force is produced by acceleration. A functionally equivalent to traditional inertial mass accelerometer measures the internal changes in heat transfer of the trapped gas. The gas representing the inertial mass is thermally nonhomogeneous. The most important advantage in respect of the traditional solid inertial mass is a shock survival up to 50000 g, leading to significantly lower failure rates.

The sensor contains a micromachined plate, with an etched cavity, adjacent to a sealed cavity filled with gas. A single heat source, centered in the silicon chip, is suspended across the trench and four temperature sensors (serially connected thermocouples) are equally spaced in respect to the sides of the heat source.

When no forces act on gas, the temperature has a symmetrical conelike distribution around heater. The presence of an acceleration in any direction will disturb the temperature profile, creating an asymmetric configuration due to a convection heat transfer (Figure 2. 20). The differential temperature, and thus voltage, becomes directly proportional to the acceleration. The sensor can measure acceleration signal in both the path of the device, along the x axes and along the y axes.

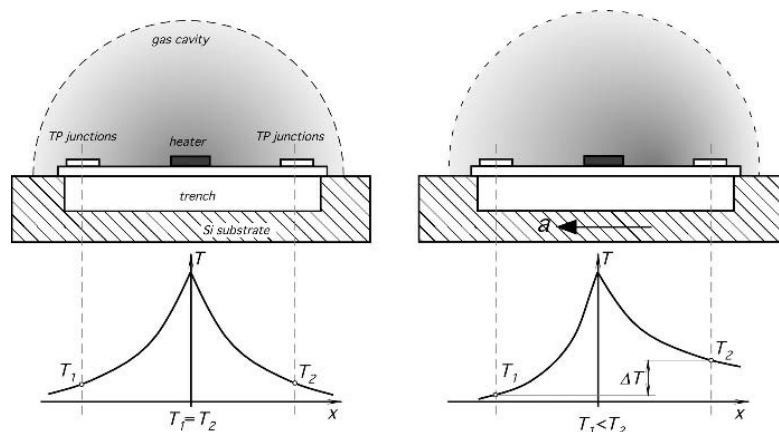


Figure 2. 20 Distribution of temperature profile in a heated-gas accelerometer: on the left, when no forces act on gas, the temperature has a symmetrical conelike distribution around heater; on the right, the presence of an acceleration will disturb the temperature profile, creating an asymmetric configuration due to a convection heat transfer.

Typical Characteristics:

Full-scale range from below $\pm 1.0g$ to above $\pm 100g$;

Can measure both dynamic acceleration (as vibration) and static acceleration (as gravity);

The analog output voltage can be in absolute (independent of the supply voltage) and ratiometric (where output voltage is proportional to the supply voltage) modes;

Typical noise floor below 1mg/Hz, allowing the measurement of sub-milli-g signals at very low frequencies;

The frequency response, or the capability to measure quick changes in acceleration, depends on the design;

The output sensitivity changes with ambient temperature (Figure 2. 21); in case, it is possible to embed on chip a temperature sensor (resistive temperature detector or silicon junction).

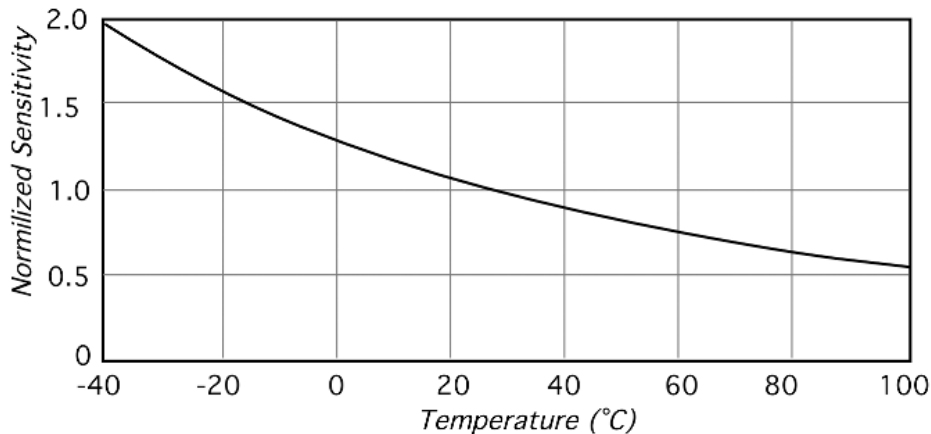


Figure 2. 21 Change of the output sensitivity with ambient temperature.

Micro-Nano Accelerometers

Many sensors use bulk micromachining, where all most critical components (such as flexures or resonant beams) are made from bulk silicon, to exploit all mechanical properties of silicon crystal.

Bulk micromachining, with an appropriate design and film process, allows extremely robust and stable accelerometers, in respect to surface micromachining techniques.

With surface or bulk micromachining it is possible to built in multiple layers on a single substrate smaller and more complex structures. Thus, multiple accelerometers can be mounted on a single chip, sensing acceleration along the three spatial directions.

Most micro- and nano-accelerometers measure acceleration with the detection of the relative motion of a proof mass and mounting substrate. A mechanical spring suspension is used to suspend the mass above the substrate. Capacitive, piezoelectric or piezoresistive techniques, based on CMOS technology, can be used to measure the displacement. The output from the chip is usually read on digital form. The chips circuits provide offset cancellation for bias stability, gain scale factor stability, zero acceleration bias stability, temperature compensation, prefiltering, noise immune digital output.

Gyroscope

A gyroscope is a device for measuring or maintaining orientation, based on the fundamental principles of the conservation of angular momentum: *"in any system of particles, the total angular momentum of the system relative to any point fixed in space remains constant, provided no external forces act on the system"*.

Gyroscopes have a high inertia, and preserve the position of the spin axes during rotary motion without external forces acting on it.

When an external force acts on the spin axes changing its direction, the joint action of the angular momentum and the external force moves the spin axes through the direction perpendicular to the plan of the force and axes itself, describing an ideal cone (*precession*).

A gyroscope, as shown in Figure 2. 22, is basically composed of:

a Rotor: free to rotate around its axis (spin axis);

a Gimbal: that allow the rotor to orientate in the three spatial directions.

When the rotor is in a rotary motion its spin axis preserves the same orientation even if the holding house changes orientation.

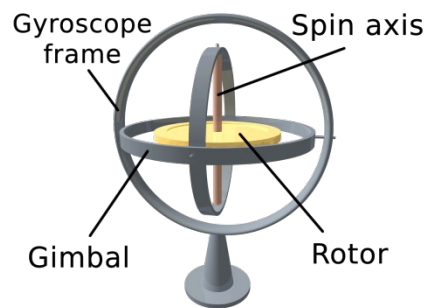


Figure 2. 22 Picture of a gyroscope, with the rotor jointed to its spin axis and the gimbal.

The device is a spinning wheel or disk whose axis is free to take any orientation. This orientation changes much less in response to a given external torque than it would without the large angular momentum associated with the gyroscope's high rate of spin. Since external torque is minimized by mounting the device in gimbals, its orientation remains nearly fixed, regardless of any motion of the platform on which it is mounted.

Mechanical (or Rotor) Gyroscope

In a mechanical gyroscope a massive disk free to rotate around a spin axes is housed within a structure for support that can rotate about one or two axes (single- or two-degree-of -freedom gyroscope).

As the spin axis remain fixed with respect to space, provides there are no external forces acting upon it; otherwise it is possible that the gyroscope delivers a torque (or output signal) which is proportional to the angular velocity about an axis perpendicular to the spin axis (Figure 2. 23).

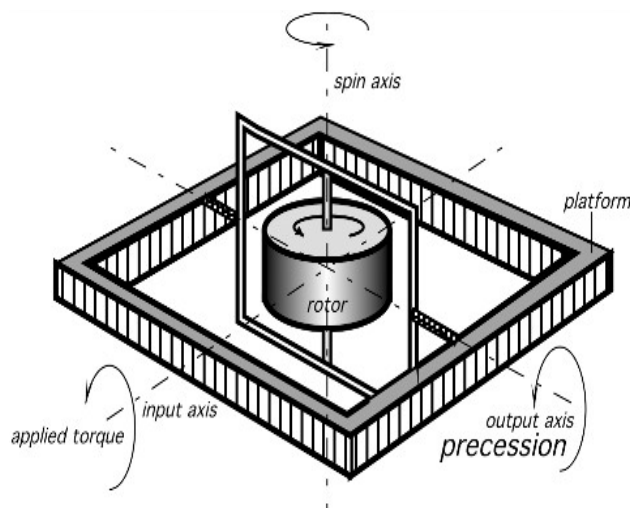


Figure 2. 23 Fundamental elements of a mechanical gyroscope

As the rotor freely rotates, it tends to preserve its axial position: if the platform rotates around the input axis, the gyroscope responds with a torque around a perpendicular axis (output), turning its spin axis around the output one with a precession movement. Using the second Newton's law related to the rotary motion, it is possible to correlate the applied torque (T) with the rate of rotation of the spin axis around the output axis (Ω):

$$T = I\omega\Omega$$

where I is the inertia of the rotor in respect to the spin axis and ω is its velocity, held constant. As rule: the direction of the precession is always in a way to align the direction of rotor's rotation with the direction of the applied torque rotation.

The accuracy of this type of gyroscope depends strictly on the effects that may cause additional torques or drifts, as friction. To reduce friction, the suspension could be eliminated by floating the rotor and the driving motor in a viscous, high-density liquid. Otherwise, using holding gas, the rotor can be supported by high pressure helium, hydrogen, or air. Another possibility is to support the rotor in vacuum using an electric field (electrostatic gyroscopes) or a magnetic field (magnetic or cryogenic gyroscopes).

All the mechanical components, such as rotors, gimbals, support bearings and motors need accurate machining and assembly, limiting the miniaturization of the device and the reduction of the cost.

Vibrating Gyroscope

The use of MEMS micromachine technology allows the design of miniaturized gyroscopes in which the rotating disk is replaced with a vibrating element (as quartz).

Vibrating gyroscopes take advantage of the techniques developed in the electronic industry and are much more robust, withstanding in various environments such as typical of many military and aerospace conditions.

Vibrating gyroscopes are based on the Coriolis acceleration. In physics, the Coriolis effect is an apparent deflection of moving objects when they are viewed from a rotating reference frame. The Coriolis acceleration of a body appears whenever that body moves linearly in a frame of reference which is rotating about an axis perpendicular to that of the linear motion. The resulting acceleration, which is directly proportional to the rate of turn, occurs in the third axis, which is perpendicular to the plane containing the other two axes.

Micromachined gyroscopes use vibration instead of rotation, with a mass suspended and made to move linearly in simple harmonic motion, and the resulting acceleration can be detected and related to the rate of motion.

Optical Gyroscope

Optical gyroscopes are based on Sagnac effect (or Sagnac interference), where two beams of light generated by a laser propagate in opposite directions within an optical ring having refractive index and radius R . One beam goes in a clockwise (**CW**) direction, and the other goes in a counter-clockwise (**CCW**) direction.

If the ring rotates with angular rate Ω , in **CW** or **CCW** direction, then light will travel different paths at two directions. Hence, using a technique for measuring the difference between the two paths (as optical resonators, open-loop or closed-loop interferometers), it is possible to measure the rotation rate Ω (Figure 2. 24).

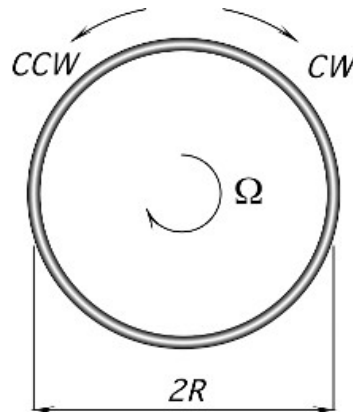


Figure 2. 24 Scheme for an optical gyroscope.

2.1.3 Haptics (UZH)

Introduction

The construction of an artificial robotic soft skin sensor poses a host of intriguing and challenging problems. Due to such difficulties, most robotic platforms, either do without skin, or de-emphasize its importance in relation to vision, audition, or proprioception. First of foremost, the skin is not a localized sensory organ, i.e., unlike vision and sound, its sensing mechanisms are distributed and diffused allowing for full-body sensory feedback. Therefore, ideally, an artificial skin should cover the whole robot body. Then, the skin should be soft and elastic, in order not to disturb the robot's motion. It should be compliant to touch and have "skin-like" characteristics to simplify interaction. Further requirements for an artificial skin are toughness and robustness against impact and shear forces.

Tactile perception is a fairly complex phenomenon, and can be defined as the sensation evoked when the skin is subjected to mechanical, thermal, chemical, or electrical stimuli. It can take many forms and includes, but is not limited to the detection of shape, chemical, or electrical stimuli. It can take many forms and includes, but is not limited to the detection of shape, size, texture, friction, or movements across the skin (as well known as discriminative touch or "mechanoreception"), the signaling of tissue damage ("nociception"), static position and movement of limbs and body ("proprioception"), sense of warmth and cold ("thermoreception"), and other related physical properties. Dario (1991) notes that, "it is interesting to observe that psychophysicists and psychologists have even coined a word ("haptics") to specifically indicate the complex interaction of proprioceptive and exteroceptive sensing and of purposive data gathering, which is at the roots of tactile perception in humans."

tions.

Design and criteria issues

Most of the research in tactile sensing so far has focussed on the development of skin like sensors trying to mimic the capabilities of human touch. Hardly any research has directly focussed on development of haptic sensing for bio-mimetic robots based on animals such as the octopus. Harmon (1982) defined tactile sensing as the ability to sense force over an array, and to be able to sense this force over a graduated scale. As a first approach to the development of artificial taction, he codified a set of tactile sensor design parameters, which lead up to a list of performance specifications. Some of these include the description of desired spatial resolution (1-5mm), frequency response (25-30Hz), sensitivity (30-1000gf/cm²) and that they must measure parameters like normal force and/or pressure, presence or absence of a contact, torque, thermal conductivity of an object, slip or shear forces. It must be noted that even the higher ranges listed fall far below human tactile sensing ability.

Come of the issues that affect haptic sensing include the following : area of coverage, conformability, compliance, toughness, wiring, digitization, difficulty of data processing, heat dissipation, scanning strategy of electrodes, materials, cross-talk, and physical parameters.

The tradeoffs involved in the design and manufacture of good tactile sensors is described below in Table 2. 1.

Table 2. 1 Tradeoffs in design of Tactile Sensors.

Accuracy	Flexibility	Practicality	Multiple Stimuli
High Resolution	Softness	Sampling Speed	Pressure
Higher Sensitivity	Folding/Bending	Implementation/Extendability	Temperature
Bigger Dynamic Range	Deformable/Stretchable	Fabrication	Stretch

Types of technologies

Force-sensitive resistors (FSR)

FSRs as well known as “conductive polymer sensors”, consist of a thin three-layered structure: an active area, a spacer, and a flexible substrate.

The device exhibits a decrease in resistance with an increase in force applied to the active surface. The active area consists of a pattern of conductors that are connected to the output pins through an elongated tail. Any force applied on the flexible substrate will push a conductive polymer thick film against the active area and will change the electrical resistance of the sensor which is measured as a voltage drop proportional to force. The relationship between the applied force and output resistance is dependent on the particular design of the active area, which is determined by the shape of the area, or the number of conductors, for instance. However, all FSRs exhibit a nearly switch-like response, requiring a break force to decrease the 1 M Ω rest resistance to approximately 100 k Ω , which is the beginning of the measurement range. The change in resistance is best measured when the active area of the FSR is attached to a flat, firm, and smooth surface. Additional problems are related to the sensors’ poor accuracy (errors up to 25%), which make FSRs unsuitable for precision measurements. Franden(2004) describes some of these properties. Piezo-resistive sensors (PRS) are also sometimes referred to as Force Sensitive Resistors as described in Noda et al (2006).

Piezo-electric materials

These materials convert mechanical stress into a proportionate output voltage potential. In tactile sensors, these are usually used in the form of a polymer, such as polyvinylidene fluoride, which must be made piezoelectric by first exposing it to a high electric field. Such films are “pyroelectric” as well, and respond to heat fluxes by generating electric charge. Furthermore they have an excellent mechano-electrical coupling. This is also one of the reasons why these materials have been successfully employed as sensor elements. Domenici and De Rossi (1992) proposed a stress-component-selective tactile sensor array, and Morten et al. (1992) introduced a resonant pressure sensor based on the piezo-electric properties of ferro-electric thick film. A new principle and the implementation of a non-scanning, fast response, arbitrarily distributed piezoelectric resonant sensor array was presented by Li and Wen (19998). Basically they determined the position of the sensing point from the time difference of the time stamps collected by the four transducers placed in the four corners of a quartz crystal plane.

Strain gauge

Strain gauges are very well known sensing devices, and consist of circuits that are capable of measuring very small changes in the resistance of one or more of their parts. Applied forces change the dimensions of the gauge which alters the resistance of the circuit.

Capacitive sensors

Capacitive sensors rely on the fact that the capacitance of a parallel plate capacitor is a function of the areas of the two plates and the thickness of an intervening dielectric medium, i.e., the distance between the plates.

Magnetic transduction

These transducers rely on the mechanical movements to produce flux density changes in magnetic fields. These measurements are usually made by "Hall effect sensors." Other such transducers employ magnetoresistive or magnetoelastic materials. When subjected to mechanical stress, these materials exhibit changes in their magnetic fields.

Ultrasonic sensing

Microphones are known to be useful for detecting surface noise that occurs at the onset of motion and during slip. Ultrasonic transmitters and receivers are used to detect changes in wavefronts due to distortion, and displacements as small as ten micrometers or less can be detected.

Electro-optical tactile sensors

Photoelectric, or optical, tactile sensors also come in different forms. Intrinsic devices involve modulation of some feature (e.g., optical phase, polarization, and so on) of transmitted light without interrupting the optical path. Extrinsic devices involve the interaction of stimuli external to the primary light path.

Micro-electro-mechanical systems

This emerging technology is also known as micromachining technique. Work on piezoresistive and capacitive micro-machined silicon-based tactile sensors has led to the design of arrays of force sensing elements using diaphragms or cantilevers as the major sensing principle. Conducting beams are easily fabricated using micro-machining techniques. Unfortunately their response to large loads is nonlinear, and has to be approximated to a linear response for small (less than 10% saturation) pressures. The "microtactile sensor array" designed by Gray and Fearing (1996) consists of small capacitive cells (capacitive tactel), which can be approximated as many parallel plate capacitors of small length and width. The most significant drawback of this sensor is its hysteresis.

Conductive rubber

Pressure conductive rubber was used by Shimojo et al.(1991) for the construction of a new type of tactile sensor.

Conductive gel

This material was used by Kageyama et al. (1999) to build a skin sensor of novel type. Conductive gel is much softer than conventional conductive materials and makes it possible to realize a soft skin without a thick cover. The sensing principle is based on the measurement of changes of electrical impedance between the electrodes mounted on both sides of the gel sheet. Despite its novel sensing principle, this sensor has at least two significant problems. First of all, the sensor becomes harder over time. Secondly, the electrical impedance of the gel increases by 20 – 30 times in less than 50 days. He also went on to describe a multi-valued touch sensor, consisting of a sandwich of a flex-circuit board, a conductive fabric, and a rubber sheet as a cover.

Conductive ink

The resistance of each sensel (sensing element) of the sensor developed by Tekscan Technology Inc. is inversely proportional to applied surface pressure. As a force is applied to the sandwich, electronics scans and measures the change in resistance from each sensel so as to determine the magnitude, location, distribution, and timing of the pressure exerted. Each sensel is actually a variable resistor whose value is high when no force is applied to it. The sampling rate of the standard "I-Scan sensor" configuration is 2.5×10^5 sensels/sec, and "Tekscan" has custom-manufactured systems that sample 5×10^7 sensels/sec.

Fiber-optic based pressure sensing

Tactex control Inc. smart fabric technology is based upon a patented fiber-optic based pressure sensing technique. These fabrics consist of thin cellular elastomers, typically of urethane or silicon. Within the fabric a large number of overlapping pressure sensing zones is constructed. An outer skin protects the fabric, and serves as a wear surface. Pressure exerted on the outer skin changes the pore size distribution in the elastomer, which in turn changes the optical scattering properties in that area – it is this change in scattering properties that is detected by the fiber optics, and interpreted as pressure.

Capacitive array sensing

Sensors based on this principle have very high sensitivity, linear response, and low hysteresis as described in Pawluck et al (1996). Their design is based on capacitive tactile array sensors developed for robotics applications. The sensor consists of orthogonal layers of copper strips separated by a dielectric. Applying pressure to the sensor's upper surface forces the copper strips closer together, increasing the capacitance at the cross-points, each of which forms an array element. Fearing (1990) noted that the change in the measured capacitance of the element is closely proportional to the local pressure above it. "Pressure Profile Systems Inc." has even managed to develop a "conformable" tactile sensor array based on the same working principle. According to the company's datasheet, the key benefit that differentiates their conformable array from existing technology is its ability to conform to complexly curved surfaces such as the human body. The tactile array sensors consist of a regular pattern of sensing elements to measure the distribution of pressure.

Micro-machined planar coil tactile sensor

Nobuyuki et al. (2000) describes a surface micromachined tactile sensor, consisting of a planar spiral coil with no substrate, which can be implanted in soft material. Planar coils are suited for this type of application because their inductance can be easily changed by deformation caused by touch.

IR-skin

The "sensory skin" described in Cheung and Lumelsky (1989), uses a whole-arm proximity sensing system for an articulated robot arm that provides complete coverage of the entire manipulator. This is necessary in order to ensure that every obstacle in the robot's path can be detected and avoided. The proximity sensing technology is based on IR arrays which are called "sensorcells." It makes the use of IR, acoustic and capacitive sensors in the same sensor skin possible. The two main components of the skin are smart sensor modules and a "flex-print circuit board skin." Module sockets are placed at regular intervals on the flexible skin and simply plugged in by the user where required. Redundant cables carrying data and power are connected to each panel. But a minimum of four cables can be used for up to 1024 sensors.

Quantum Tunneling Composite

They use the principle of Quantum tunneling, in composite materials of metals and non-conducting elastomeric binder, used as pressure sensors. When pressure is applied, the metal particles move closer and electrons can tunnel through the insulator. This principle is used in the the Shadow Robot Hand (<http://www.shadowrobot.com/tactile/overview.shtml>) for tactile sensing.

Applications

Most of the research in tactile sensing so far has focussed on the development of skin like sensors trying to mimic the capabilities of human touch and therefore most of the application demonstration have revolved around humanoid robot tactile sensing and haptic interaction projects. Some of the other applications are in Human Machine Interfaces, Virtual Reality, Wearable Computing, Medical applications, Ergonomics, Automobile industry and in Sports science.

2.1.4 Proprioception (IIT)

Proprioceptive system of the octopus

The Octopus ability to be aware of the orientation of the arms, to perceive their movements (whether self generated or externally imposed), and to state the amount of resistance opposing any movements constitute proprioception or kinaesthesia as it is usually termed. Kinaesthesia or Proprioception consists of three qualities. These are the sense of position, the sense of movement, and the sense of force. To substitute these sensations in the robotic Octopus prototype system different sensing technologies can be considered. The following section introduces the principle of operation of some of these technologies mainly related to the sensing of the motion/displacement and force/torque quantities.

Proprioceptive sensors

Displacement sensors

By far the most common motions in robotic or mechanical systems are linear translations or angular rotations. More complex motions are usually composed by the above primitive motions. The first part of this section provides a list of the available sensing technologies usually employed to measure linear and rotational displacements.

Resistive Sensing

The simplest way to measure a linear or rotary displacement is by using a variable resistor or potentiometer.

Variable resistors are mechanically link to the motion to be measured, either along a fixed linear axis or along a rotary axis in the case of the angular motion. The variation in their resistance is used to determine the linear or the angular displacement.

Bend Sensors

A special type of a resistive sensor is the flexible bend sensor that can be used to measure the deformation of surface to which it is attached. Conductive ink between two electrical contacts on a flexible material changes resistance as the material bend and stretches. This resistance variation can be used to determine the bending of the sensor.

Optical Encoders

The principle of the optical encoder is based on the use of photo interrupts to generate a series of pulses. By counting the generating pulses with appropriate circuitry the motion or displacement can be monitored or measured. There are two basic versions, the absolute encoders and the incremental or relative encoders. In general incremental encoders provide better resolution in a lower cost and more compact size and they are the most common option. The main drawback of the incremental encoder is that the absolute position is not known in the startup and some calibration procedure is required in order to obtain it.

Resolvers

A resolver is usually used to measure rotary displacement around a fixed axis. It typically provides sine and cosine analogue outputs. Resolvers are very robust and usually are preferred over encoders despite the fact that are less accurate and requires more complex support circuitry. Some resolvers provide also a encoder type output for compatibility.

Inductive sensing (LVDT)

The linear variable differential transformer (LVDT) is an inductive sensor which consists of a tube and a plunger. The displacement of the plunger is the motion to be measured. The tube is wrapped around with at least two coils and excitation coil and a pick up coil. An alternative signal is usually used to drive the excitation coil. The plunger carries a ferromagnetic slug which when it moves changes the magnetic coupling of the excitation and the pickup coil. As a result the level of signal detected by the pickup coil changes according to the magnetic coupling which varies as a function of the motion of the ferromagnetic slug.

Capacitive Sensing

Capacitive sensors can be used to measure small linear motions of a few millimeters. Capacitance change can be produced either by changing the distance between the two capacitor plates by vertically translating the two planes or by modifying the size of the overlapping between the two plates by translating the two planes relative to each other along their planes. In the first case the capacitance variation is a nonlinear function of the distance between the two plates while in the second case the capacitance changes linearly as a function of the size of the overlapping area.

Hall effect

Hall effect sensors can be distinguished into simple digital switch sensors and analogue sensors. They both produce a digital or analogue output according to the intensity of the magnetic field. The analogue type produces an output which is proportional to the strength of the magnetic field. The analogue Hall effect sensors can be used to detect both linear and angular motions. Two of these sensors can be arranged in a right angle to detect the sine and cosine of the angle of the rotation magnet, therefore effectively creating an absolute sensor.

Accelerometers

Acceleration is well related to the motion and it can be used as a basis quantity for the measurement of other motion parameters such as velocity and position. The basic accelerometer consists of a mass that is free to move along a sensitive axis. The majority of accelerometer sensors are based on this principle although the sensing technology used for their implementation varies from electromechanical systems to piezoelectric, piezoresistive, strain gauges and capacitive based devices. Accelerometers can be used for general purpose motion measurements, vibration and shock sensing.

Force and Torque Sensing Principles

The second group of proprioceptive sensors are those related to the sensing of the force and torque modalities. The fundamental principle of operation for the mechatronic force/torque proprioceptive sensors results from the physical response/mechanical behavior of a fixed or free to move body under the application of the force/torque load. When a fixed body is loaded with a force/torque it will behave elastically until a critical value of normal stress or shear stress will be reached and then it will deform plastically. During the elastic deformation the body is temporarily deflected and when the external load is removed it returns back to the original position/size. Determination of the applied force can be done by directly measuring the deflection caused on the fixed body. In the free to move body case, applying an external force to a free to move mass will generate a certain acceleration the level of which can also be used for the determination of the applied force/torque load. In general an unknown force/torque modality can be measured by:

by balancing the unknown force/torque against a standard force/torque generated by a known mass and a structure of links or levers.

by measuring the acceleration of a known body mass.

by measuring the pressure generated by the load on a specific body area.

by measuring the deflection caused on an elastic body with the application of force/torque.

The above methods for measuring force and torque loads can result on different sensor designs based on various sensing principles. The design and selection of the sensor working principle are usually governed by the implications of the sensor application. The following section introduces the different type of sensors used to measure a force or torque quantity.

Strain gauges

Metal foil strain gauge has been in use for many years and is the fundamental sensing element for many types of sensors, including pressure sensors, load cells, torque sensors, position sensors, etc. The foil strain gauges are available in a wide choice of shapes and sizes to suit a variety of applications. They consist of a pattern of resistive foil which is mounted on a backing material. They operate on the principle that as the foil is subjected to stress, the resistance of the foil changes and this can electrically be measured.

As opposed to metal strain gages, semiconductor strain gages depend on the piezoresistive effect of the semiconductor material and measure the change in resistivity with stress as opposed to strain. The semiconductor bonded strain gage is a thin slice of silicon substrate with the resistance element diffused into a substrate of silicon. As in the case of the metal strain gauges, the basic effect is a change of resistance with strain. In the case of a semiconductor, the resistivity also changes with strain, along with the physical dimensions. The net result is a much larger gauge factor than is possible with metal gauges.

Capacitive sensors

A capacitive sensor consists of two plates separated by air gap or a dielectric material. Applying a force on one of the two plates can result in the change of the thickness of the gap between the two plates which produces variation in the capacitance. This capacitance variation can be used to measure the applied force/tension. Usually the force is applied onto a membrane that is attached in one of the capacitor plates or to the capacitor plate itself. Among the other sensing principles, capacitive-based sensing is known as one of the most effective means for detecting extremely small deflections of structures. Capacitive sensing schemes represent an alternative to strain gauges offering very good sensitivity to very small deflections without direct temperature dependence.

Force sensing resistors

The working principle of Force sensing resistors (FSR) is based on the fact that certain thick film polymer devices exhibit decrease of the resistance with the application of the force. An FSR sensor is made up of two parts The first is the resistive material applied to the film. The second is a set of contacts applied to the film. When a force is applied to the sensor a better connection is made between the contacts and the film and this results in the decrease of the resistance of the sensor element. FRS are considered less expensive than other sensing devices and are appropriate in applications where high accuracy is not necessary. FSRs should not be used when precise force sensing is necessary as sensor parts may demonstrate variation in the resistance.

Piezoelectric sensing

Piezoelectric materials generate an electric charge when placed under mechanical stress. Unlike the sensors mention so far that can measure static forces, piezoelectric force sensors are mostly used for dynamic- force measurements such as oscillation, impact, or high speed compression or tension. Any force applied to the piezoelectric sensing element produces a separation of charges within the atomic structure of the material, generating an electrostatic output voltage. The polarity and the magnitude of the voltage generated depends on the atomic structure of the material and the direction in which the force is applied. The piezoelectric effect is reversible, that is if a potential is applied between the surfaces of the crystal of the piezoelectric material it will cause the deformation of the material changing its physical dimensions.

Magnetoresistive sensing.

The principle of operation of these sensors is based on the fact that certain metal when cooled to low temperatures show a change in the resistivity when subjected to an applied magnetic field. In practice these devices have severe disadvantages because of their high sensitivity to ambient temperature changes. The semiconductor magnetoresistive sensor consists of magneto resistors (D-type InSb/NiSb semiconductor resistors whose value can be magnetically controlled), which are mounted onto an insulated ferrite substrate. The sensor is encapsulated in a metallic or plastic package. A permanent magnet, which supplies a biasing magnetic field, is fixed on the base of the sensor.

Table 2. 2 Comparison of Displacement sensing technologies.

Property	Resistive	Bend Sensor	Optical Encoder	Resolvers
Absolute	Yes	Yes	Yes	Yes
Relative	Yes	Yes	Yes	Yes
Repeatability	Good	Average	Excellent	Excellent
Accuracy	Good	Average	Excellent	Excellent
Amplification	Not Required	Not Required	Not Required	Not Required
Circuitry Complexity	Low	Low	Low	Average
Size	Average/Small	Average/Small	Average	Big

Property	LVDT	Hall Effect	Capacitive	Accelerometers
Absolute	No	Yes	Yes	No
Relative	Yes	Yes	Yes	Yes
Repeatability	Good	Good	Good	Average
Accuracy	Good	Average	Good	Average
Amplification	Average	Not Required	Average	Average
Circuitry Complexity	High	Low	Average	Average
Size	Big/Average	Small/Micro	Small/Micro	Small/Micro

Table 2. 3 Comparison of Force and torque sensing technologies

Property	Strain Gauges	Capacitive	FSR	Piezoelectric	Magnetoresistive
Static	Yes	Yes	Yes	No	Yes
Dynamic	Yes	Yes	Yes	Yes	Yes
Repeatability	Good	Good	Average	Good	Average
Accuracy	High	Average	Low	Good	Average
Amplification	High	Average	Do not require	Average	Average

Circuitry Complexity	Average	Average	Low	Average	Low
Size	Small/Micro	Small	Average/Small	Small/Micro	Small
Temperature Influence	Average/High, require compensation	Low	Average	Low	High require compensation

Conclusions

Looking at the Octopus arm motions, it appears that the Octopus has a great ability to control its arms and perform reaching and grasping actions. Considering the proprioceptive system of the Octopus though it appears that the Octopus performs all these arm motions with the minimum proprioceptive information. The arms of the Octopus contain tension sensors allowing the Octopus to determine whether its arms are stretched or not. These tension receptors give to the Octopus some indication of the posture of its arms however this information is not adequate to allow the Octopus to be aware of the exact position of its arms.

As a result, the real octopus does have the ability to reconstruct in the brain of the overall shape of the object it is grasping. It can detect local texture variations through its excellent touch sensing system, but cannot integrate the information into a larger picture (Wells, 1978).

Considering now the robotic Octopus the selection and the number of the proprioceptive sensors is greatly depends on what are the sensory requirements from the arm kinematics and control point of view.

Following the real Octopus paradigm this implies that tension sensors on the soft structure of the arm will be required to give localized tension information that can be used also to identify the local bending of the arm. Candidates sensor technologies may include strain gauges, capacitive, FSR or magnetoresistive techniques depending on the required signal accuracy. In general all these technologies can be miniaturized and are suitable for the limit space of the robotic platform.

In addition to the tension sensors and expanding more the proprioceptive system of the real Octopus, the robotic platform could also integrate positional sensors to support the realization and execution of the platform control system. Depending on the posture information required different sensors can be considered. For rough tracking of the arm body or end effector movements accelerometers may be proved to be adequate to provide this information. More accurate knowledge of the arm posture may require the use of more sophisticate 3D shape sensing techniques. These may be realized on the arm structure itself, e.g. by incorporating bundles of bending sensors along the arm or through kinematics and measurements of the actuator displacements. For the second case a variety of sensors may be considered from resistive to capacitive or Hall effect sensors depending on the properties of the displacement to be measured. This can be clarified more after the selection of actuators.

Wells. Martin John. Octopus: physiology and behavior of an advanced invertebrate. London : Chapman and Hall ; New York : distributed in the U.S.A. by Halsted Press, 1978.

2.1.5. Vision Sensors (FORTH)

Visual system of the octopus

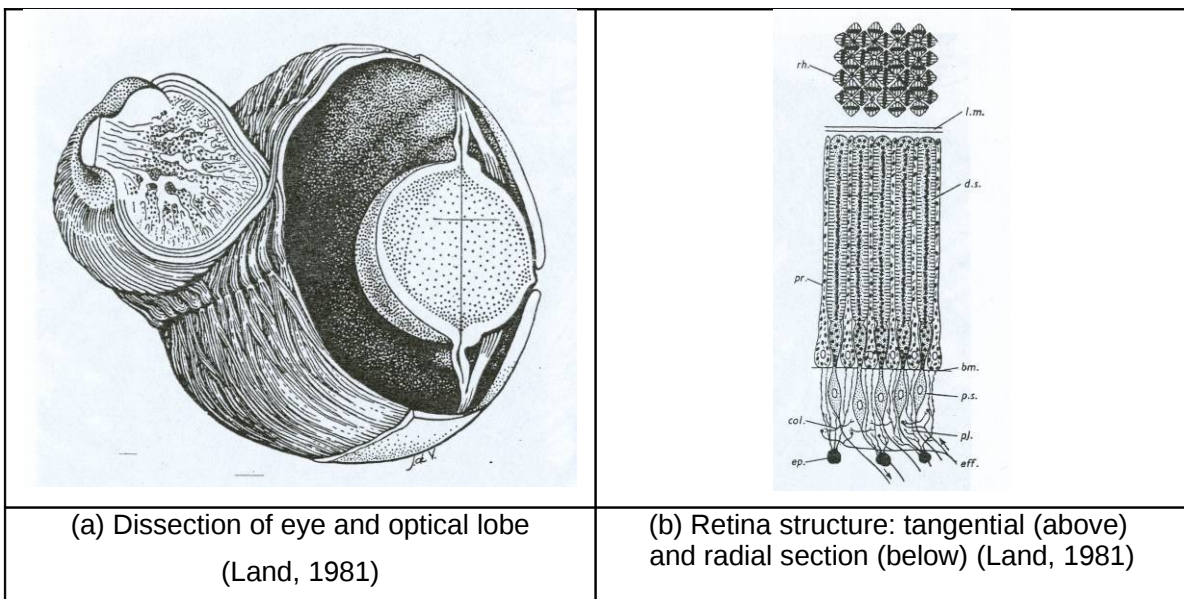
The sense organs of cephalopods, in particular of the octopus, like the rest of their nervous system, is highly developed (Brusca and Brusca, 1990). Cephalopods have large high-resolution eyes, and the optical lobes of their brain contain more neurons than in the whole of the rest of their central nervous system. This allowed them to develop a repertoire of visual behavior comparable to that of higher

vertebrates (Land, 1981). The cephalopod camera eyes are an example of convergent evolution with those of vertebrates: the cornea, iris and lens arrangement are very similar.

Cephalopod eyes are large, spherical, possess Matthiessen's ratio lenses, have a mobile iris, and a repertoire of eye movements (all these characteristics parallel the ones in fish). The lens has a fixed shape and focal lens. The cornea probably contributes little to focusing, because there is almost no light refraction at the corneal surface. An iris diaphragm controls the amount of light entering the eye, and the pupil is a horizontal slit. The eye accommodates to varying light conditions by changes in the size of the pupil and by migration of the retinal pigment.

The retina comprises closely packed (density of 70,000 per mm²), long (about 200 μm in Octopus), rod-like photoreceptors, composed of arrays of microvilli, as in insects. The length and narrowness of the photoreceptors indicate that photon capture and resolution are maximized. The sensory ends of the photoreceptors face the lens, pointing toward the front of the eye (*direct eye*), as opposed to fish and other vertebrates. The rods connect to retinal cells that supply fibers to the optic ganglia at the distal ends of the optic nerve. Adjacent receptors have their microvilli oriented at right angles, thus, neighboring receptors respond best to light whose planes of polarization are also at right angles. Therefore, the whole retina can be seen as an analyzer of polarized light. This may allow the detection of fish which camouflage themselves with a, nearly invisible to ordinary light, mirror surface.

Cephalopod eyes are believed to produce a perfectly focused image for monochromatic light. These animals are thought to be color-blind, therefore, chromatic aberration is probably unimportant. They can discriminate among objects by size, shape, and vertical versus horizontal orientation, although octopuses are probably quite nearsighted.



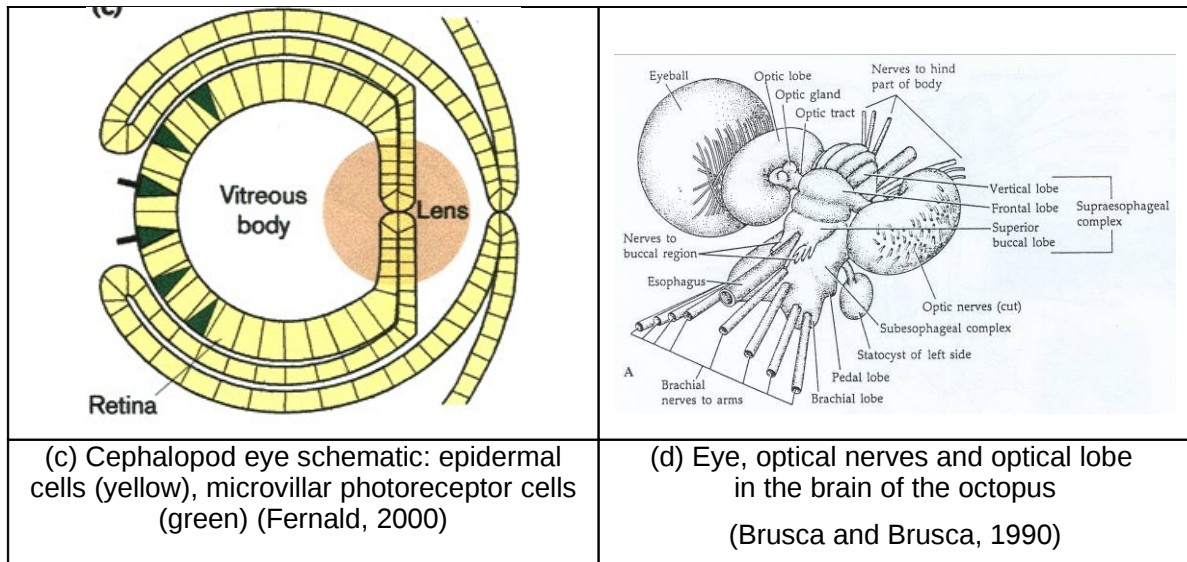


Figure 2. 25 Octopus eye.

Vision sensors

Imaging sensors are a rich source of information for sensing and estimation. Imaging sensors come in a wide variety of configurations, varying according to imaging geometry, image resolution, sensor technology and the range of sensed spectral bands. The typical case of visual sensor is the CCD camera.

A charge coupled device (CCD) camera is an apparatus which is designed to convert optical brightness into electrical amplitude signals using a plurality of CCDs, and then reproduce the image of a subject using the electric signals without time restriction. Charge coupled devices or CCDs are arrays of semiconductor gates formed on a substrate of an integrated circuit or chip. The gates of the CCD are operative to individually collect, store and transfer charge. When used in image applications, the charge collected and stored in each gate of the array represents a picture element or pixel of an image. The CCD image sensor includes an image sensing section, which performs photoelectric conversion, and a storage section, which is arranged separate from the image sensing section and temporarily stores charges acquired by the photoelectric conversion.

In the usual three-CCD perspective color camera, there are three charge-coupled detector (CCD) arrays, each receiving a portion of the visible spectrum, corresponding roughly to the human perception of red, green, and blue colors. A common, and less expensive alternative, is a single-chip CCD camera. In this case, a special spatial array of color filters, usually referred to as a Bayer filter is employed. The resulting spatial array is subsequently processed (a process referred to as demosaicing), to provide color information for each pixel. Digital colour cameras generally use a Bayer mask over the CCD. Each square of four pixels has one filtered red, one blue, and two green (the human eye is more sensitive to green than either red or blue). The result of this is that luminance information is collected at every pixel, but the colour resolution is lower than the luminance resolution. Better colour separation is reached by three-CCD devices (3CCD) and a dichroic beam splitter prism, that splits the image into red, green and blue components. Each of the three CCDs is arranged to respond to a particular colour. Some semi-professional digital video camcorders (and most professionals) use this technique. Another advantage of 3CCD over a Bayer mask device is higher quantum efficiency (and therefore higher light sensitivity for a given aperture size). This is because in a 3CCD device most of the light entering the aperture is captured by a sensor, while a Bayer mask absorbs a high proportion (about 2/3) of the light falling on each CCD pixel.

CCD sensors are often referred to with an imperial fraction designation such as 1/1.8" or 2/3", this measurement actually originates back in the 1950s and the time of Vidicon tubes. Compact digital

cameras and Digicams typically have much smaller sensors than a Digital SLR and are thus less sensitive to light and inherently more prone to noise.

Apart from the CCD in a digital camera, the lens is the most important element to ensure a quality image. Most digicams have zoom lenses which allow you to vary their focal length from wide-angle to telephoto. Focal lengths are indicated in millimetres. On conventional 35mm cameras, lenses shorter than 50mm are considered wide-angle while longer focal lengths are telephotos. A 50mm lens is considered "normal" because it sees the scene in the same proportions as the human eye does. Although some DSLRs have full frame sensors, the equivalent on most digicams would be a 6 or 7mm lens, as most CCDs are much smaller than 35mm film. For clarity purposes however, we will refer to focal lengths as compared to 35mm because CCDs on digicams are not uniform in size and their focal lengths and angle of view vary widely.

In geometric optics, lens distortion is a deviation from rectilinear projection, a projection in which straight lines in a scene remain straight in an image. It is a form of optical aberration. Although distortion can be irregular or follow many patterns, the most commonly encountered distortions are radially symmetric, or approximately so, arising from the symmetry of a photographic lens.

Most photographic lenses exhibit optical vignetting to some degree. The effect is strongest when the lens is used wide open and will disappear when the lens is stopped down by a few stops. Together with natural vignetting, optical vignetting causes a gradual darkening of the image towards the corners. This illumination falloff often goes unnoticed but it may become disturbing when the subject has large faces with an even colour or brightness. The contrast of the recording medium also plays a role: the higher the contrast, the more pronounced the effect.

Foveated imaging sensors

Mimicking the information saving approach of the human retina has been able to soften the trade-off between image resolution and image dimension. Foveated sensors have an increasing resolution from the periphery up to the center achieving at the same time a high resolution in the focus point and a broad field of view while limiting the amount of information to be acquired and processed. The pixels are randomly accessible allowing the acquisition of smaller regions. The retina-like configuration gives a more than 30 times reduction in the image dimensions still providing a good perceptual representation thanks to the optimal match between sensor's resolution and retinal resolving power. Such an advantage can be used for a faster frame acquisition or for a lower processing load. Such retina-like cameras have a digital output with a rectangular image in *log-polar* format where each ring of the sensor is mapped into a line of a rectangular grid. The log polar mapping is conformal and any "traditional" local processing can be used without modifications (e.g. edge detection, filtering etc.). A simple remapping through a look-up table is sufficient to convert it into a *regular* image. Log-polar images have higher resolution at the center, where the attention is focused on, and the rest of the visual field is covered at a coarser resolution, still enabling the detection of events at the image periphery. The main advantages of using a non-uniform image sampling mechanism, such as the log-polar images, are related both to perceptual and algorithm complexity issues. Foveatic sensors and imaging are illustrated in Figure 2. 26 and Figure 2. 27.

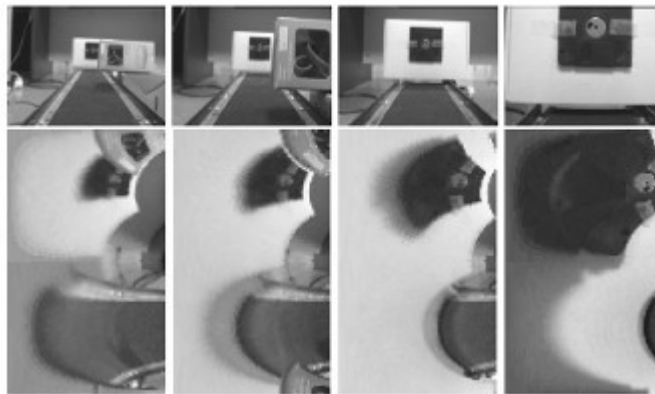
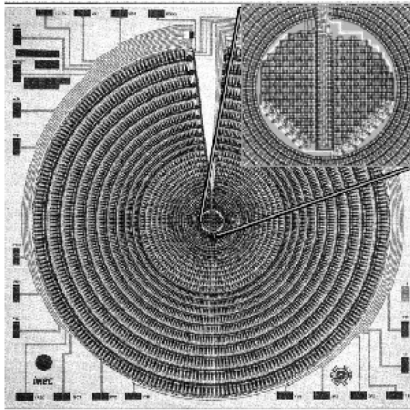


Figure 2. 26 Foveatic sensors: a foveatic (log polar) CMOS visual sensor (left) and perspective images and their corresponding logpolar transformations (right).



Figure 2. 27 Foveatic imaging: a foveatically sensed image (left) and the corresponding original image (right).

The use of an anthropomorphic retina-like visual sensor, and the advantages of polar and log-polar mapping for visual navigation, has been investigated in (Tistarelli and Sandini, 1993). It is there demonstrated that the motion equations, that relate the egomotion and/or the motion of the objects in the scene to the optical flow, are considerably simplified if the velocity is represented in a polar or log-polar coordinate system, as opposed to a Cartesian representation. The analysis is conducted for tracking egomotion, but is then generalized to arbitrary sensor and object motion.

A CCD sensor with a small foveal region with constant resolution, and a relatively large peripheral region, where the receptors' density decreases exponentially with eccentricity is described in (Kreider, 1993; Bandera, 1990; Sandini and Tagliasco, 1980). The circular geometry of the sensor's sampling structure provides several advantages over conventional imagers. The log-polar transformation provides data compression, rotation and magnification invariance around the central region of the

sensor. It is an elegant way to deal with the trade-off between resolution and amounts of data. But this structure has disadvantages as well: lower resolution compared to conventional imagers, the complexity of design and use, and the need for gaze control. These types of sensors are particularly attractive for robotic applications, as well as docking, tracking, and time-to-impact applications.

In (Pardo et al., 2004) a technique that allows high-speed movement analysis is presented, using the accurate displacement measurement given by the feature extraction and correlation method. It is demonstrated that it is possible to use the time to impact computation for object segmentation. This segmentation allows the detection of objects at different distances.

Binocular vision systems

An important issue in the realization of an autonomous robot with stereoscopic vision is the control of vergence. Together with version, it determines uniquely the position of the fixation point in space. Vergence control is directly related to both depth perception and *binocular fusion*. In (Manzotti et al., 2001), a method of extracting a global disparity measure for vergence control is presented, which does not require a priori segmentation of the object of interest. The method uses images acquired by retina-like sensors and, therefore, the computation is performed in the log-polar plane. The technique is global, in the sense that it is an integral measure over the whole image, and computationally inexpensive, considering that the goal was to use it in the robot control loop, rather than to accurately measure some 3D world features. Moreover, it is robust and independent of the average illumination, as well as of other features of the target, such as size, shape, and direction of motion. It provides a precise and linear estimate of the vergence error, which is the only requirement from the control point of view. Binocular vision and corresponding sensor are illustrated in Figure 2. 28.

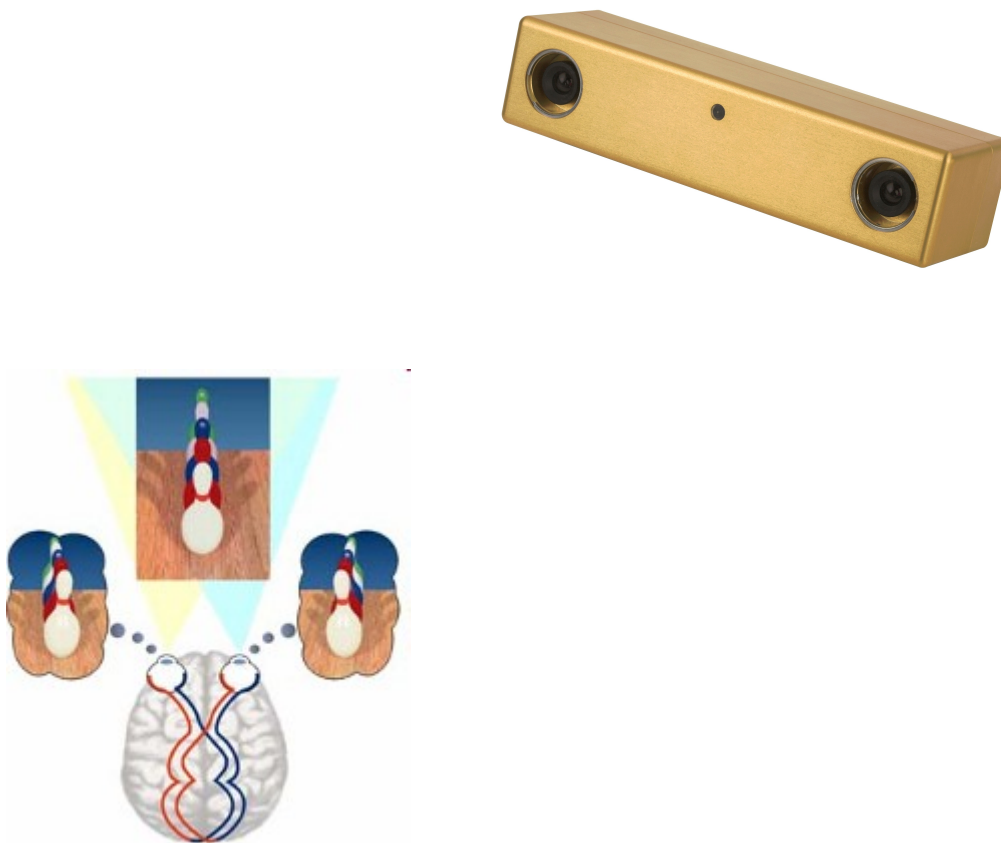


Figure 2. 28 Binocular vision: illustration of binocular vision in humans (left), and a binocular vision sensor by Point Gray Research (right).

Humanoid vision systems

Among the robotic realizations that are targeted at humanoid vision, some aim at integrating information provided by foveal and peripheral cameras. (Ude et al., 2003), in particular, describe a system that uses shape and color to detect and pursue objects through peripheral vision and then recognizes the object through a more detailed analysis of higher-resolution foveal images. The classification is inferred from a video stream rather than from a single image and, when a desired object is recognized, the robot reaches for it and ignores other objects. Common alternatives to the use of two cameras per eye consist of using space-variant vision and, in particular, log-polar images. As an example, Metta (Metta, 2001) describes an attentional system that should be extended with modules for object recognition, trajectory tracking, and naive physics understanding during the natural interaction of a robot with the environment.

Panoramic vision systems

By combining a traditional perspective camera with a mirror, creating a so-called *catadioptric system*, it is possible to create imaging geometries that map fields of view as large as a hemisphere into a single image. Such systems are inspired by insect compound eyes, and are useful, for example, for surveillance. Their geometric properties provide for stable position referencing for mobile navigation (Burschka, et al., 2003). Panoramic imaging is illustrated in Figure 2. 29.

Many insects, like the dragonflies, have additional small eyes on their head, called ocelli, in addition to their compound eyes. The ocelli only see a limited part of spectrum, like UV and green, and are very useful in determining attitude with respect to the horizon, as they can eliminate false signals caused by a setting sun. For example, consider two eyes, one sees UV and the other green. The UV sees a dark ground, a light sky and very bright sun. The green eye sees a uniform picture and a very bright sun. Appropriate processing of the two signals removes the common feature, the sun, and eliminates many effects caused by varying sky color, resulting in a correctly detected attitude. This system is superior to a conventional system of rate gyroscopes: it gives an absolute attitude reference, while gyros accumulate noise.

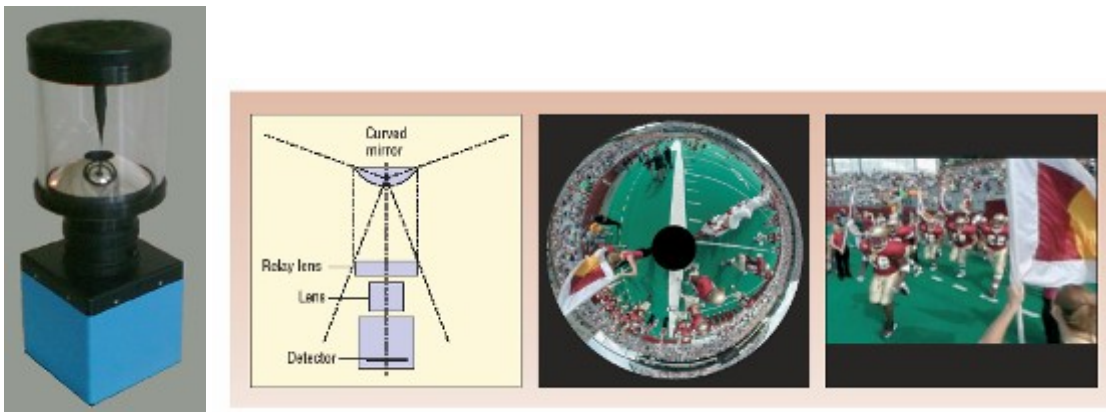


Figure 2. 29 Wide-angle imaging using a catadioptric camera: left to right: a panoramic sensor, its image formation geometry, panoramic image, and perspective warping of a portion of the panoramic image.

The NASA *bioinspired engineering of exploration systems (BEES)* investigated insect-inspired strategies to obtain novel solutions for navigation, hazard avoidance, altitude hold, stable flight, terrain following, and gentle deployment of payload (Thakoor et al., 2002). Such functionality provides potential solutions for future autonomous robotic space and planetary explorers. Features are mapped to a stack of cellular strata within the retina. Each of these representations can be efficiently modeled in semiconductor cellular nonlinear network (CNN) chips. Other artificial approaches to the fabrication of vision sensors inspired by compound eyes can be found at (Jeong et al., 2006) and (Meneses and Michel, 1998).

Optical flow sensors

Several visual systems calling upon optic-flow monitoring are particularly useful in the context of navigation tasks and are implemented in a variety of robots. The biological knowledge thus acquired was exploited to implement optoelectronic devices, based on visual motion detector elements, analogous to the fly Elementary Motion Detectors (EMDs) (Reichardt, 1961), (Zanker and Zeil, 2001), allowing a terrestrial robot to wander in its environments, while avoiding obstacles (Shen), or aerial robots to track a contrasting target (Viollet and Franceschini, 2001) or to automatically perform terrain-following, take-off or landing (Ruffier and Franceschini, 2005).

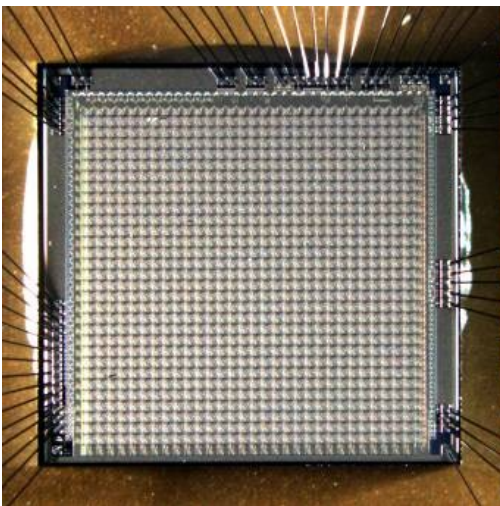


Figure 2. 30 An optical flow sensor, which estimates 2D optical flow in real-time.

The desert ant *Cataglyphis*, while probably merging optic-flow and odometry monitoring to evaluate its travel distance, is able to use its compound eyes to perceive the polarization pattern of the sky and infer its orientation. This affords it with accurate navigation capacities, that make it possible to explore its desert habitat for hundreds of meters while foraging, and return back to its nest on an almost straight line, despite the absence of conspicuous landmarks, and despite the impossibility of laying pheromones on the ground, since these would evaporate almost instantaneously. Inspired by the insect's navigation system, mechanisms for path integration and visual piloting have been successfully employed on mobile robot navigation in the Sahara desert (Möller et al., 1998).

Neuromorphic Vision Sensors

Biomimetic neuromorphic sensors are distinct from conventional image sensors in that their goal is not to capture an image, but, rather, to extract visual features of the surrounding environment, that will aid in the processing of the captured information. Although interest in such sensors has been stimulated by the work of C. Mead and his group on silicon-based analog neural systems in the mid 1980s (Maed, 1989; Mead and Ismail, 1989), it was K. Fukushima who in the early 1970s developed an electronic model of the retina incorporating the center-surround receptive field and subsequent multi-layered processing network (Fukushima and Miyake, 1982; Fukushima et al., 1970).

Several research groups have since developed biologically inspired vision sensors, modeling different aspects of the visual pathway for various applications (for more detailed overviews, see (Fossum, 1997; Va der Spiegel et al., 1997; Koch and Li, 1995; Moini, 1999; Etienne-Cummings, 2001). One such sensor realizes a compact, low-power, low-cost, wide-dynamic-range, single chip for tracking applications, fabricated in CMOS technology, containing a foveated retina with logarithmic response to intensity, and with edge detector, motion detector and centroid localization capabilities (Etienne-Cummings et al., 1997; Etienne-Cummings et al., 2000). Another such sensor decomposes an input image into line segments grouped into four orientations, and then specifies line stops and intersections, and can be used for character recognition, for autonomous navigation and face and other recognition tasks. The line features carry rich information about the shape and structure of objects in the scene,

and are key for the recognition of these objects (Attneave, 1954; Nishimura, 2001). The feature detection method is based on template matching in a 3x3 window, combined with a non-linear threshold function. Processing on this sensor is done by the same circuits in a serial fashion, and, for that reason, the convolution unit for template matching has a programmable kernel, allowing for a compact implementation and hierarchical, spatially parallel and temporally serial processing.

Octopus-like Neuromorphic Vision Sensors: The octopus retina is able to distinguish between patterns that are aligned either vertically or horizontally in space, but is unable to discriminate mirror-image oblique objects. Both the retina structure and this functionality have been mimicked in an analog VLSI chip called *O-Retina* (Gopalan et al., 2001). (Momeni and Titus, 2006), on the other hand, deals with the implementation of the octopus' ability to discriminate objects based on their state of polarization (*polarization vision*). More precisely, the octopus retina can differentiate optimally between the horizontal and vertical direction of vibration of linearly polarized light.

Polarization vision is suggested to be useful for orientation and navigation, increasing the contrast between objects and their surroundings, and particularly for detecting transparent prey, breaking through camouflage, and increasing detection range. Because on-chip devices, such as transistors or diodes, are only sensitive to light intensity, the information encoded in the state of polarization has to be extracted and provided to the chip in terms of intensity. The device that can perform this operation is a birefringent crystal with a metal pattern on top of it, which is called *micropolarizer* in the following. For the sake of brevity, the analog VLSI chip together with the micropolarizer is dubbed *P-Retina*.

The function implemented is the discrimination of orthogonal directions of vibration of polarized light. On-chip image acquisition is performed by two photodiodes. Typically, these photodiodes have the ability to react differently to polarized light. A "difference circuit" then takes the difference of the two photodiode currents. The current-to-voltage converter implements a logarithmic dependence of output voltage on input current. The output of this compressive element is fed into a voltage follower which drives both one node of the rectangular resistive network implemented by active devices (MOS transistors) and its R_{bias} circuit, which is necessary for properly biasing this network. The input follower voltage output of each pixel is connected to this resistive network. Its function is to average all these voltages both spatially and temporally and, thus, model the lateral spread of signals through the actual artificial retina. Spatial averaging is caused by the influence of voltages on other nodes which have some physical separation from the node under consideration. Temporal averaging is a result of parasitic capacitances, which exist in all physical devices, at each node. This parasitic capacitance corresponds to the membrane capacitance in biological networks, but it is neglected for all following considerations since the system is not used to obtain temporal information. Finally, the node voltages are taken to the output through a buffer or follower.

2.2 Actuation Technologies

2.2.1 Introduction (SSSA)

An actuator is a device that modifies the mechanical state of a system to which it is coupled.

Actuators can be seen as a system that establishes a flow of energy converting some form of input power (typically electrical power) into mechanical power. The final goal of this exchange of energy may be either to effectively dissipate the net mechanical energy of the system, for example, like a decaying passive frictional mechanism, or to increase the energy level of the system.

An actuator is composed by three essential elements:

Energy source, that provide the power required to the actuator during the work time

Transducer, that is the core of an actuator, is defined as "a device, which *transforms energy from one domain into another*" (Rosenberg and Karnopp, 1983) and specifically, in the case of actuators, from electricity (but not only) to mechanical power.

Motion converter, that adapts the force and the velocity produced by the transducer in order to make them usable by the system

These three components are not always all included in an actuator and combining them 4 classes of actuators can be defined (Figure 2.31):

Effector: in this case only the transducer, powered without limitations, is present and it is directly coupled with the final user. Some examples of this class are electromechanical driver with high frequency response as acoustic diffuser or some direct-drive haptic interfaces.

Motor: composed by transducer and motion converter, but without power source (thus without power source limitations). This is the most common actuator, particularly used where direct actuation is not suitable and broad energy is available.

Autonomous effector: an effector with an embedded source power, but without the possibility of external connections for energy supplying.

Autonomous motor: it is the complete system, where the transducer needs a motion converter for final usability and in the meantime it is constrained by an internal energy source. This is the most common configuration.

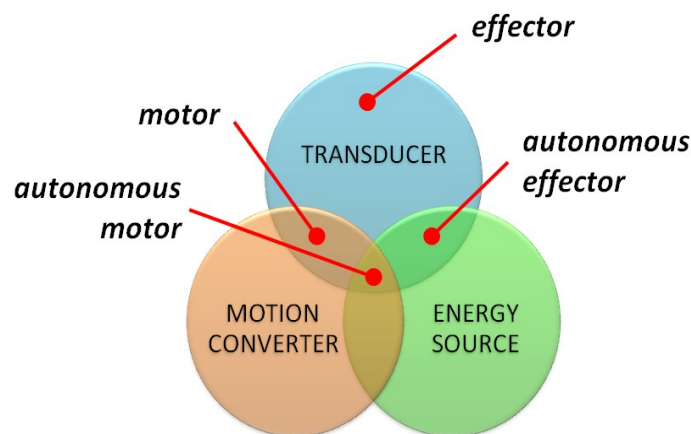


Figure 2. 31 Different kind of actuators that can be obtained by the combination of energy source, transducer and motion converter.

In order choose an actuator for a specific application some parameters have to be considered. These parameters allow a classification and a comparison between them on the base of their performances evaluation. In the follow the most important will be illustrated.

Stress, σ , is the typical force (F) per cross-sectional area (A) under which the actuator materials are tested, and **peak stress** is the maximum force per cross-sectional area under which a material is able to maintain position (also known as blocking stress). For most technologies, stress developed scales linearly with cross-sectional area (whose surface normal is parallel to the direction in which actuation is occurring).

$$\sigma = \frac{F}{A} \quad \left[\frac{N}{m^2} = Pa \right]$$

Strain, ε , represents the displacement ($l_f - l_0$) normalized by the original material length (l_0) in the direction of actuation. Typical strain is the strain that is often used in working devices, whereas *peak or max strain* is the maximum strain reported. The peak strain generally cannot be obtained when operating at peak stress.

$$\varepsilon = \frac{l_f - l_0}{l_0} \quad \left[\frac{m}{m} \right]$$

Strain rate is the average change in strain per unit time during an actuator stroke. Typically the maximum reported rate is given. The maximum strain rate is usually observed at high frequencies where strains are small.

Power density, P_v , is the power output (P_{out}) per unit volume (V) of actuator material and represents a measure of the rate of energy delivery at the mechanical port. Typically only the mass of the material itself is considered. Peak power density can be found from the maximum product of simultaneously measured stress and strain rate divided by density. Because of the interdependence of load and rate, peak power is in general less than the product of peak stress and peak strain rate normalized by density.

$$P_v = \frac{P_{out}}{V} \quad \left[\frac{W}{m^3} \right]$$

Work density, W_v , is the amount of work generated in one actuator cycle (W_{out}) normalized by actuator volume (V). It is very important to note that this does not include the volume occupied by electrolytes, counter electrodes, power supplies, or packaging, unless otherwise stated. These additional contributions to actuator volume do not always scale linearly with work output and therefore need to be considered separately. Also it is emphasized that the work density is not simply the product of peak stress and peak strain.

$$W_v = \frac{W_{out}}{V} \quad \left[\frac{W}{m^3} \right]$$

Time constant, τ , is the time taken for the output parameter of a first order system to reach 63.2% of its final value upon the application of a step input.

Frequency bandwidth, f , is the available bandwidth of an actuator defined by the “cutoff frequency”, that is the frequency at which a decay of 3 dB in the output velocity of the actuator is observed that corresponds to the frequency at which strain drops to half of its low frequency amplitude. Limitations on bandwidth and strain rate can result from a range of factors including speed of delivery of the input energy (e.g., RC charging time), rates of diffusion or heating, internal dissipation, inertia related effects including speed of sound, and kinetics associated with the energy transduction method.

Time constant and frequency bandwidth are related by the following expression:

$$f = \frac{1}{2\pi\tau} \quad [Hz]$$

Efficiency, η , is the transduction process of an actuator and is defined as the ratio of work generated (L_U) to input energy expended (E_i). The listed efficiency has not always been achieved in practice, and sometimes requires additional circuitry to attain. Ideally, actuators are lossless devices, and, thus efficiency in an ideal situation should be close to 100%. In practice, various different dissipative phenomena take place in the transducer or accompanying components, producing lower efficiency. Stored electrical energy and even thermal energy can in principle be recovered in order to improve efficiency.

$$\eta = \frac{L_U}{E_i} \left[\frac{J}{J} \right]$$

Electromechanical coupling refers to the proportion of input energy that is transformed into work, including external work done by the actuator and stored internal mechanical energy generated in the actuator itself. The values represent a best case. The coupling is not necessarily the same as the efficiency. In fact in a number of actuators the efficiency can be much higher than the coupling because input electrical or thermal energy can be recovered. The coupling is nevertheless important as it indicates how much energy in excess of the energy being converted to work must be shunted back and forth between the power supply and the actuator.

Cycle life is the number of useful strokes that the material is known to be able to undergo. Cycle life is often highly strain and stress dependent. Frequency dependence can arise due to dissipation and heating.

Elastic modulus, E , is the material stiffness (K) multiplied by sample length (l_0) and divided by cross-sectional area (A). Generally it is the instantaneous value that is reported, before any creep is induced. It is important as it determines the actuator's passive ability to reject load changes and disturbances, and along with the density and mass determines the frequency beyond which inertial effects become important. Once inertial forces become significant resonance may occur, and at still higher frequencies strains will decrease (typically with the inverse square of frequency).

$$E = K \frac{l_0}{A} \left[\frac{N}{m} \frac{m}{m^2} = \frac{N}{m^2} = Pa \right]$$

Mechanical work in common machines and appliances are most commonly gained through electromagnetic motors. However, some limitations of conventional motors, such as low power-to-mass ratios, low efficiencies, and the need to convert rotary to linear motion, allow opportunities for actuating materials in several applications. The use of actuating materials is an alternative strategy that may be important where conventional strategies fail.

Several classes of materials have been discovered that couple light, chemical energy, heat, a magnetic field, or an electric field to mechanical motion of useful magnitudes. These materials can exploit basically four kind of transduction mechanisms:

Fluid-mechanical transduction. Some traditional actuators (pneumatic and hydraulic actuators) convert the pressure of a fluid into mechanical energy, either rotational or translational. (section 2.2.2 and 2.2.3)

Thermomechanical transduction. In this energy conversion process, the input energy is in the thermal domain and the output energy in the mechanical domain. Several actuators can be developed by following this conversion scheme:

Shape Memory Alloys (SMA). In this type of actuators, the input thermal energy triggers a phase transition in the alloy, which results in the shape recovery of a previously deformed state. These actuators are discussed in detail in section 2.2.5.

Thermally active polymer gels. Some polymer gel actuators respond to thermal stimuli. These are included in the section 2.2.6.

Magnetomechanical transduction. These actuators establish an energy flow from the magnetic domain to the mechanical domain and vice versa. Again, several actuators can be developed, depending on various different transduction phenomena.

Electromechanical transduction. The energy in the input electrical domain is transformed into mechanical energy. In most of the following actuator technologies, the transduction process is reversible:

Piezoelectric actuators. The converse piezoelectric effect resulting from the interaction of an imposed electric field and electrical dipoles in a material results in a deformation. This deformation is used to drive the plant. The converse piezoelectric effect can be used directly or through geometrical transducer concepts. (section 2.2.4)

Shape Memory Alloys (SMA). These actuators have already been mentioned in connection with thermomechanical transduction. Thermal energy is usually supplied through resistive heating (Joule effect), and, hence, these can also be considered electromechanical transducers. (section 2.2.5)

Electro Active Polymers (EAP). Within the broad family of EAP actuators, dry type polymers directly exploit Maxwell forces or the electrostrictive phenomenon to obtain mechanical energy from electrical input energy. In addition, some ionic EAPs (also referred to as wet EAPs) are triggered by small electric fields. (section 2.2.6)

Physical principles

Many actuators are based on the same actuating principle, so, in order to minimize redundancy, in this section a brief but exhaustive explanation of the physical principles used for actuation will be given.

Piezoelectric effect

Certain materials have the characteristic of generating an electric potential when deformed by an external force. This characteristic is called direct piezoelectric effect. It naturally exist in symmetrical crystals, such as quartz and tourmaline. Piezoelectric material also has an inverse piezoelectric effect: when a voltage is applied to a material with piezoelectric property, it will produce a expansion or contraction movement. Figure 2.32 is an illustration of inverse piezoelectric effect.

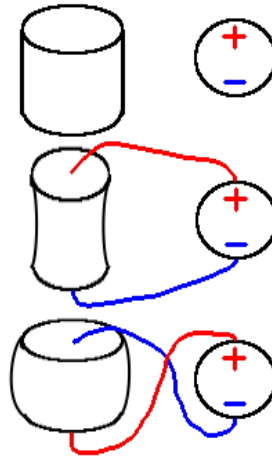


Figure 2. 32 The reverse piezoelectric effect.

The inverse piezoelectric effect, is the basis of piezoelectric actuators.

Maxwell stress effect

The Maxwell stress effect is defined by the Columbian attraction between two electrodes at different voltage spaced by a dielectric material. The applied electric field generates a charge imbalance between the electrodes that tend to move closer, squeezing the dielectric material. This effect is negligible in the case of rigid dielectric materials, but very remarkable in the case of soft materials.

Electrostrictive effect

Electrostriction is a property of all electrical non-conductors, or dielectrics, that causes them to change their shape under the application of an electric field. The cause of this dimensions changing is the randomly-aligned electrical domains within the material. When an electric field is applied to the dielectric, the opposite sides of the domains become charged and attract each other, reducing material thickness in the direction of the applied field (and increasing thickness in the orthogonal directions due to Poisson's ratio). The resulting deformation is proportional to the square of the polarization. Reversing the electric field does not affect the direction of the deformation (unlike piezoelectric effect).

This effect and the previous one dictate the mechanical performance of quite all the Electroactive Polymers

2.2.2 Hydraulic Actuators (IIT)

Hydraulic actuation has a long and successful history dating back to ancient times when the power of water was used to turn wheels and exert forces. In more recent times hydraulic actuators have used pressurised oil, typically at 5-300bar, due to its low compressibility. Hydraulics can be used in both linear and rotary configurations, Figure 2.33. In both cases the principal of operation is the same with the pressurise oil being used to exert a force on a cylinder head or vane which converts the energy into motion. The general linear mechanism consists of a piston encased in a chamber with a piston rod protruding from the chamber. The piston rod serves as the power transmission link between the piston inside the chamber and the external world. There are two major configurations of this actuator: single or double action. For the single action configuration, it can exert controllable forces in only one direction and uses a spring to return the piston to the neutral or un-energized position.



Figure 2. 33 Conventional Linear and rotary hydraulic actuators.

In the case of rotary actuation, the power unit is a set of vanes attached to a drive shaft and encased in a chamber. Within the chamber the actuator is rotated by differential pressure across the vanes and the action is transmitted through the drive shaft to the external world.

Due to the high pressures involved and the incompressibility of the fluid resultant forces are high as are system bandwidths. However there are drawbacks to the actuator most notably the high mass resulting from the need to use high strength materials due to the high pressures involved, however the systems still attain high power to weight ratios. The system is also difficult to seal leading to oil leakage, which make it unsuited to many indoor environments. Additionally, the hydraulic fluid is flammable and pressurized so leaks could pose an extreme hazard to equipment and personnel. This adds the undesirable aspect of additional maintenance to maintain a clean sealed system. Other drawbacks include lags in the control of the system due to the transmission lines and oil viscosity changes from temperature.

Table 2. 4 summarises the main characteristics of a Hydraulic actuation system.

Table 2. 4 Main Characteristics of Hydraulic Actuation

Characteristic	
Basic System	Power (Pump, regulators), pipes, Valves, Actuators, Cooling system
Required components	
Size of components	Bulky
Weight of components	Big
Working medium	High Quality Oil or Water Based Solutions,
Actuator Type	Rigid Metal Cylinder, Hydraulic Motor
Input Power Supply	24V-380V, 5-300bar
Electronic drivers complexity	Simple
Efficiency	Less than %60
Force/Power to Weight Ratio	High
Safety of Operation	Low
Temperature Sensitivity	High, Heat exchangers can be used to reduce the effect
Environmental Friendly	No

Possibility for miniaturizing	Low
Load Variation sensibility	Low
System Bandwidth	High
System Stiffness	High

2.2.3 Pneumatic Actuators (IIT)

Pneumatic actuators usually come in a form of a traditional pneumatic cylinder. The principle of operation in the traditional pneumatic cylinders is similar to that of the hydraulic cylinders. The main difference is that pneumatic actuators use a compressible gas (i.e. air) as the medium for energy transmission instead of oil. As a result pneumatic power is a simplified and cleaner version of hydraulics as it uses fluids in gaseous form instead of liquid. This makes the pneumatic system more passively compliant than the hydraulic system. With pneumatic actuators, the pressure within the chambers is lower than that of hydraulic systems resulting in lower force capabilities. Additionally, installation, operation and maintenance is easier and cost is lower compared to hydraulics. Due to the medium which is compressible, control of motion is handled differently than hydraulics. While compliance is desired in a hydraulic system, force and speed are wanting in a pneumatic setup therefore the methodology to get these performance aspects is left to ingenuity of software control and nozzle design. Apart from the traditional form of rigid metal cylinder, the pneumatic actuators regularly also appear in form of non rigid structures such as rubber bellows, flexible tubes or muscles.

Pneumatic bellows

Pneumatic bellows offer a simple alternative to traditional pneumatic cylinders and they have the advantage that they have no moving parts (Y. Hayakawa et al., 1993). The actuator is made of a flexible tube that does not deform in a radial direction but is able to be contracted axially through the collapsing of concertinas located along its length. The usual mode of operation is to have the bellows compressed to its minimum length and then apply a pressurised air source to the inside of the actuator. In an attempt to reach its minimum energy state i.e. the position with maximum actuator volume, the bellows expands longitudinally and in so doing generates an expansive force. When the internal pressure is released the force that the actuator has moved causes the bellows to again become compressed (passive return), or alternatively by actively evacuating air from the bellows a contractile force can be produced (active return).

Unlike conventional pneumatic cylinders where a seal is required between the moving cylinder head and the actuator body, a bellows has no moving parts and therefore such seals are not required. Linear motion control of a bellows actuator, however, can be problematic due to its non-rigid structure. Consider the example shown in Figure 2.34 where a bellows is being used to generate an expansive force F applied to the block. As the bellows attempts to reach its minimum energy state (maximum volume) instead of simply extending in length it may buckle as can be seen and bellows expansion occurs but no useful force is applied to the block. To overcome this problem some form of guide rail or rod is used to prevent this buckling occurring much like a standard pneumatic cylinder.

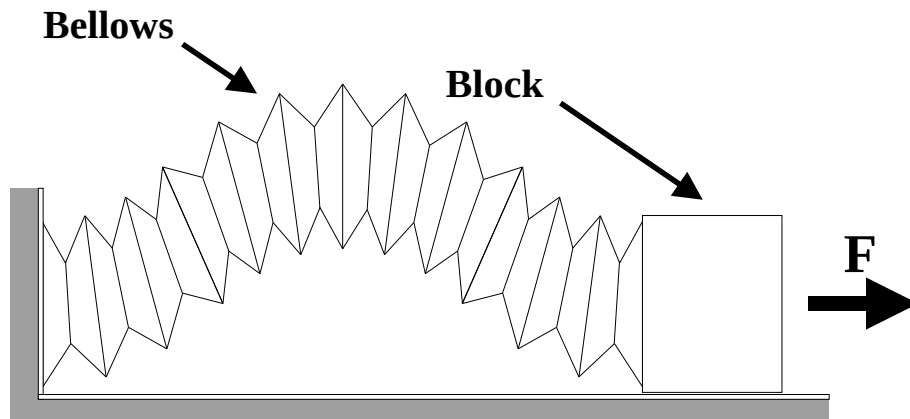


Figure 2. 34 Pneumatic bellows used as an actuator.

Pneumatic Group Actuators/Continuum Actuator

Another type of flexible pneumatic actuator is the Pneumatic Group Actuator or Continuum Actuator, Figure 2.35. The actuator is composed of multiple flexible silicon tubes, mounted between base plates, that when pressurised elongate. There are three tubes between each of the plates which means that if a single tube in a group is pressurised it will elongate whilst the others remain at their resting length, this results in a curvature of the actuator as seen in the figure.

A very similar system known as a Continuum Actuator or the 'Elephants Trunk' (J.B.C. Davies et al., 1998) use three parallel metal bellows to achieve the same functionality. Unlike most other forms of actuator these systems can be used to create mechanically simple manipulators without the need for a large numbers of additional components. The reason for this is that the system generates motion by 'element deflections' rather than through the use of links and joints, that is to say the actual body of the actuator forms the mechanical structure of the manipulator.

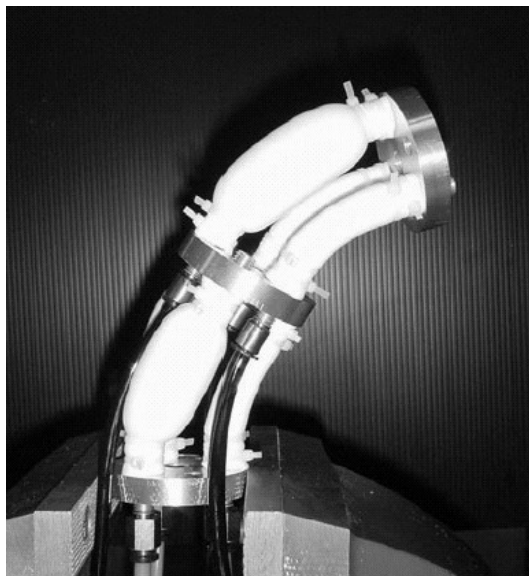


Figure 2. 31 Pneumatic Group Actuators.

Pneumatic Muscle Actuator

Another type of non rigid pneumatic actuator is the McKibben muscle or pneumatic Muscle Actuators (pMA), Figure 2.36 (H F Schulte, 1962; K Inoue, 1987). The pneumatic Muscle Actuators (pMA) is constructed as a two-layered rubber/nylon cylinder. It consists of an inner layer made from butyl rubber tubing, with two end-caps forming the termination connectors to seal the muscle cylinder. These end-caps can be made of nylon, aluminium, brass, steel or indeed any material depending on the specific

operational requirements. One of the end-caps is sealed, closing the muscle cylinder, while the other acts as the air input conduit. Around the rubber tubing there is a flexible outer sheathing formed from high strength interwoven (but not bonded) double helix nylon fibres. The sealed chamber acts as a pressurised containment unit. The flexibility of this structure means that it can be stretched or compressed without damage, but at the same time this outer shell prevents the delicate rubber liner from over-inflating and rupturing. To prevent energy losses due to the initial expansion of the rubber liner, the rubber layer has a diameter comparable with the rest diameter of the flexible wall. The muscles are available in a number of sizes providing variable force potential and actuator displacement ranges. Muscles lengths can range from under 10cm to 400cm and diameters range from less than 10mm -70mm.

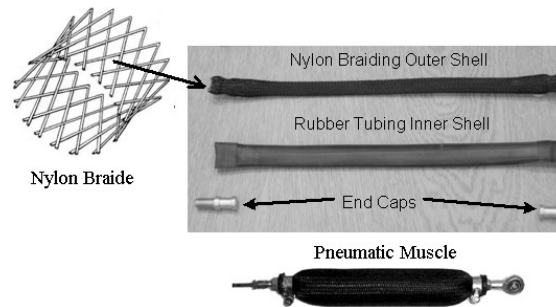


Figure 2. 36 Pneumatic Muscle actuator.

Error: Reference source not found reports on the main characteristics of the Pneumatic actuation system.

Table 2.5 Main characteristics of the pneumatic actuation

Characteristic	
Basic System Required components	Compressor, Pipes, Filters, Valves, Actuators, Dryers
Size of components	Average
Weight of components	Average
Working medium	Air, Nitrogen
Actuator Type	Metal Cylinder, Rubber based expandable bellows or tubes
Input Power Supply	12V-380V, 0.2-30bar
Electronic drivers complexity	Simple
Efficiency	Less than %40
Force/Power to Weight Ratio	Medium
Safety of Operation	Medium
Temperature Sensitivity	Medium, usually not an issue since the medium is exhausted to the atmosphere
Environmental Friendly	Yes
Possibility for miniaturizing	Medium
Load Variation sensibility	High
System Bandwidth	Low
System Stiffness	Medium

2.2.4 Piezoelectric Actuators (UZH)

Piezoelectric actuator is a device that uses the piezoelectric effect to convert a voltage applied to it into mechanical movement. It normally consists of a number of thin sheets of piezoelectric elements, so that a large amount of displacement can be induced by a low driving voltage (Figure 2.37).

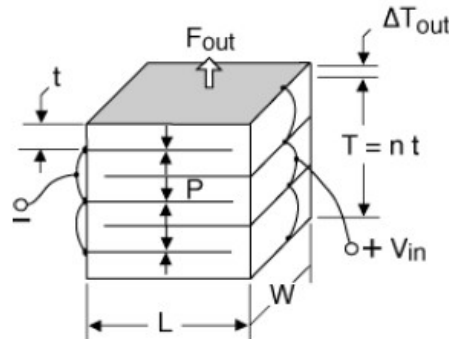


Figure 2. 37 Stack of piezoelectric elements, that amplify the displacement maintaining low the required voltage.

All devices using one of the piezoelectric effects can be considered as piezoelectric actuators according to the broadest meaning. The following classification can be applied on the base of effects and uses.

- (1) Sensors for dynamic force and electric generators for vibration energy harvesting based on direct piezoelectric effect.
- (2) Vibration, sound and ultrasound generators that use the inverse piezoelectric effect They offer deformations in the range of 300 ppm with field of 600 kV/m. This field requires high voltages, except at resonance.
- (3) In a restricted sense, piezoelectric actuators refer to controllable actuators using multi layer piezo ceramics to make solid-state actuators using electrically-induced deformations. The multi layer piezo ceramics reduce the required voltage outside resonance. The maximum electric field can reach up to 2 MV/m with a voltage of less than 200V, leading to an active deformation of about 1000 ppm.

Some of its typical performances are summarized in Table 2.6.

Table 2. 6 Typical performances of piezoelectric actuators.

Characteristic	
Power consumption	300-1000 mW
Operating temperature	up to 100 °C
Vibration frequency	up to 100 kHz
Strain	Commercially available materials offer strains of about 0.1%; state-of-the-art materials have about 0.2% strain output, and emerging single-crystal ceramics promise up to 0.5% strain, but may have a reduced modulus of elasticity
Driving	need high voltage and high frequency driving circuitry
Work density	excellent
Specific power	109,000 W/kg (a typical value)
Strain rate	Depends

Elastic modulus of piezoelectric element	40 GPa
Efficiency	up to 68%

Piezoelectric actuators have the advantages of high actuating precision and rapid response speed. Typical applications of this kind of actuators are high precision positioning, piezoelectric buzzes, inkjet heads in printers, ultrasonic motors, and, more common in everyday life, telephone receivers. They also can be driven in very small scales enabling them to be used in mini robots and they can be embedded in laminated composites or injection molded plastics.

Meanwhile, they can be designed in such a way that use as piezoelectric actuators and sensors at the same time. For example, THUNDER (Thin-layer composite unimorph ferroelectric driver and sensor) actuators developed by NASA at the Langley Research Center is commercially available. One limitation is the difficulty to use it in "instrumentation grade" sensors since piezoceramics has non-linearities and hysteresis. But for typical closed-loop active structural control systems, these factors can be effectively ignored.

Potential application in OCTOPUS

It possibly can be embodied in octopus arm prototype to form the local bending motions.

2.2.5 Shape Memory Alloy Actuators (IIT)

Shape Memory Alloys (SMA) actuators usually consist of a wire made from a metal such as titanium-nickel which undergo a reversible material deformation when heated. As the material is heated this causes a reduction in the wire's length, while the removal of heat means that the material cools and returns to its original length. This unusual behavior is based on the reversible transformation from the martensite into the austenite phase of a shape memory alloy. Martensite, the low temperature phase, is relatively soft whereas Austenite, the high temperature phase, is relatively hard. Consider for example the highly simplified two-dimensional representation of the material's crystalline arrangement shown in Figure 2.38

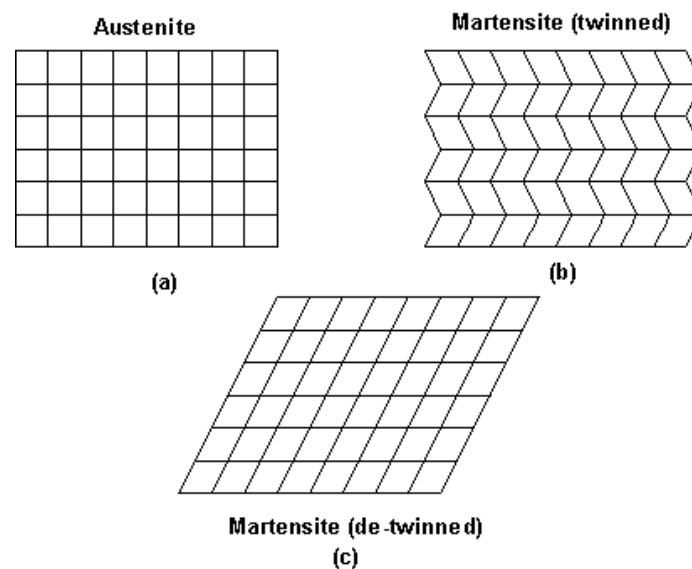


Figure 2.38 Shape Memory Effect and the crystalline Arrangement.

Each box represents a grain of material with its corresponding grain boundaries. The grains form a heavily twinned structure, meaning they are oriented symmetrically across grain boundaries. The

twinned structure allows the internal lattice of individual grains to change while still maintaining the same interface with adjacent grains. As a result, Shape Memory Alloys can experience large macroscopic deformations while maintaining remarkable order within its microscopic structure.

From the different the Shape Memory Alloys that have been discovered so far, Nickel-Titanium (Ni-Ti) has proven to be the most flexible and beneficial in engineering applications. This alloy has greater ductility, more recoverable motion, excellent corrosion resistance and stable transformation temperatures (Waram, 1993). Apart from the small size (the diameter of wire can be as small as few microns) and the high forces developed the SMA actuators have also some other advantages. They can be used as direct linear drives requiring no force or motion amplification. All the above allow the miniaturization of the actuation system in order to overcome space limitations. In addition, the voltages levels necessary for the operation of these actuators is low requiring simple power supplies and driving (Grant, 2000).

However despite all the above advantages these actuator have low bandwidths due to the slow cooling time of the material although this can be improved by the use of forced cooling. They exhibit nonlinear behavior and wide hysteresis. The wires also have relatively small displacements (typically 5-8%). Other than the above actuation fatigue over repetitive cycles remains an open research issue. Shape memory actuators are often used in bundles (De Laurentis, 2002) of parallel wires as greater forces can be produced without increasing the time required for individual wires to cool.

Table 2. 7 Main Characteristics of the SMA Actuation.

Characteristics	
Basic System Required components	Power supply, current driver, SMA wire, cooling system
Size of components	Small
Weight of components	Small
Working medium	Shape memory effect, wire deformation
Actuator Type	Single metal wire or bundles
Input Power Supply	2V -
Electronic drivers complexity	Simple
Efficiency	%5
Force/Power to Weight Ratio	Medium
Safety of Operation	High
Environmental Friendly	Yes
Possibility for miniaturizing	High
Actuator Strain	5-8%
System Bandwidth	High
System Stiffness	Medium, can be adjusted in antagonistic configurations

2.2.6 Electro Active Polymer Actuators (SSSA)

Electro Active Polymers are an emergent class of materials that have the capability to modify their dimensions and shape when an electric stimulus is applied. This class of polymers can be divided into 2 major group: the first one undergo to dimensional change in response to an electric field (electronic EAP); the second one is the group of materials that needs the presence and movement of ions to make actuation possible (ionic EAP).

Electronic (dry) EAP

Dielectric elastomers

Dielectric elastomer actuators (DEAs) are basically elastomeric or rubber materials which are incompressible but highly deformable. An electric field is applied across the sheet thickness through two compliant electrodes. The electrostatic interaction between the two electrodes with opposite electric charge causes a significant stress in the dielectric, known as Maxwell stress, which can compress and elongate the dielectric material at high strain rates (Figure 2.39). This stress is proportional to the square of the applied field and to the dielectric constant. For practical use of dielectric elastomers, low modulus (~1 MPa) and high dielectric strength (>100 MV/m) are required to reach strains of up to 380% at high applied fields. More typically, strains are 10-100% (very high in respect to the 20% observed in our skeletal muscle).

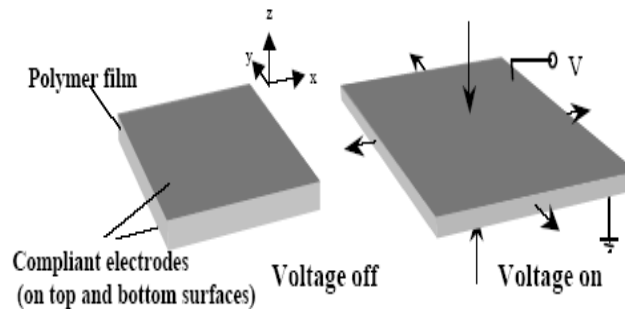


Figure 2. 39 Functional scheme of a dielectric elastomer: the two compliant electrodes tend to move closer when a voltage is applied thanks to the Maxwell stress effect.

The elastomer employed is often a silicone, acrylic or polyurethane elastomer, sometimes loaded with heavy particles such as TiO₂ to increase the dielectric constant. The compliant electrodes can be made of conductive pastes, spin-coated conductive rubbers, sprayed graphite particles, or superelastic CNT sheets. The key to large strain is to make both the electrodes and the dielectric elastomer highly compliant without sacrificing dielectric strength and conductivity.

Electromechanical coupling is typically 60-80% for acrylic and up to 90% for silicone elastomers. The large strains resulting from the actuation lead to high work per unit volume per stroke in these actuators (the 3.4 MJ/m³ maximum is 400 times that of our muscle). The electrostatic energy stored within a dielectric elastomers increases in proportion to the field squared, while the mechanical energy density is roughly proportional to the fourth power of field. As a result, mechanical energy density and electromechanical coupling are maximized by operating close to breakdown and using materials with the maximum dielectric strength. Dielectric strength can be increased by prestraining the elastomers, which also serves to amplify strain.

Dielectric elastomers can sustain a frequency bandwidth up to 1 kHz for some kind of materials due to the charging time that acts as limiting factor in the rate of response.

Even if high voltages are required, the currents they produce are very low because of their capacitive nature.

Since it is the field in the dielectric and not the voltage that drives the actuation, it is possible to maintain the same field while reducing the required voltage by using thinner sheets of elastomer or by increasing dielectric constant. But, using dielectric materials, it is worth noting that the high electric field required for operation can lead to a dielectric breakdown that is rapidly reached if the thickness or the dielectric strength are too low.

Despite these technological limitations dielectric elastomers are one of the most studied polymer actuators and numerous applications are being developed, mainly for robotics applications.

Ferroelectric polymers

Ferroelectric materials, like ferromagnets, have dipoles that can be aligned producing permanent dimensional changes in response to an applied electric field (electrostrictive effect). Inorganic ferroelectrics, such as barium titanate, can reach a deformation on the order of 0.1%, much less than ferroelectric polymers, which can strain by an incredible 5-10%. Like inorganic piezo- and ferroelectrics, ferroelectric polymer actuators are fast and have a high work density (1 MJ/m³).

A key disadvantage of ferroelectric polymers is that there is substantial hysteresis. A large field must be applied in the opposite direction of the initial field in order to reverse the polarization, and substantial energy is dissipated.

To date, the best actuator performance has been obtained from poly(vinylidene fluoride)-based (PVDF) polymers copolymerized with trifluoroethylene, forming P(VDF-TrFE). The electronegativity of the fluorine causes high polarity in the polymer backbones. Field-driven alignment of polar groups produces reversible conformational changes that are used for actuation, as depicted in Figure 2.40. The application of a field perpendicular to the chains leads to a transition between the nonpolar (alpha phase) and polar (ferroelectric beta phase) forms. The result is a contraction in the direction of polarization and an expansion in the other two normal directions. Usually, this transition is facilitated adding a small mass fraction of a bulky monomer such as chlorofluoroethylene (<10%) to the P(VDF-TrFE), in order to disrupt long-range order. The imperfections are used to bring the Curie point below room temperature, such that a nonpolar, paraelectric phase dominates at normal operating temperatures. The result is an effective elimination of domains and of hysteretic behavior that is a characteristic of ferroelectrics. The resulting material is known as a relaxor ferroelectric. Strain is at a maximum at stresses of ~20 MPa, and electromechanical coupling reaches 0.42.

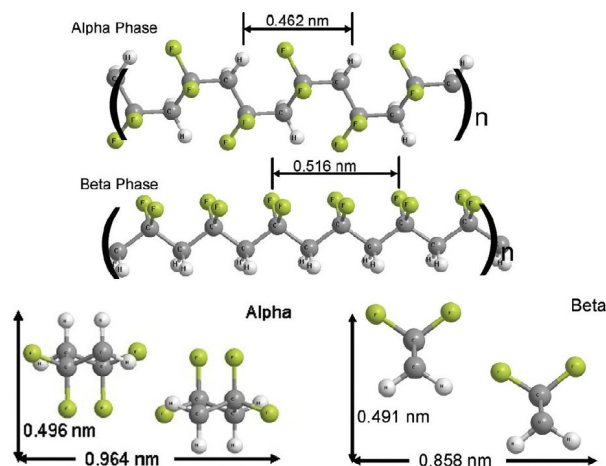


Figure 2. 40Ferroelectric alpha phase and beta phase: the transition between them can be reached applying an electric field perpendicular to the chains that leads to a contraction in this direction and an elongation in the normal directions.

The elastic modulus of the ferroelectric relaxors (0.3-1.2 GPa) is 1000 times higher than in DEAs, the dielectric constant is ~20 times higher, and the dielectric strength is similar. Overall, this leads to smaller strains, but similar energy densities (~ 1 MJ/m³) and electromechanical coupling.

Fields and voltages are very high (~100 MV/m, >1 kV), but, as in dielectric elastomers, increasing dielectric constant and reducing thickness are options for lowering the voltage. In general, polymers with high polarizability associated with a large (and preferably fast) conformational change in the polymer backbone are desirable.

Electrostrictive graft elastomers

The graft elastomer contains flexible backbone chains that have side chains, called grafts. Neighbouring backbone grafts physically cross-link, forming crystal units. Figure 2.41 illustrates the graft elastomer structure.

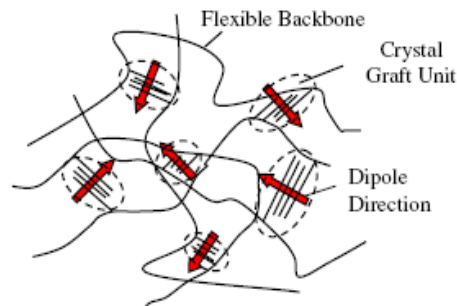


Figure 2. 41 Illustration of a graft elastomer structure: flexible backbones are connected by crystal graft unit with a dipole moment that can be driven by external electric fields.

The flexible backbone chain and the crystal graft unit consist of polarized monomers, which contain atoms with electric partial charges, generating dipole moments. Upon application of an electric field to the polymer, force is applied to each partial charge. Each dipole moment consists of two partial charges, each with the same magnitude, but one is in positive direction and the other is negative. Therefore, two forces applied to the two partial charges of one dipole moment would have the same magnitude but would point in the opposite direction, forming a force moment. Rotation of the dipole moment is induced by the force moment (Figure 2.42).

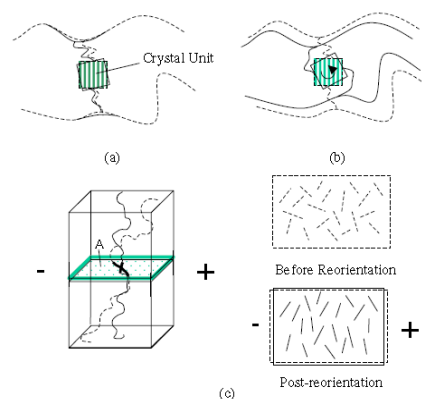


Figure 2. 42 A crystal unit connecting to polymer backbones (a) that can be induced to rotate by an external electric field causing the two polymer chains to move closer (b); Reorientation of backbone chains and dipole moments of polarized monomers (c).

At rest, monomer dipole moments of backbone chains are randomly orientated, canceling each other out. The applied electric field induces the rotation of the whole unit. Both local backbone reorientation and crystal unit rotation induce deformation. In addition, local reorientation of backbones and rotation of crystal units generate a second electrical field, inducing an additional strain due to the Maxwell effect.

Applied fields on the order of 10 MV/m are needed to induce strains reaching 2.5%, and provide an elastic energy density of ~ 0.5 MJ/m³. These results are obtained using a chlorotrifluoroethylene and trifluoroethylene backbone with P(VDF-TrFE) polar sidechains, producing a comparatively stiff matrix ($E = 0.6$ GPa). Fields are lower than those required for relaxor ferroelectrics, but so are actuator strains. Because of the size of the polar grafts, actuation rates are lower than for relaxor ferroelectrics.

Liquid crystal elastomers

Liquid crystals are known to change phase and orientation under the influence of an electrostatic force.

By incorporating mesogens into a compliant polymer backbone or as side chains, field-induced changes in phase can be used to produce actuation (Figure 2. 43). 4% of electrostrictive strains have been obtained at 133 Hz using field amplitudes of 1.5 MV/m on a thin sample of 75 nm.

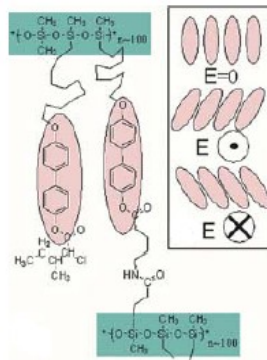


Figure 2. 43 Structure of a liquid crystal elastomer: the polymer backbone (green rectangles) are cross-linked by mesogens (pink ovals) that can be oriented by external electric field (right rectangle).

The modulus of these polymers is low, and the combination of low modulus and relatively low actuator strains leads to low work density. Work density can be improved by using a stiffer polymer (2% strains at 25 MV/m with a work density of 0.02 MJ/m³), but this has so far resulted in lower bandwidth. This performance still does not match that of high performance relaxor ferroelectrics, but investigations are still at an early stage. Minimizing dielectric loss is important for high-frequency operation in liquid crystal elastomers, as in other field driven actuators, since high loss reduces efficiency and leads to heating and failure.

Ionic (wet) EAP

CNT actuators

Carbon nanotubes, CNTs, come in two structural configurations: single-walled CNTs (SWNTs) can be thought of as a single layer of graphite (called graphene) rolled into a cylinder of nanometre diameter (Figure 2. a) with a length about 1000 times their width. Multi-walled CNTs (MWNTs) are obtained from nested SWNT structures which in turns are developed from graphene sheets (Figure 2. b).

Individual SWNTs or very long MWNTs have exceptional mechanical properties. The tensile modulus of SWNTs (640 GPa) approaches that of diamond, while their tensile strength is thought to be 20-40 GPa, about ten times higher than any other type of continuous fibre.

While mechanical properties in this range are observed for individual SWNTs, those observed for assemblies of these nanotubes in nanotube yarns and sheets are much lower, which restricts the performance of actuators based on nanotube yarns or sheets.

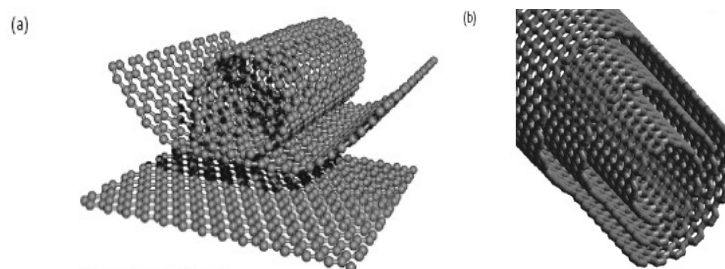


Figure 2. 44 Single walled carbon nanotube (SWNT) with rolling graphene sheets (a) and a multi-walled carbon nanotube (MWNT) (b).

The actuation principle of operation of CNTs is based on the use of these structures as electrodes in electrochemical supercapacitors.

At high levels of charge injection into CNTs, the predominant cause of actuation is electrostatic, as with DEAs. However, the electrostatic forces are repulsive interactions between like charges injected into the nanotubes, rather than between two electrodes. A voltage applied between an actuating nanotube electrode and a counter electrode (usually another CNT), both dipped in an ion containing solution, leads to charging (Figure 2.45 a, b)

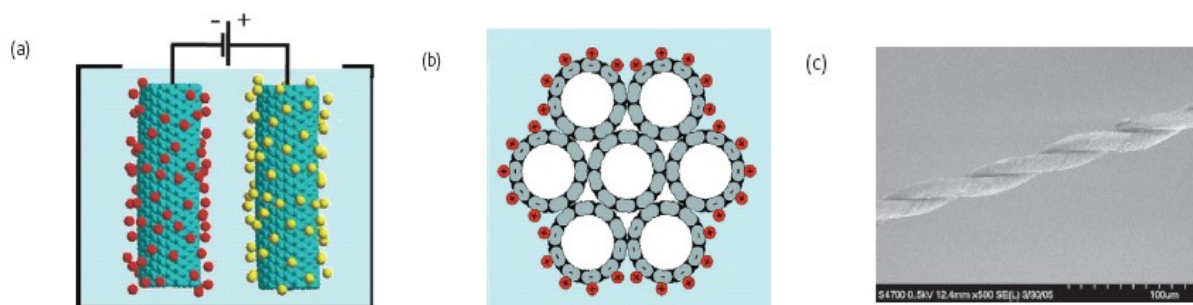


Figure 2. 45 Charge injection driven by electric field in two SWNTs (a) and in a bundle of SWNTs where the charges are injected at the external surface (b); example of a MWNT yarn (c)

Electrostatic repulsive forces between like charges on the CNTs work against the stiff carbon-carbon nanotubes bonds to elongate and expand the nanotubes, though quantum mechanical effects can predominate over electrostatic forces at low levels of charge injection. Apart quantum mechanical effect, quantum chemical effect and electrostatic double layer effect (that is the most predominant) result in expansion of the CNT structure too.

Actuation is generally achieved in films or yarns (Figure 2.45 c) composed of many nanotubes. The response times is on the order of 10 ms, with effective strain rates of 19%/s and effective power-to-mass ratios of 270 W/kg. The achievable response rate decreases with increasing nanotube yarn or sheet thickness, increasing interelectrode separation, and decreasing electrolyte ionic conductivity.

Work densities in CNT fibers and yarns are ~ 1 MJ/m³ (as in DEAs and ferroelectric polymers), as calculated from elastic modulus and strain. The energy densities thought to be achievable for individual nanotube actuators are unmatched by any actuator technology. Coupling is presently <1%, likely the result of the tremendously large energy needed to deform individual nanotubes ($E = 640$ GPa) and the fact that this energy cannot presently be effectively used for actuation because of low bulk modulus ($E \sim 15$ GPa) compared with the individual nanotube modulus.

Strains are relatively small (<2%) compared with other polymer actuators (but an order of magnitude larger than found in typical piezoceramics).

Conducting polymers

Electron conducting polymers (CPs) are typically materials that present semiconducting behavior when undoped and conducting when doped with donor or acceptor ions. Doping is typically achieved chemically or electrochemically.

The mechanism of actuation is based on the dimensional changes resulting from electrochemical uptake or expulsion of ions and solvent (Figure 2.46). Depending on the conducting polymer/electrolyte couple used, electron insertion into one electrode can be accompanied by a volume increase as cations are inserted or a volume decrease as anions are removed. Similar processes can occur at the counter-electrode. Expansion appears to be primarily perpendicular to the polymer chain orientation for oriented polymers, suggesting to the first order that ions and accompanying solvent are slotted between chains, as shown in (Figure 2.46)

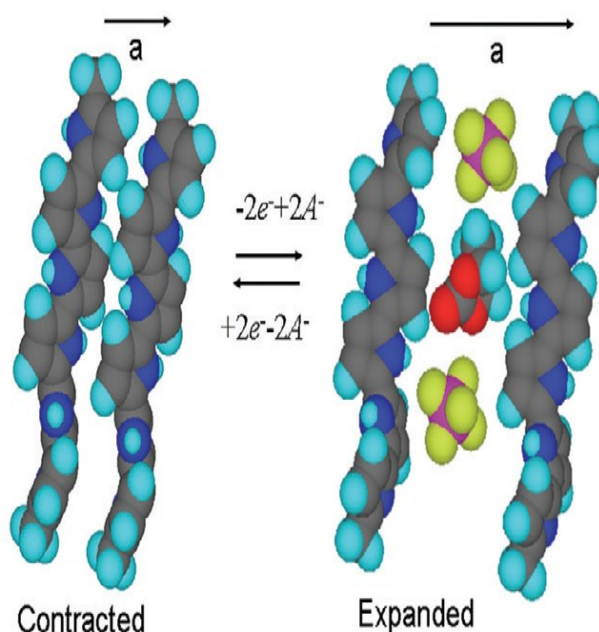


Figure 2. 46 Uptake and expulsion mechanism at the base of the dimensional change on CPs: a difference of potential forces ions to be intercalated between polymer chains.

The most used conductive polymer types are polypyrrole, polyaniline and polythiophene:

Polypyrrole, used in membranes, under different potentials can be polarized increasing its permeability by several orders of magnitude. The volume change is a consequence of the movement of very mobile small anions such as ClO_4^- present in the electrolyte solutions. The application of a voltage across the polymer matrix will result in the insertion and transfer of ions out of the polymer in order to maintain electroneutrality.

Polyaniline films, PANI, undergo volume changes as a consequence of its electrochemical oxidation/reduction under acidic conditions. The redox reaction occurs in conjunction with the flow of protons and electrons into the polymer matrix.

Polythiophene, PT, is the latest discovered material of this class, but it is receiving increasing attention because of its different actuation mechanism. For example, in polymethylthiophene intercalation of solvated anions or cations is not solely responsible for volume changes of the polymeric matrix. PT oligomers are relatively flat macromolecules and it is possible for these systems to form extended arrays in the solid state via π - π aromatic stacking interactions. Upon oxidation, these π - π aromatic stacking interactions are increased and consequently PT systems contract upon oxidation which in turn promotes large strains.

Strains are typically 2-10% and rates of actuation tend to be low (between 1 and 10%/s) because of the relatively slow transport of ions within the polymer, but it depends mainly on the size of the anions and cations, their solvation shell, the applied potential and the thickness of the polymer film.

High strengths (on the order of 100 MPa or higher), high typical stresses (\sim 1-34 MPa) and low voltages required (\sim 2 V) make this kind of materials very interesting as artificial muscles. Operating voltage can be increased in order to improve actuation rate, but without a proper control of the provided high voltage, a degradation in electrolyte and/or polymer can be caused. Work densities approach 100 MJ/m³.

CPs are virtually able to sustain forces at zero current consumption, that means they can constitute an effective blocking mechanism at a very low energy cost.

The advantage of conducting polymers over electronic EAPs is their low operating voltage. They feature higher strains and are cheaper than CNTs, but they are slower because of the actuation mechanism is based on ionic diffusion. Like CNTs, the electromechanical coupling is low (<1%) that makes for poor efficiency.

Ionic polymer-metal composites

This type of electrochemical artificial muscle employs a polyelectrolyte as an ion exchange membrane and metal thin layers as electrodes (Figure 2.47a). The polyelectrolyte is sandwiched between the two flexible electrodes, which interpenetrate the polyelectrolyte. When a voltage is applied between the electrodes, as shown in Figure 2.47b, the counterions tend to diffuse to the corresponding electrode, thus solvated mobile cations move toward the oppositely charged electrode, resulting in swelling near this negative electrode, shrinkage near the positive electrode. This migration causes also the deflection of the multi layered structure toward one of the metal electrode.

The polyelectrolytes usually used in IPMCs are Nafion (SO₃⁻) or Flemion (COO⁻) and thin layers of platinum or gold are commonly used as electrodes.

The ionic groups on the polymer backbone form hydrophilic clusters where the polar solvent and the mobile ions accumulate. These clusters are surrounded by hydrophobic regions composed of the nonpolar parts of the polymer. Channels through these hydrophobic regions enable ion and solvent transport necessary for actuation.

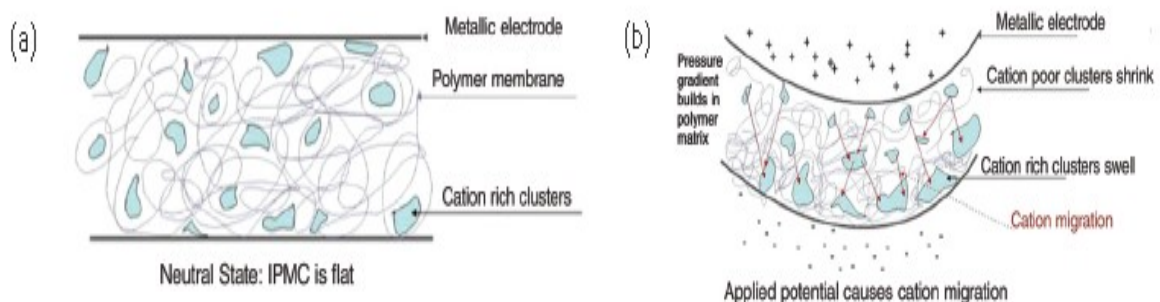


Figure 2. 47 Structure of an IPMC at rest (a) and when a voltage is applied (b): the cation migration, driven by the electric field, causes the bending of the structure.

Typical actuation strains are about 0.5 %, but can reach 3% under applied voltages of <7 V. Substantial bending in these cantilevertype actuators is caused when one side of the material contracts and the other expands (Figure 2.47b) but after an immediate response a relaxation phase occurs, limiting the bending capability. Reported stresses of actuation can reach 30 MPa.

IPMCs have been actuated at up to 100 Hz, with fast transport being achieved because of the ease of transport through the highly porous polyelectrolyte.

Active gels

Gel actuators are constituted by lightly cross-linked polymer networks that contain solvent.

The presence of the solvent inside the polymer network determines the physical properties (stiffness, shape etc) of the gel. By electrical means, polymer gels are able to swell by the uptake of solvent within the polymer matrix (Figure 2.48b) The actuation process is directly related to the ability of these structures to take up or expel the solvent in response to external stimuli. The gel expansion depends upon the rate of flow of solvent into the gel matrix. Electricity is not the only mechanism that can be used to change the equilibrium swelling, but also temperature, chemical, pH and light have been tested.

The main problem with gels is the same of all ionic electroactive polymers that have a response time that depends on ions diffusion. In order to achieve fast response times (less than 1 second) the diffusion distances should be of the order of 1 mm or less and the design of the device has to take into account its surface area to volume ratio.

However, the small dimensions, useful to increase actuation velocity, will limit the generated force (which is proportional to the volume or mass of gel) but this issue can be compensated by having many elements acting in parallel.

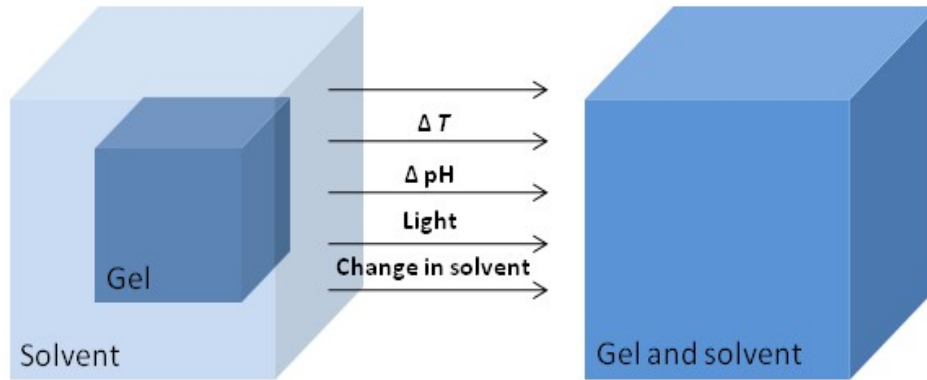


Figure 2. 48 External stimuli can activate mechanism of solvent uptake or expulsion.

Table 2. 8 Comparison among EAP technologies.

Actuator type	Strain (max) (%)	Stress (max) (MPa)	Work density (max) (J/cm ³)	Specific power (max) (W/g)	Max strain rate (%/s)	Elastic module (MPa)	Max efficiency (%)
Dielectric Elastomers	25 (>300)	1.0 (7.0)	0.01 (3.4)	0.5	>450	0.1 – 10	80
Ferroelectric Polymer	3.5 (10)	20 (45)	0.32 (1)	NA	>2000	800	40
Electrostrictive Graft Elastomers	2.5	NA	0.5	NA	NA	600	NA
Liquid Crystal Elastomers	2 (4)	0.12 (0.45)	0.02	NA	1000	100	75
Carbon Nanotubes	<2	>10	1	0.01 (0.27)	19	1000 (sheet) 10000 (fibre)	<1
Conductive Polymers	2 (20)	5 (34)	0.1 (1.0)	(0.1)	10	800 – 3000	1
Ionic Polymer - Metal Composites	0.5 (3.3)	3 (30)	(0.006)	0.003	3.3	50 – 100	1.5 – 3
Active Gels	30	0.2 (1.2)	NA	0.001	NA	<10	NA

3. Survey of Bio-inspired Soft Robots and Control Schemes (IIT, FORTH)

3.1 Introduction

Human limbs, which mostly inspired the design of robot manipulators, are discrete mechanisms with rigid links connected by single degree of freedom joints. Conceptually, rigid-links and low degree of freedom devices are able to meet the majority of manipulative and locomotive tasks. However, some creatures make use of alternative methods based on a very high degree of freedom backbones or made from soft structures.

Muscular hydrostats such as elephant trunks, mammal and tongues and octopus arms are soft structures that can bend, extend and twist. Such structures, exhibits unique capabilities including extremely enhanced maneuverability and ability of navigation through extremely complex paths. There are many examples in nature of mobile structures made from soft materials. The deep study of the morphology and functionality of soft systems can help to understand these unique structures and lead to new developments in robotics.

Focusing on the octopus arm in particular the potential of soft structures can be easily observed, however, the realization of such a robotic structure needs first to overcome significant challenges in all areas from the mechatronic system to the modeling and control. The following sections summarise some of the work done in the last years towards the implementation and control of robotic systems that try to emulate the biological soft structures.

3.2 Soft and Hyper Redundant Robots - Analysis and Control Challenges.

In the hard robots the position of each joint is often measured with a high-resolution encoders. Based on this information the mobility of a stiff robot can be easily studied by analysing the forward kinematics to accurately determine the shape and tip position of the robot. In the same way, the inverse kinematics in rigid structures can be used to determine the joint positions that provide a desired tip position. Using the forward and inverse models effective control techniques then can be developed to guide the motions of the rigid manipulator.

On the other hand the development of high-performance model-based control algorithms for continuum manipulators is a challenging problem for several reasons Due to the

continuous nature of these tentacle-like manipulators, mathematical models based on joint angles and link lengths do not supply an easy and physically realizable description of the manipulator's shape. As a result controlling but also sensing their motions and postures is a very challenging task. Part of the difficulty of the control problem arises from the fact that the sensing of the shape of the continues structure is not straightforward. Their body is a continuum structure, so exact measurement of the shape and tip position is difficult. This is directly related to the control problem. Deciding what to measure and how to use the information from the sensors to control the soft arm motion is also not clear. In the literature there have been several different approaches, which researchers have studied for the control of continuum robot manipulators as well many studies on how a real Octopus controls its arms. A survey of these techniques and studies are a reported in the following sections.

3.3 Octopus Arm Control

In the biological systems with rigid non redundant skeleton structures the execution of motions is initiated by a series of commands generated by the nervous system. These commands are send to the corresponding actuators which finally move the limb toward the target while constrained by the non redundant rigid skeleton structure. This is process is very different from that found in biological systems which are lacking of a rigid skeleton structure such as the hydrostats. Due the theoretical infinitive DOFs soft biological systems use more complicate procedures when controlling their motions. As an example Octopus arm movements provide an extreme example of controlled movements of a flexible arm with virtually unlimited degrees of freedom. The octopus arm movements while reaching a target were studied by Gutfreund (1996). In that study kinematic invariance in movement was examined in order to identify general principles of the motion planning control. Results from this study demonstrated that the octopus actuates its arm for locomotion, reaching for objects or searching by a wave-like propagation of arm stiffening that travels from the base of the arm toward the tip. Analysis of the bend-point path in 84 reaching movements suggested that the bend-point tends to move within a single plane in a simple, slightly curved path connecting the centre of the animal's body with the target location. The authors proposed that this strategy reduces the immense redundancy of the octopus arm movements and hence simplifies motor control.

In similar manner and according to studies from Gutfreund (1996) the coordination between different arms is performed by the Octopus in a similar way by propagating a bend in each of the arms. The arms can either move together or move one after the other.

Generally in soft structures, this propagating bend can be generated either passively or actively involving muscle contraction along the arm. Studies by Hochner (1995) indicated that the bend propagation in the octopus arm is associated with a wave generated by the octopus muscle activity. According to the constant volume constraint for muscular-

hydrostats, contraction of the longitudinal muscles on one side of the arm and simultaneous activation of the transverse muscles, to resist increase in arm diameter, should result in the formation of a bend, Kier (1985). Hence, a propagating bend would be generated by a wave of coordinated local contractions.

In other studies performed by Sumbre (2000a) results indicated that octopuses use strategies similar to vertebrates for transferring an object from one place to another. The octopus temporarily configures its arm into a stiffened, articulated, quasi-jointed structure based on three dynamic joints. Rotational movements around these joints bring the object to the mouth. Certain kinematic characteristics in octopus arm motion such as relationship among rotation angles along the arm remain invariant at the joint level rather than at the end-effector level, suggesting intrinsic control co-ordination. This may indicate that a kinematically constrained articulated limb may provide an optimal solution for precise point-to-point movements, Sumbre (2005b).

3.4 Soft and Hyper Redundant Robots Design

Robotic systems with a (very) large number of degrees of freedom, whose morphology is analogous to that of snakes, eels, elephant trunks and tentacles are called *hyper-redundant*, Chirikjian (1994, 1995, 1995a). Over the past several years, there has been a rapidly expanding interest in the study and construction of them. Some robotic implementations of hyper-redundant systems are typically serially-connected, multilink articulated mechanism where each joint of the mechanism has one or more actuated degrees of freedom, endowing these robots with quite complex shape-changing capabilities. Other realization of hyper-redundant manipulators may consist of truly flexible physical structures or of a soft structure with a large number of degree of freedom (HDOF); they are usually referred as continuum and serpentine robot mechanisms, respectively. They move by bending through a series of continuous arcs producing motion which resembles that of biological tentacles.

These capabilities of the hyper redundant robots are currently being investigated in the context of three main research directions, namely: (a) developing manipulator-like devices, mounted on either a fixed or a mobile base, in order to increase and enhance their reach, and (b) developing mechanisms which are capable of self-propulsion by these internal shape changes and (c) developing control techniques to effectively regulate the mobility and posture of these machines. The first direction is surveyed in Robinson (1999), Walker (2005) and Chiaverini (2008) and references therein. The present section focuses on the second and third directions.

Most of the robot devices, which are trying to mimic the soft continuous or hyper-redundant biological systems shown in Figure 1, are made from a combination of hard and soft materials, Figure 2 and 3.



Figure 1: Some of the organisms providing inspiration for the morphology and motion control of hyper-redundant or continuous locomotion and manipulation robots.

Inspiration for the development and motion control of hyper-redundant robotic locomotion systems stems from organisms such as snakes, eels, marine worms, nematodes, larvae, etc. (see figure below) with the prime biological paradigm being that of the snake, hence the prevalence of the term "snake-robot" in the literature.

The advantages associated with hyper-redundant locomotors were first investigated in pioneering studies by Hirose and Burdick, and include terrain adaptability, modularity and redundancy, as well as their potential for use as combined locomotors and manipulators, Hirose (1993, 2004), Ostrowski (1998). Such robots can have locomotive capabilities that outperform those of wheeled and legged robots in difficult-to-negotiate three-dimensional terrains. Moreover, their shape also allows sensors and actuators to be distributed down the length of the mechanism, enabling a greater range of interaction

between the environment and the mechanism, compared to conventional robotic systems. Examples of hyper-redundant locomotion robots are provided in the following figure 2.



Figure 2: Hyper-redundant robotic locomotion systems.

In a similar manner hyper redundant manipulators trying to replicate the morphology of the biological soft continuum manipulators such the elephant trunk or the Octopus leg

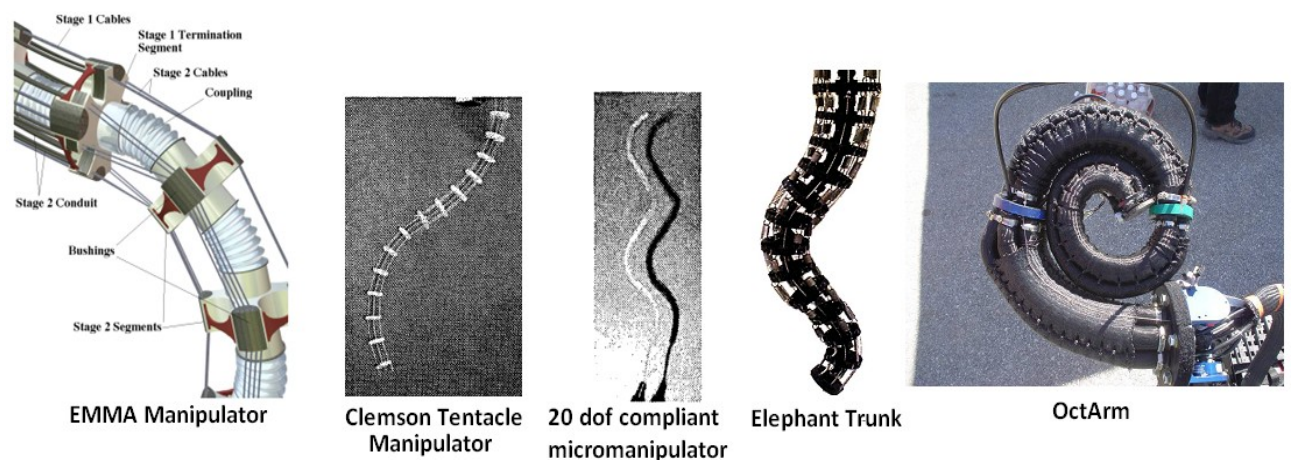


Figure 3. Hyper-redundant manipulator systems.

3.5 Soft and Hyper Redundant Robot Control

A. Gait generation (open-loop control):

Much like their biological counterparts, hyper-redundant robots can achieve a variety of locomotion gaits through appropriate coupling of their internal shape changes (typically lateral and/or transversal waves travelling along the body) to external motion constraints. The latter arise from the interaction with the locomotion environment, and, as illustrated in the following figure, may take the form of differential friction (associated with different friction coefficients in the normal and tangential direction of motion), Burdick (1993), Sato (2002) and La Spina (2007), non-holonomic constraints (typically associated with the use of non-slipping wheels) Krishnaprasad (2001), Tanaka (2006), Mori (2002) and Ostrowski (1998), or even push-point resistance contacts (snakes also routinely employ such obstacle-aided schemes for locomotion), Transeth (2008), Tanaka (2006), Bayraktaroglu (2006) and Hirose (1993).



Figure 4: Interaction with the locomotion environment through passive wheels [HF04] (left), blade-like modules generating differential friction [ST09] (middle), and via push-point contacts [TLGP08] (right).

The kinematics of hyper-redundant robots have been modelled by a number of different techniques, including formulations based on the Denavit-Hartenberg convention Poi (1998), backbone continuous curves Chirikjian (1990, 1991, 1994) and models exploiting non-holonomic constraints, for undulatory systems employing wheels Krishnaprasad (1994, 2001), Ostrowski (1996,1998) and Bayraktaroglu (2006).

The analysis of the dynamics of hyper-redundant robots has been based on variants of the Newton-Euler and Euler-Lagrange formulations, as well as on geometric mechanics (for an overview, see Transeth (2006, 2009)). It is worth pointing out that, in a number of cases, the developed analytical tools for hyper-redundant locomotors have much in common with early models employed to theoretically study the undulatory propulsion of organisms such as eels Taylor (1952), Lighthill (1975), snakes, Gray (1950), protozoa Gray (1955) and Holwill (1967), polychaete, Clark (1976) and worms Gray (1968), etc.

The undulatory robotics literature has mainly focused on mechanical design and open-loop control for gait generation. These gaits have been inspired by the gaits exhibited by snakes (lateral undulations, sidewinding, concertina, climbing, see figure below), worms, and caterpillars (for an overview, see Transeth (2006). For hyper-redundant systems whose morphology combines an elongated, articulating body with active lateral appendages (akin to legs or paddles), motion control schemes have been developed based on the gaits exhibited for salamanders [ICC05], centipedes and polychaete marine worms Sfakiotakis (2008, 2009).

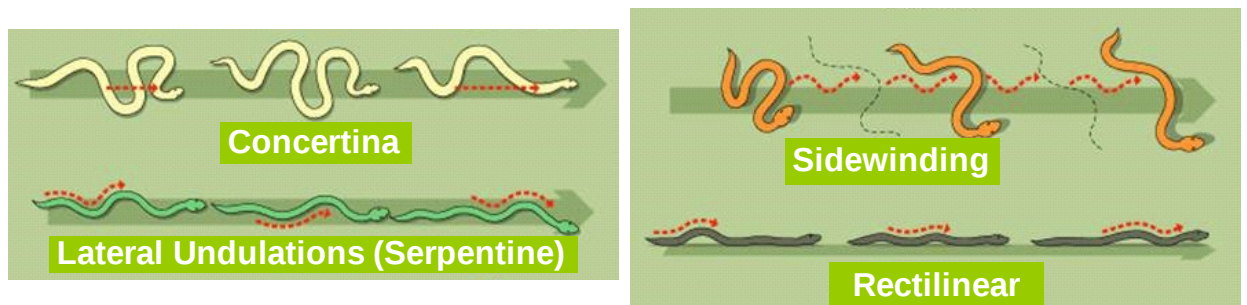


Figure 5: The main locomotion gaits of snakes.

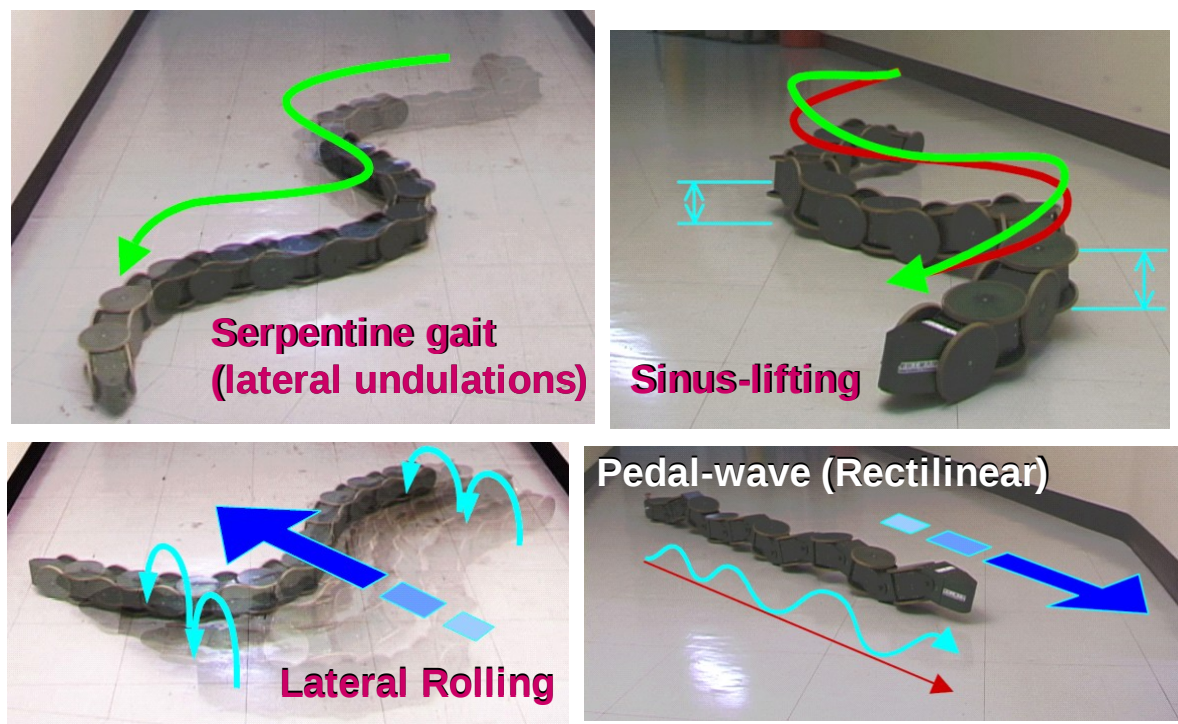


Figure 6: Different locomotion gaits, obtained with the ACM-R3 robot, featuring a total of 20 degrees of freedom Mori (2002).

By far the gait most widely studied is locomotion via lateral undulations (also referred to as *serpentine locomotion*), involving the propagation of a lateral travelling wave along the mechanism. In the great majority of robotic prototypes, both terrestrial and aquatic, retrograde (head-to-tail) waves are employed for forward propulsion. Recent investigations of robotic prototypes utilizing direct (head-to-tail) body waves for propulsion demonstrated the feasibility of such an undulatory mode and are presented, along with the relevant analysis, in La Spina (2007) and Sfakiotakis (2007, 2009). The travelling wave is generated (see figure below) via either prescribing explicit trajectories for the mechanism's joints, based on mathematical formulations of appropriate body curves (such as the serpenoid curve, see Hirose (1993), or via neural-control schemes, such as Central Pattern Generators Sfakiotakis (2007), Inoue (2007) and Arena (2006).

While most of the existing undulatory robots utilize passive wheels to realize serpentine locomotion, Hirose (1993, 2004), Ostrowski (1996,1998), Ma (2002), Krishnaprasad (2001), Yamakita (2003), Tanaka (2006), Mori (2002) and references therein , more recent work addresses robots which crawl on their underside, and do not rely on wheels, Sato (2002), Sfakiotakis (2007, 2008 and 2009), Worst (1996), and Lipkin (2007), as well as undulatory swimming prototypes Ayers (2000), McIsaac (2002), Hirose (2004), Crespi (2005) and Arena (2006).

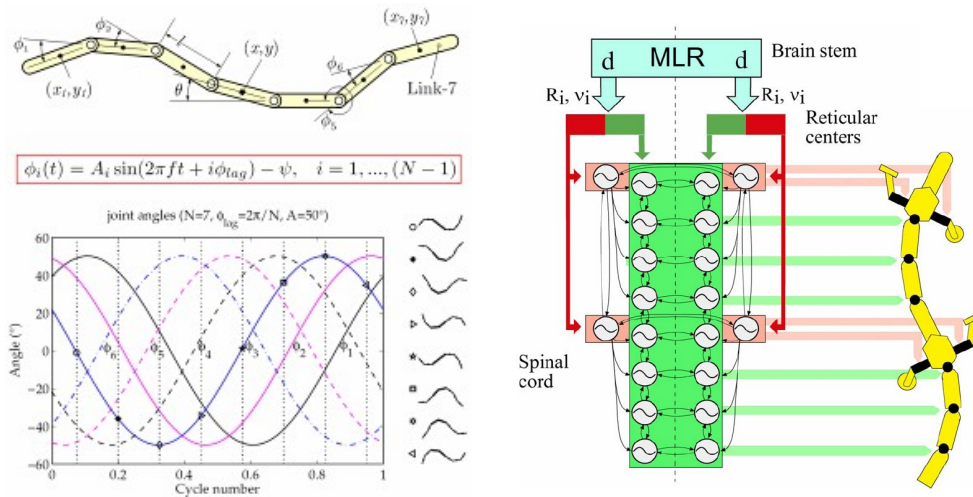


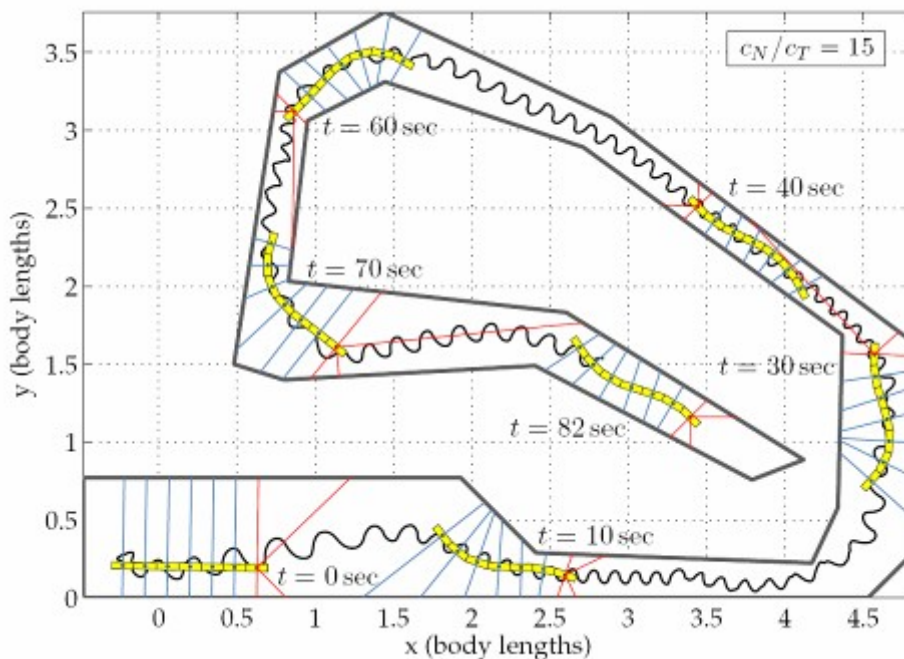
Figure 7: (Left) Travelling wave generation by explicitly prescribing the temporal variation of the joint angles Sfakiotakis (2006). (Right) Illustration of a CPG-inspired neural-control scheme of a salamander-like robot [ICC05].

B. Sensor-based reactive behaviors (closed-loop control):

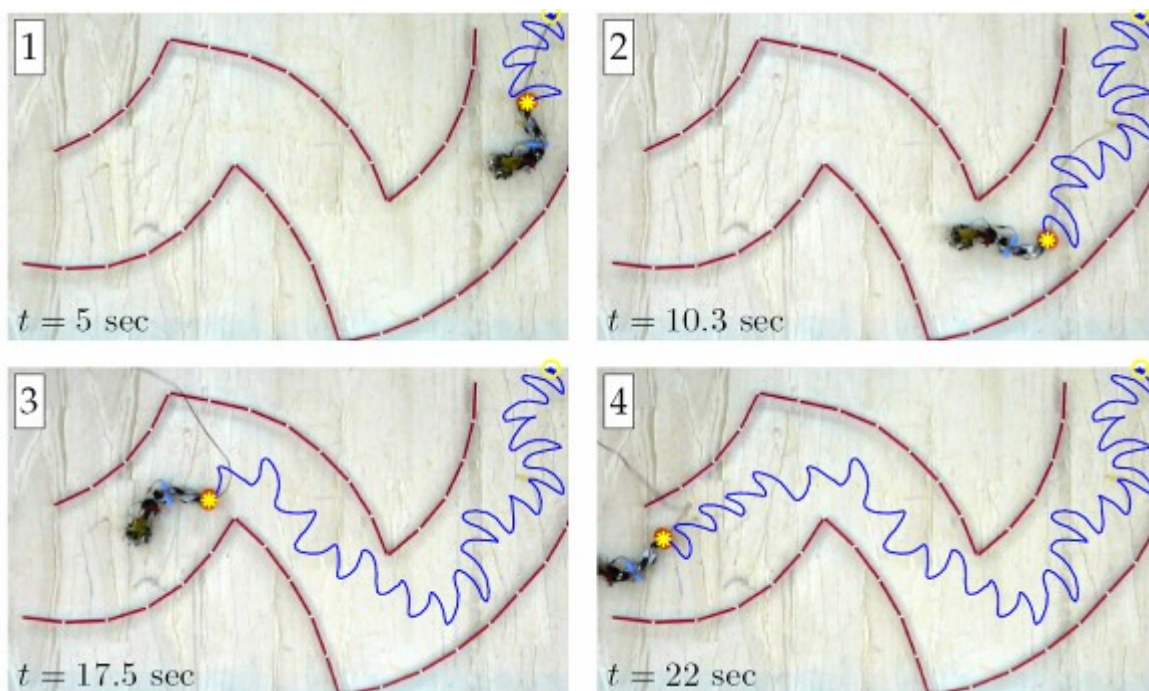
Regarding closed loop control schemes, *trajectory tracking* for, mainly wheeled, snake-like robots, has been studied, either assuming that perfect system state information is available, or using position information from an external (static) vision system Sato (2002), Mo (2003), McIsaac (2002), and Lapierre (2005). However, on-board exteroceptive sensors are necessary in order to enhance the autonomy of undulatory robots, so that they become able to operate in the complex environments for which they are intended. In this case, sensor-based closed-loop control schemes for navigating these robots, via the modulation of the joint oscillation parameters, are needed.

Some first steps in this direction explore, at a lower level, the use of sensors to identify substrate properties for modulating the parameters of the travelling wave Inoue (2007), or selecting an appropriate gait over varying terrain, Li (2004) and Chen (2008).

At a higher level, exteroceptive sensors (e.g., distance, vision) allowing the implementation of more complex behaviors (e.g., path following, obstacle avoidance) have been considered. One of the first such investigations appears to be the ACM-III wheeled serpentine robot, which is equipped with tactile sensors along its body, and demonstrates advancement inside narrow labyrinths and adaptive coiling around objects, Hirose (1993, 2004). The GMD snake robots feature tactile sensors, infrared sensors, cameras and lasers for applications like pipeline inspection Walker (1996), Kolesnik (2002). The lamprey robot in Ayers (2000) is reported to use a compass, inclinometers and sonars for eliciting behavior switches in response to environmental perturbations. The use of on-board distance sensors for determining orientation errors in the direction of locomotion of an undulatory robot is described in Ye (2004). In Tanaka (2006) force sensors, mounted on the head link of a pair of undulatory robots, are exploited for implementing a cooperative object transportation task. Control schemes, implementing reactive centering and swarming behaviors for undulatory robots, based on distance sensor data, are described in Sfakiotakis (2007, 2007a) (see figure below). Vision-based homing behaviours for undulatory robots, generated by extending nonholonomic image-based visual servoing strategies and using epipolar geometry, are developed in Lopez (2009).



(a) Reactive centering behavior: Simulations of a 7-link undulatory robot employing distance sensors to traverse a corridor, adapting the amplitude of its body wave to the width of the corridor.



(b) Reactive centering behavior: Experiments with a 5-link robotic prototype, equipped with infrared distance sensors.

Figure 8: Bio-inspired closed-loop control of undulatory robotic locomotor [ST07]

Focusing more on the hyper redundant manipulator, there have been several different approaches, which researchers have also studied for the control of continuum or hyper redundant manipulators.

Set-point controllers for continuum manipulators are proposed by Ivanescu (2002, 2005), Gravagne (2002) and Suzuki (2002). For the control a hyper redundant planar space manipulator, Ivanescu (2002) proposed the use of an energy based control law described by simple energy relationship of the dynamic model. Later Ivanescu (2006) extended this by proposing a control method which was based on the artificial potential method. It was shown that the control of a 3D space hyper redundant 3D arm to a target position is possible if the artificial potential is a potential functional whose point of minimum is an attractor of this dissipative control system. The same method could be used to constrain the manipulator motion in order to avoid e.g. obstacles.

It has been showed by Gravagne (2002) that under the assumption that distributed damping exists on the backbone of a soft robotic manipulator, a PD plus feed-forward controller can exponentially regulate the configuration of a multi section continuum manipulator. Suzuki (2002) described sliding mode and impedance control techniques for hyper-flexible manipulators. The use of an external camera for shape estimation and set-point regulation of soft robotic arms was also proposed by Chitrakaran (2007) and Hannan (2005).

There are also very few techniques, which target the more general tracking control problem for continuum manipulators with one of the exceptions being shape tracking control, Mochiyama (1999), where the manipulator follows a desired shape prescribed by a time-varying spatial curve.

A motor scheme for the control of a single-joint robot arm actuated by McKibben artificial muscles is proposed by Eskiizmirliler (2002). In this approach, classical control elements of the cybernetic circuit are replaced by artificial neural network modules having an architecture based on the connectivity of the cerebellar cortex and whose functioning is regulated by reinforcement learning. After learning, the model accurately pilots the movements of the robot arm, both in velocity and position.

To simplify the inverse kinematics, Gravagne (2000) proposed mapping infinite-dimensional arm configuration space to the finite-dimensional actuator space by using natural and wavelet decompositions. Gravagne (2004) used manipulability and force ellipsoids to analyse the directional dependence of motion and force exerting capabilities of soft robotic manipulators. A combination of conventional controller with neural network-based learning for the OctArm manipulator was presented by Braganza (2006).

One of the greatest assets of a continuum soft manipulator is its inherent passive compliance. Passive compliance, i.e., compliance built into a mechanism via purely mechanical means, can often eliminate the need for complex and expensive force/torque sensors and feedback systems. Additionally, compliance is necessary for successfully accomplish a whole arm grasping algorithms for hyper-redundant robots Gravagne (2002a). The ellipsoid method appears to be a useful tool to deal with the analysis of the compliance as well as for the development of the controller.

A vibration-damping setpoint controller was proposed by Gravagne (2001). By selecting a central point on the robot and controlling the trajectory of that point the inverse dynamics of a gel robots were simplified by Otake (1996). Accurate control of soft robots requires model-based prediction of the set of possible configurations. Dynamic models that accurately describe large-scale deflections of soft robots and cover their entire workspace are currently too complicated to be used for control. Current control approaches, based on simpler models, are not guaranteed to be stable or effective for large deflections Gravagne (2001). Also, including distributed forces such as gravity, and structural stability of multiple section robots into control schemes is a challenging problem. Work by Yekutieli (2005) showed that a simple command producing a wave of muscle activation moving at a constant velocity is sufficient to replicate the natural reaching movements of octopus arms with similar kinematic features.

Finally a robot developed by Kim (2003) is another example of a soft robot where the actuation used is based on Ionic Polymer Metal Composites. The robot locomotes on the ground by using ciliary motion. In each cycle, the front and the rear legs are alternately pushed downward and folded upward.

3.6 Evolutionary Design of Bio-inspired Systems (FORTH)

The aim of research in the field of biologically-inspired systems is to uncover the working principles of natural organisms and help implement artificial agents, that can successfully tackle real-world situations. Existing approaches emphasize the impact that physical dynamics have on biological organism morphology and control strategies, extracting useful guidelines, which are further interpreted in a computational context to support artificial system design. Well-established knowledge, regarding the natural mechanisms triggered to produce some specific behavior of biological organisms, significantly support the design of artificial models. However, many aspects of the natural systems' operation remain unknown and cannot be directly integrated into the system.

In order to avoid arbitrary human assumptions (that can potentially harm the implementation process), we may provide the artificial systems with some internal plasticity dynamics, and let them self-organize, according to the physical properties of the environment, similar to the biological evolutionary process. Following this approach, bio-

inspired system design emphasizes the reciprocal coupling of the control mechanism (i.e., of the central nervous system), of the body of the agent and of the operating environment.

In order to sufficiently explore alternative hypotheses, an automatic mechanism is necessary to identify and validate possible configurations. Evolutionary algorithms may provide an effective and systematic means to address this issue, mainly due to their well-known capacity to explore the problem domain in a global, rather than a local, manner. Therefore, artificial evolution can be used as a powerful tool for exploring natural working principles. In the past, evolutionary processes have been used extensively in designing artificial neural networks, considered as the computational counterpart of the biological central nervous system, for the case of artificial agents. Additionally, evolutionary processes have been employed in studying the situated robotic characteristics emerging from agent-environment coupling, including aspects of neural control, developmental maturation, and morphological design.

Below, we summarize the main research direction in the fields of evolutionary neural networks and evolutionary robotics.

A. NeuroEvolution

[Genetic Algorithms](#) are inspired by analogies to natural evolution: the rules of evolution ([selection](#), [recombination](#)/reproduction, [mutation](#) and, more recently, [transposition](#)) are, in principle, simple, yet, over millions of years, have produced remarkably complex organisms. Appropriate abstractions of this process are used in [genetic algorithms](#).

Artificial neural networks (ANN) can effectively approach many computational and engineering problems due to their well known ability to model non linear functions. In order to apply ANNs to a specific practical problem, an optimization method is necessary to adequately tune network parameters. Evolutionary algorithms are powerful stochastic optimization methods, that can adequately address ANN tuning, without using gradient information. Typically, during evolutionary tuning, a parametric description of the network is encoded in artificial chromosomes, which are further evolved according to some problem-specific fitness criteria. The basic scheme of the evolutionary procedure is graphically depicted in Figure 9. The algorithm is as follows:

step1. Randomly generate an initial population of chromosomes.

step2. Compute the fitness for each individual in the current population.

step3. Select individuals with a probability proportional to their fitness.

step4. Generate a new population using crossover on the selected individuals.

step5. Apply mutation to introduce noise in the obtained solutions. Go to step 2 until a satisfactory solution is obtained.

step6. Display the solution with the highest fitness.

In the sequel we describe the main approaches on ANN evolution.

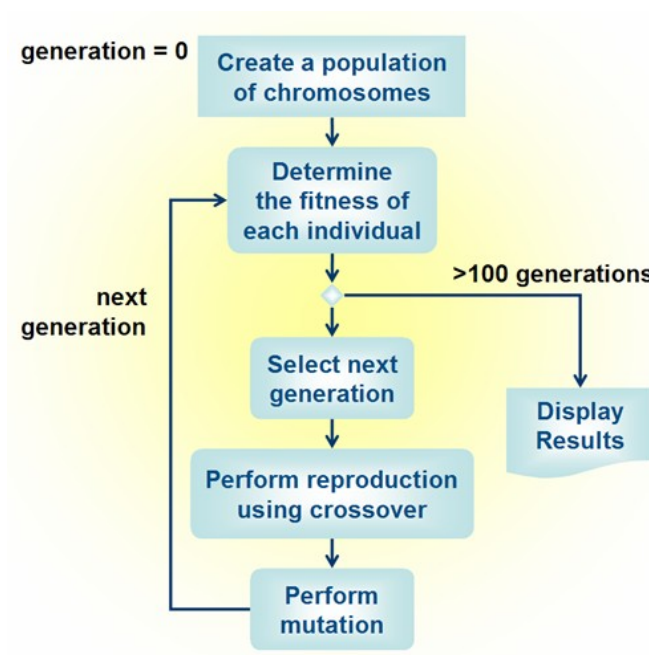


Figure 9. The artificial evolutionary optimization procedure.

Direct / Developmental / Implicit encoding of networks

An important issue for the success of neuroevolutionary procedures is how the specialized properties of the neural network will be encoded in properly structured chromosomes, which facilitate the identification of high-fitness ANNs. The current encoding schemes can be classified into three main classes: direct, developmental and implicit, Floreano (2008). The *direct* methods have been mainly used for evolving fixed-size networks. In particular, following this approach network parameters (synaptic weights, neuron biases, time-constants, etc.) are directly encoded in the genotype. This direction has been very successful especially when dealing with small size networks Chandra (2006) and Chellapilla (2001). However, using appropriate network topologies can significantly affect our ability to solve a problem. The main problem on this direction is that the evolution of the structure renders the network too fragile (i.e. structural changes usually lead to decreasing fitness, even if they have the potential to further increase the fitness in later evolution). Neuro-evolution of augmented topologies (NEAT) is one of the most successful methods for evolving the structure and the weights of ANNs, emphasizing on meaningful crossover between individuals with different chromosome length, Stanley (2002). Besides parametric and structural optimization,

direct encoding approaches are not very efficient with large network structures, because the length of the genetic string and its evolvability do not always scale well with network size.

In order to evolve large networks, the chromosomes may encode the details of a *developmental* process, which will ultimately produce the neural network. For example, Gruau (1995) proposed a genetic encoding scheme for offline neural network development based on cellular duplication and differentiation. Other approaches used encoding schemes of the life-time development of a neural network, Nolfi (1994). The developmental process for these approaches is determined both by genetic and by environmental (sensory-motor) factors. Despite the ability of developmental approaches to generate large networks from compact genetic representations, it is not clear to what extent the network size contributes to solve difficult problems.

A more recent approach for representing neural networks is based on *implicit* encoding, that assumes a certain amount of environmental principles to be represented into the chromosome. Gene Regulatory Networks (GRN) simulate the interaction among genes, in order to implicitly represent internal network interactions. Several artificial evolutionary systems have been recently implemented, inspired from biological gene regulation processes, resulting in complex and efficient NN structures, Eggenberger (1997), Hallinan (2004) and Quick (2003). For example, GRN models may rely on the diffusion of chemicals, which can either directly influence the phenotype of the agent or regulate the expression of genes, Bongard (2002). This approach has been further extended for evolving networks of any kind of dynamical devices, Mattiussi (2007).

Neural Models

The type of neurons employed for the construction of ANNs significantly affects its ability to address a given problem. The more abstract model for approximating neural firing is the integrate-and-fire model that involves a non-linearity mechanism for turning an internal continuous variable (summarizing input) into a firing rate, Dayan (2001). The influence of one cell on another is given by the product of the pre-synaptic cell's firing and the strength of the connection. Due to their simplicity and computational tractability, integrate and fire models have been used widely for implementing feed-forward neural networks. The main shortcoming for such neurons is that they are unable to implement time-dependent memory, which is necessary to address dynamic phenomena. In the leaky-integrate-and-fire model, the memory problem is solved by adding a "leak" term to the process of integrating pre-synaptic input, therefore producing a dynamic neuron model. Continuous Time Recurrent Neural Networks (CTRNNs) are the most widely used structures that are based on leaky integrators, Beer (1992). Due to their dynamic nature these models are more difficult to train with learning algorithms that use gradient descent, correlation and reinforcement learning. Evolutionary processes instead can effectively

tune CTRNNs, an approach that has been extensively used in robotic applications Tuci (2003). Furthermore, in order to simulate spike-based (i.e., impulse-based) communication between cortical neurons, researchers utilize spike neuron models, Hodgkin (1990), that may work at various levels of biological abstraction. A simple way for implementing spiking neurons is to take the dynamic model of CTRNN neurons and thresholding its output for determining when spikes are emitted. Evolutionary algorithms have been successfully employed for evolving spiking neural networks, Hagrais (2004) and Floreano (2003).

Evolution of learning – Neuromodulation

An important advantage of using evolutionary algorithms for designing and optimizing ANNs is that evolution can be combined with other learning methods, producing new and very effective training schemes. For example, back-propagation learning has been combined with evolutionary processes for taking care of parameter initialization issues, Ng (1999) and Alba (2004). Similarly, evolution is combined with reinforcement learning strategies, either to adjust their performance when performing meta-level optimization, or explore alternative adaptation strategies, being more natural and more efficient than the ordinary action-critic models. Evolutionary algorithms have been employed also for the evolution/optimization of the learning procedure. For example, learning rules have been parametrically described as linear combinations of measures based on pre- and post-synaptic neural activities. Learning rules are evolved to take a final form that facilitates network adjustment, Chalmers (1990). The evolution of Hebbian-like learning rules have shown to significantly support the adaptability of the network to changing operating conditions [FM98]. Similar approaches have been implemented for spiking neural networks, using parametric descriptions of the spike-timing dependent plasticity (STDP), DiPaolo (2003). In general, it is suggested that, the interaction of artificial evolution with other learning procedures, amounts to smoothing the fitness surface around optimal solutions, which can be explored more effectively during the learning process, Hinton (1987) and Mayley (1996).

The interaction between life-time learning and evolution has been described long ago, and is currently known as the Baldwin effect, Smith (1987). This is based on the assumption that the organisms having more rich learning capacity have larger number of offsprings. Currently, there are two ways for combining evolution with run-time learning, i.e. based either on Lamarckian or on Darwinian principles. The first assumes that the characteristics acquired through learning are coded back into the genotype, while the latter does not allow any direct chromosome adaptations from epigenetic learning.

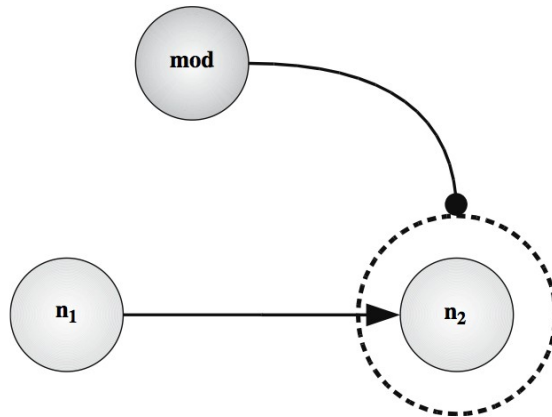


Figure 10. Neuromodulatory neurons permit the implementation of a value-based learning mechanism in artificial neural networks. The basic learning mechanism changes the weight of the link between the two neurons n_1 and n_2 according to their activity. The neuromodulatory neuron *mod* modulates (strengthens or suppresses) the basic learning mechanism, Mattiussi (2008).

More recently, a new approach for combining learning and evolution has emerged, inspired by the neuromodulatory mechanisms, that regulate the behavior of animals. These works aim at furnishing neural networks with reinforcement learning-like capacity following the general mechanism depicted in Figure 10. Neuromodulatory architectures are largely inspired by the functionality of cortical neurotransmitters, using specialized neurons that modulate the process of synaptic weight adaptation between ordinary neurons, therefore developing sub-networks capable of learning only in particular circumstances, Mattiussi (2008). For example, based on Analog Genetic Encoding, it has been possible to develop learning mechanisms that outperform hand-designed value-based schemes, Soltoggio (2007). Another approach for evolving neuromodulatory controllers is based on GasNets, where specialized neurons emit “gases” that diffuse through the network, modulating the profile and the activation function of surrounding neurons Husbands (1998). These networks have been shown to be very effective in problems requiring the emergence of neural pattern generators or timers, Magg (2006).

B. Evolutionary Robotics

In evolutionary robotics, artificial agents are considered as autonomous organisms, that are free to develop their own body-brain structure based on environmental interaction and with minimum human intervention. Over the last decades, a growing body of work focused on evolving controllers for mobile (wheeled) or walking (legged) robotic systems. These works, summarized in Floreano (2008), use a variety of ANN structures to control robotic systems. Besides the implementation of artificial agents with advanced behavioral and cognitive capacities, evolutionary robotics can be used in brain science as a useful research tool that can uncover important principles of neural processing, and thus

provide new explanations for natural cognitive phenomena, Tamburrini (2005). This is because the neural controllers emerging from evolutionary procedures can manifest interesting biological-like characteristics, Ruppin (2002). Such examples can be found in several recent studies Borrett (2005), Maniadakis (2007), Suzuki (2005). However, since biological reality is much richer than the implemented artificial agent models, results should be carefully considered when interpreting assumptions for biological systems.

Critical issues

The majority of research works in the field of Evolutionary Robotics rely on realistic simulation environments used for evaluating the performance of candidate controllers. The best fitted controllers are subsequently transferred into physical robots. However, the well-known gap between simulation and reality (differences in sensors, effectors, motion dynamics, etc.) makes controllers, that work well in simulation, operate poorly in real world conditions. In order to cope with these problems, the designers of robot controllers follow several methods, such as: (i) including independent noise to the sensors and the effectors of the simulator, Jacobi (1995), (ii) using minimal simulations, i.e. modeling only those characteristics that are relevant for the emergence of the desired behaviors Jakobi (1993), (iii) evolving the plasticity mechanisms of the system, rather than its parameter values, so that the controller will be enriched with the capacity to adapt in real life conditions Urzelai (2001), Eggenberger (2004), (iv) simultaneously evolving the controller and the morphology of the robot, so that the one can adapt to the other Bongard (2005), (v) continuing evolution after embodiment on the physical robotic system, Floreano (1994).

Evolution on real robots

Important guidelines for successfully evolving robotic controllers are given in Bianco (2004). More specifically, ANN controller evolution requires the use of implicit and general selection criteria, in order to favor organization of the evolving individuals and repeatedly change environmental conditions. In particular, implicit selection criteria (e.g., maintain high stamina/energy value) leave evolving individuals free to select their ways for solving the underlying problems. This is obviously not the case when using explicit criteria (e.g., shortest path to the charging station), that reduce self-organization during controller optimization. The promotion of agent structure organization aims at building systems that are gradually larger, more complex and more advanced than their predecessors, being capable to face and solve incrementally more sophisticated problems. Finally, keeping a certain level of environmental stability but allowing reach dynamic changes to occur in the environment, makes necessary the emergence of agent's adaptation capacity, and supporting its ability to cope with unexpected circumstances in the future.

Coevolution in distributed systems

When dealing with the design of complex distributed systems the effectiveness of the evolutionary procedure can be significantly facilitated by considering the structural characteristics of the particular system. This is particularly the approach followed by coevolutionary algorithms which utilize separate populations to evolve partial entities of the problem, Potter (2000) and Darwen (2002). In order to formulate a composite problem solution, individuals within different populations have to be selected, put together and operate in parallel. In other words, coevolution breaks down the overall problem into smaller pieces and then solves partial problems taking also into account the dynamics of their interaction. Coevolutionary approaches are broadly distinguished in competitive and cooperative.

More specifically, competitive coevolutionary models are suitable for problems that can be stated in the form of two or more opponent entities (e.g., in predator / prey scenarios), Kicinger (2005). In particular, each opponent utilizes the others as test cases in order to estimate its fitness quality. Following this approach, competition takes place between partial evolutionary processes, i.e. the success of the one implies the failure of the other, Olsson (2001). The fitness of a candidate solution is proportional to the number of test cases it solves, while the fitness of a test case is proportional to the candidate solutions which fail to solve it. As a result, it is expected that each opponent will become increasingly more efficient by exploiting the weakness of the other, and also eliminating its own weak points.

The cooperative scheme provides an appropriate framework for evolving distributed systems consisting of non-linearly interacting components that need to be co-adapted on one another, Wiegand (2001). The standard approach to applying cooperative coevolution is based on the natural decomposition of a problem into its partial components, Wiegand (2003). In particular, the structure of each component is assigned to a different subpopulation. Then, components are evolved simultaneously, but in isolation from one another. In order to evaluate the fitness of an individual from a given partial population, collaborators are selected from the other subpopulations, and the combined chromosome is decoded to form a complete solution of the problem which is further tested and evaluated. As a result, each component achieves successful performance only by helping the other components to also perform in an efficient way. The crucial role of component interaction in cooperative coevolution, enforces the coupling of partial structures and the formulation of successful composite solutions. Cooperative coevolution has been successfully applied in robotics for implementing distributed multi-agent systems, which are capable of solving complex tasks by means of developing an integrated collective functionality, Cho (2001) and Baldassarre (2004) and communicate, Quinn (2001) or implementing distributed brain-inspired models Maniadakis (2008).

Modular robots

Modular self-reconfigurable robots are complex distributed systems, composed of multiple robotic units. Depending on the type of the elementary units and their particular hardware characteristics, assembling algorithms can be categorized in: (i) lattice reconfigurations, where robotic elements may attach at discrete locations on a lattice formed by other modules in the collection, (ii) mobile reconfigurations, where robotic elements can move independently through the environment and, potentially, link to each other, and (iii) chain/tree reconfigurations, where open or closed kinematic chains of elements attach to each other to form complex systems for a recent review see Yim (2007).

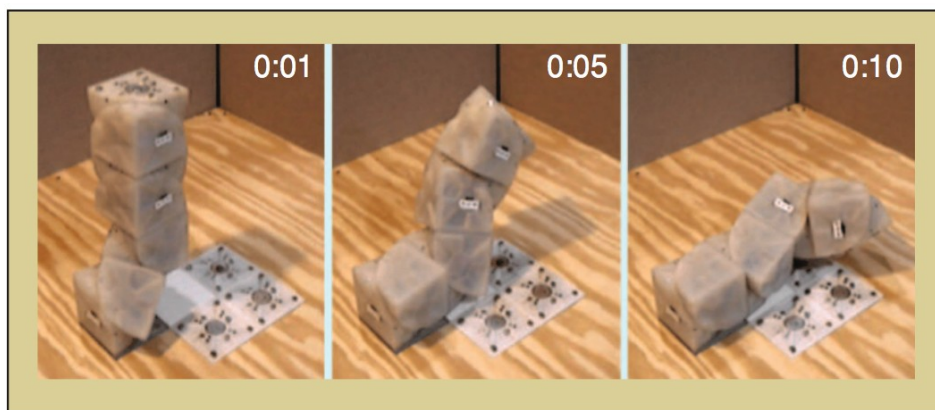


Figure 11. Four Molecubes are assembled in a complex robotic creature.

For example, the work on Molecubes, Zykov (2007), aims at using cubical robotic elements with one rotational degree-of-freedom (DoF) aligned with their diagonal, to form gradually larger creatures (see Figure 11). Similarly, the work on SuperBot, uses elements of three DoF (pitch, yaw, and roll), that can adequately communicate and share power. The work on the Swarm-bot modular robots, Mondada (2004), describes teams of autonomous robots which can physically connect to each other, forming dynamical assemblies that can navigate on rough terrains, or go through narrow passages. In particular, elementary robotic units equipped with small gripper devices are evolved to formulate multi-agent assemblies. The composite creature formed is driven by a leader elementary robot, that dominates the remaining elements, while the controller of the leader is copied to the remaining robots. Similar to Swarm-bots, other works employed evolutionary algorithms to design controllers for elementary components are summarized in Tuci (2006).

Another approach based on modular robotics aims at simultaneously evolving both robot bodies and their controllers. For example, Framsticks offers various genotypes and fitness functions to co-evolve morphology and control of virtual stick creatures, Komosinski (2001). Hornby and Pollack compared direct and generative representations

for body-brain co-evolution and found that the latter ones achieve better performance, Hornby (2001). Using L-systems as generative encoding (i.e. define a complex object by successively replacing parts of it using a set of rewriting rules), they evolved neural controlled robots that are more complex and use more parts than those in previous work. A novel multi-cellular electronic circuit, capable of evolution and development, is described in Roggen (2004). All cells contain the complete genetic description of the final system, similar to living organisms. Through a mechanism of development, cells connect to each other using a fully distributed hardware routing mechanism. Useful research directions for implementing open-ended modular self-assembled robotic systems are provided in Bianco (2004).

Evolutionary hardware

The works discussed so far consider robotic systems with static and predefined morphologies. In order to avoid the gap between simulated and real operating conditions, evolutionary procedures may run by physically instantiating candidate solutions to be evaluated in real-world conditions, Walker (2003). Along this line, existing works can be mainly classified in: (i) developing robot controllers following a finite training phase, that terminates before the robot is applied to a task (i.e., the controller is not adapted during task execution), and (ii) developing a controller that is adapted while performing the task (i.e., in a life-long adaptation mode).

Summarizing the methodologies that have been used so far, we see that using physical robots for evolution is time consuming, and, therefore, only simple worlds and tasks are investigated, Hornby (2000) or small sized populations are evolved, Floreano (2004). Using a mixture of simulation and physical robots is a promising approach, if the controller is frequently tested and adapted in the real world, Wilson (1997), which however requires heavy involvement of the trainer. Additionally, controller plasticity can significantly support robot adaptation to new operating conditions, Floreano (2001).

Field programmable gate arrays (FPGA's) can significantly support the evolution of hardware controllers. They are reconfigurable electronic circuits made up of logic gates, that can be configured at run-time. The first use of onboard evolution for controlling a robot was made in Thompson (1995), where, a wall-avoidance behavior was evolved in a wheeled robot. Keymeulen et al. have also evolved FPGAs to control a visually guided robot, Keymeulen (1998). The robot's task was to follow a ball whilst avoiding obstacles, being adapted to new situations such as movement of obstacles and loss of individual sensors. Two FPGA's were used, with the first executing the current best genotype, while the second used a simulation of the world to perform evolution. The simulated model of the world was built by the robot as it moved around. After every 10 generations, the currently best genotype was transferred to the first FPGA for execution. Thus, although evolution took place in a simulation, the simulation was running on the robot itself.

Robotic Body Evolution

Besides the previously described research directions, aiming at evolving controllers for pre-existing robots, the capacity of evolutionary procedures to explore complex configurations has been recently employed in studies investigating the physical morphological properties of the robots. Early such works evolved the properties of robot sensors, Cliff (1993). Later, using simulated environments, the synthesis of 3D creatures leaving in a world with realistic physics was investigated, based on competitive evolutionary scenarios [Sims94]. The advancement of simulation environments enabled the evolution of physical structures considering stresses and torques Funes (1998). This made possible the simultaneous evolution of controllers together with parameters determining robot morphology, Lund (1997) and Marbach (2004).

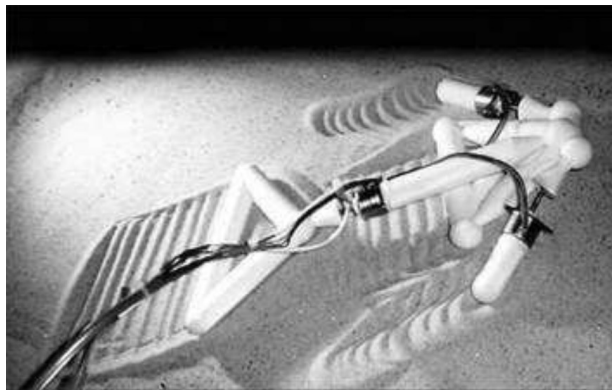


Figure 12. The artificial creature evolved by Lipson (2000) in action.

A noticeable step in artificial agent evolution has been performed by Lipson and his group, within the framework of the Golem project, where autonomous creatures were evolved in simulation out of basic building blocks, including neurons, bars and actuators (bars could connect together to form complex structures, neurons could connect to each other and to bars whose length they would control via linear actuators) Lipson (2000). The artificial creatures have been evolved using the criteria of moving as far as possible in a certain time period. Then, the fittest individuals were implemented in robotic hardware, based on rapid manufacturing processes (3D printers, etc.), and successfully tested in real-world conditions (see Figure 12), implying that, in the future, we might discover novel robot bodies and controllers that can effectively address real-world problems. Significant guidelines for taking advantage of the coupling between body morphology, neural processing, and generation of behavior during robot design are provided in Pfeifer (2005).

4. Survey of Behavioral/Sensory-motor Control Architectures (UZH)

4.1. What is a Behavioural architecture?

There are a large body of research in robotics purporting the design of architecture for the control of robotic agents. Even before attempting to summarize the results in literature, it is important to try and define some of the terms we commonly encounter. The first such term is that of an “architecture”.

What is an Architecture?

Here are a few example definitions from Literature on the topic of Robot Architectures.

Arkin (1998) defines an architecture as, “a Robotic Architecture is a discipline devoted to the design of highly specific and individual robots from a collection of common software building blocks”. He then goes on to highlight some of the other definitions in literature such as for instance Mataric (1992), “An architecture provides a principled way of organizing a control system. However, in addition to providing structure, it imposes constraints on the way the control problem can be solved”. Russel and Norvig (2003), define an alternate version of the Cognitive Architecture, as “models of human reasoning”. These definitions bring in different perspectives to the development of architectures, i.e. the software development perspective, the control oriented and the cognitive perspectives, wherein the first Arkin definition is rather abstract and general.

Control Architecture

Pfeifer and Scheier(1999) on the other hand makes a very clear definition of a “Control Architecture” for a robot as something which essentially specifies how the various parts of the low-level specification, the primitives, should be connected to produce the desired behavior. The control architecture thus implements the hypotheses about mechanisms underlying the intended behavior of the agent.

What is Behavior Control

One view on the general issue underlying the problem of behavior control is how an agents sensory input should be mapped to the motor output in order for the robot to be able to fulfill its tasks. The “behavior architecture” may thus be construed to mean a control architecture developed to solve the problem of behavior control. However, this is a more of classical perspective on Behavior control. For the Octopus, it is important to keep in mind the sensori-motor couplings. The dynamical systems perspective, for

instance shows that there may not be a linear flow of causality from Sensors to Motors as implied by the classical view of Behaviour Architecture. This view is presented in Fig. 1.

Pfeifer argues that the particular control architecture chosen for an agent crucially depends on the purpose for which the robot was designed. If the goal is to model natural intelligence such as in the Octopus Project, the main considerations are biological or psychological plausibility whereas to fulfill tasks, it must be chosen to implement efficient task-related behaviors.

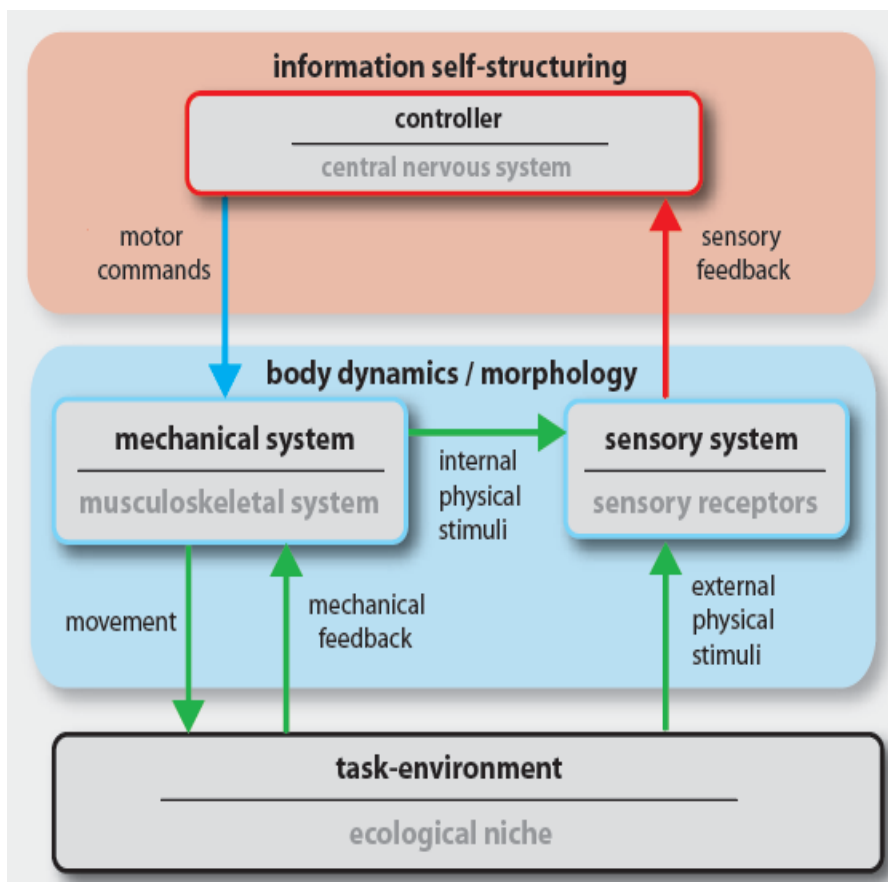


Figure 4.1. Sensori-Motor/Behavior Control Architectures in the view presented in Pfeifer et al (2007)

Floreano (2008) notes that in the design of bio-inspired robotics, there are several degrees of bioinspiration, ranging from loose metaphors to high-fidelity replicas of specific parts. The goal in this case, is to capture and reproduce the mechanisms that provide better performance for a given engineering problem. But if the aim is the design of a biologically inspired agent in order to understand intelligence, it can be argued that the choice of architecture must reflect the biological inspiration, since its no longer an engineering problem that needs a solution.

4.2. Classification of Architectures

There are a number of surveys in robot literature which try to classify Behavior and Sensory-Motor Control Architectures. However, classification is not an easy job since the distinctions are not so well defined. The following section tries to highlight some classification schemes which make it easier to understand and analyse Behavior/Sensory-Motor Control. Some of the Classification schemes and sample projects presenting them are shown below in Table 4.1.

Table 4.1 Some Classification schemes for Behavior/Sensory-motor Control Architectures

Application oriented	Biological	Model-based	Hybrid	Reactive
model-based, hybrid	enactive hybrid	Shakey (Nilsson, 1975), Stanford Cart (Moravec 1980), Stanley (Thrun, 2008)	Loosely Coupled Parallel Processes (Pfeifer et al 1999, 2007), MOSAIC (Wolpert et al, 1998)	Tortoises (Grey Walter 1967), Vehicles (Braitenberg, 1984), Subsumption Architecture (Brooks 1986)
Cognitivist		Emergent/ Connectionist		Enactive
Symbol-based (Russel Norvig 1995), SOAR (Newell et al, 1993), ACT-R (Byrne, 2003), many more		Neural Network Architectures (extended Kohonen, ART); Emergence (Hofstader 1985),		Embodied mind (Varela et al., 1991; Pfeifer and Bongard, 2007; Vernon et al., 2008); Extended Braitenberg (Braitenberg, 1986); Dynamical Systems (Kuniyoshi, 2007);

4.2.1. Biological vs. robotic

Traditional artificial intelligence views intelligence as being closely akin to what computers do – the information processing metaphor. This view has had many important successes, but not in building robots to work in the real world. One representative example of this view is the symbolic approach developed by Newell and Simon(1975), who asserted that a physical symbol system has the necessary and sufficient means for generating a general intelligent action. Traditional AI encountered many problems such as robustness and generalization, sequential nature of programming, its centralized way of information process, and so on.

The embodied AI is a synthetic approach which view intelligence as emerging when loosely coupled and parallel systems interact with each other and with the real world. The synthetic approach will involve creating simulations, but will also involve the building of systems – autonomous agents – that exist in the real world. They will behave without the intervention of human control. Whether simulated or embodied agents are studied will

depend on the situation, but both are likely to be required. Pfeifer et al (2007) and Pfeifer and Bongard (2007) provide an extensive survey of successful bio-robotics research. Some of the robots in this category include the Ant Navigation model of Sahabot in Lambrinos et al (2000), Webb's cricket (1994) and the MIT Cog(1998).

The methodology for studying naturally intelligent systems in this approach is synthetic, meaning that one has to build artificial agents to mimic natural ones. And this approach has three goals: Build an agent for a particular task; study general principles of intelligence; model certain aspects of natural system. Through the synthetic methodology, synergies between robotics and biology are uncovered, wherein, it no longer becomes a case of merely a biologist providing inspiration for roboticists, but also it is a mutually beneficial process wherein the biologists can learn answers to many of their problems.

4.2.2. Model-based vs. reactive

This classification would also be similar to the a traditional top-down vs. bottom-up division of systems, where model-based approaches are typically top-down whereas reactive architectures tend to be bottom-up.

Arkin (1998) notes that the model-based approach dominated robotics research for the for the first thirty years, during which time AI research developed a strong dependence upon the use of representational knowledge and deliberative reasoning methods for robotic planning. Hierarchical organization for planning was also mainstream: A plan is any hierarchical process in the organism that can control the order in which a sequence of operations is performed. Hierarchical control is seemingly well suited for structured and highly predictable environments (e.g., manufacturing).

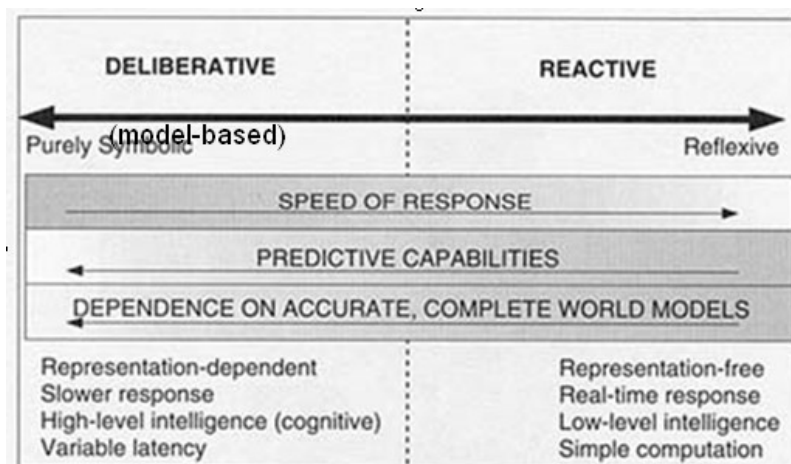


Figure 2 Spectrum of model-based and reactive methods

Reactive systems, however, were developed in response to several of the apparent drawbacks associated with the hierarchical design paradigm including a perceived lack of responsiveness in unstructured and uncertain environments due both to the requirements of world modeling and the limited communication pathways; and the difficulty in engineering complete systems as incremental competency proved difficult to achieve, that is, virtually the entire system needed to be built before testing was feasible.

Model Based

Traditional Artificial Intelligence has tried to create intelligent systems in a top-down approach. This has involved attempting to imitate thought and reason to produce intelligence. Brooks (1991) refers to this as a Sense Model Plan Act (SMPA) model. The agents first sense their environment through various sensors into the world and then uses this data to build a complete (as complete as possible) model of the world. Then, using this model, the agent produces a plan to achieve its goals and finally acts on the plan. Most of the agents processing time is spent in sensing the environment and building models. Very little of the time is used in planning and acting. The agents (robots) tended to be very slow and were not able to react to changes in the environment very well since the internal models frequently needed updating and were often incorrect.

Some Examples of Classic Model Based Robots are:

Shakey : The Artificial Intelligence Center at Stanford Research Institute conducted research on a mobile robot system nicknamed “Shakey” from 1966-1972. Endowed with a limited ability to perceive and model its environment, Shakey could perform tasks that required planning, route-finding, and the rearranging of simple objects. It was a pioneer and forerunner of many techniques used since. Many aspects of the project are summarised in Nilsson (1984).

Stanford Cart : The Stanford AI lab cart was a card-table sized mobile robot controlled remotely through a radio link, and equipped with a TV camera and transmitter and designed to understand difficulties in teleoperating a lunar rover. Moravec (1980) describes an attempt to program it to drive through cluttered indoor and outdoor spaces, gaining its knowledge about the world entirely from images broadcast by the onboard TV system. It performed obstacle detection, avoidance, and modelled the world through which it could then plan its path. The cart was very slow in its motion.

Stanley : The robot Stanley, was the Stanford University's successful entry into the 2005 DARPA Grand Challenge. Stanley, as described in Thrun et al (2005) was developed for high-speed desert driving without human intervention. The robot's software system relied predominately on state-of-the-art AI technologies, such as machine learning and probabilistic reasoning. Stanley represents the state of the art in the Model based approach to robot control.

Reactive (and Embodiment based)

Grey Walter Turtles : Walter (1967) started building three wheeled, turtle like, mobile robotic vehicles for educational purposes. These vehicles had a light sensor, touch sensor, propulsion motor, steering motor, and a two vacuum tube analog computer. Even with this simple design, Grey demonstrated that his robots exhibited complex behaviors. He called his creation Machina Speculatrix after their speculative tendency to explore their environment. They were the inspiration for many later works

Braitenberg Vehicles : Braitenberg vehicles (1984) were conceived in a thought experiment to illustrate in a evolutive way the abilities of simple agents. The vehicles represent the simplest form of behavior based artificial intelligence or embodied cognition, i.e. intelligent behavior that emerges from sensorimotor interaction between the agent and its environment, without any need for an internal memory, representation of the environment, or inference. They were a series of agents of increasing complexity and were the basis for the Extended Braitenberg Architecture.

Subsumption Architecture : Brooks (1986) Subsumption architecture was the first approach towards Behavior Based Robotics. Subsumption is a method of decomposing a robots control architecture into a set of task achieving behaviors or competences. The Control architecture is then built by incrementally adding task achieving behaviors on top of each other although its not hierarchical in the traditional model-based robotics sense, which is why it can be called as hierarchical reactive.

Walknet : Cruse (1991) proposed a reactive control scheme with a decentralized architecture for hexapod walking on the basis of his observation that the gait emerge from a strong dependence on sensory feedback and local communication between the legs, and complex interaction with the environment. This is described in greater detail in the Example architecture section.

Hybrid Architectures

These architectures combine elements of both Reactive and Model based approaches. They usually use techniques like predictive models augmenting or improving the performance of reactive control architectures. One important point to be noted however is that the models are not typically formulated in symbolic terms like those in the model-based approach. A large number of architectures have been proposed since the introduction of subsumption architecture which combine the ideas of reactive and model based techniques to varying degrees. In order to convey their flavour and due to reasons of space, only 2 are highlighted here.

MOSAIC : Wolpert and Kawato (1998) proposed a new modular architecture, the modular selection and identification for control (MOSAIC) model, for motor learning and control based on multiple pairs of forward (predictor) and inverse (controller) models. This is described further in the examples.

Emulation Theory of Representations : The emulation theory of representation is developed and explored in Grush (2004) as a framework that can revealingly synthesize a wide variety of representational functions of the brain. The framework is based on constructs from control theory (forward models) and signal processing (Kalman filters). The idea is that in addition to simply engaging with the body and environment, the brain constructs neural circuits that act as models of the body and environment. The framework is initially developed within the context of motor control, where it has been shown that inner models running in parallel with the body can reduce the effects of feedback delay problems.

4.2.3. Cognitivistic , Emergent/ Connectionist, Enactive

This axis of the classification is a more philosophical one, but it has also strong impacts on the actual design of behavioral architectures. One can identify three paradigms in the history of AI, which we will refer to as cognitivism, connectionism, and enactive approach.

Cognitivism was the first paradigm of the emerging field of Artificial Intelligence in 1950's. The aspects of intelligence that were modeled were the high-level cognitive functions, such as problem-solving, representation of knowledge and reasoning, and planning (see e.g. Russel and Norvig, 1995). The *computer* was not only the *tool* on which these models could run, but also quickly became the leading *metaphor for mind*. The essence of this paradigm is that the key to intelligence is computation with symbols that represent the world. The keywords are *algorithmic nature*, *symbolic computation* and *representation*. Thus, this approach is intrinsically model-based (see previous section) and body is of marginal importance here. While it was very successful in formal domains and practical applications (such as chess, search engines etc.), it turned out to be very difficult to deal with real-time behavior in unstructured environments. This approach also suffers from the frame problem and symbol-grounding problem (see e.g. Pfeifer and Scheier, 1999). The cognitivist paradigm is also known as *functionalism*, *computer functionalism* or *GOF AI* (Good Old-Fashioned Artificial Intelligence).

The second paradigm is connectionism (Hofstadter, 1985). It rests on the idea that many complex phenomena, such as autonomous intelligent behaviour of a robot, are emergent properties of parallel events in a network of simple active elements with links between them. The most popular example are neurons and artificial neural networks, which have become a frequently used formalism to model pertinent phenomena. The focus here is still on computation performed within the 'brain'. However, rather than sequential, centralized and symbolic as in the cognitivist case, the computation is parallel, distributed and so-called subsymbolic in its nature.

The Enactive viewpoint has been introduced in the early ninetieths as a contrast to classical cognitive and emergentist approaches in AI, which could not cope with some

issues on inner experiencing of organisms, feelings or real understanding (Varela et al., 1991). In the cognitivist approach, the robot constructors impose their model of the world on the agents and robots (the model is typically simplified for the robot's particular tasks). Thus, the robot has a representation of the world that it has not acquired itself. In connectionism, the conditions are imposed by the design. Varela et al. (1991) offer a different view. The agent is viewed not as an input/output machine but rather as a network consisting of multiple levels of interconnected, sensorimotor subnetworks that are embodied in the environment. Cognition is then viewed as embodied action. The approach of embodied cognitive science (e.g. Pfeifer and Scheier 1999) is compatible with this approach, but offers a more pragmatic view – oriented toward actual design of intelligent systems.

4.3. The “Substrate” underlying the architectures

In the previous sections, we have outlined some conceptual differences between different behavioral architectures. In the end, it is inevitable that these architectures be also implemented. The means to implement them – or the ‘substrate’ – differs. Different architectures have often their natural or native substrates associated with them. Sometimes, the implementation is even inseparable from the conceptual level of the architecture.

Computation on symbols

This is the native ‘substrate’ (the physical substrate is a computer) for model-based cognitivist approaches. A world model is created and represented in a symbolic manner (e.g. in predicate logic). Plans can be executed on this representation by using automated inference procedures, for instance. Many of today's robots are built with a significant symbolic computation component in their architecture.

Finite state machines

A prominent example of use of this substrate is Brooks' subsumption architecture. Finite state machines that are used as small computational units linking sensors to motors. They do have internal states, which however does not imply symbolic representation (Brooks, 1991). For example, Brooks' original augmented Finite state machines can enable the state transition after a period of time has elapsed. They can be applied in a centralized or decentralized, and in a hierarchical or non-hierarchical manner (Brooks' particular case in decentralized and hierarchical). We can conclude that this particular substrate is pretty universal and can be used under different paradigms.

Dynamical systems

Dynamical systems represent a philosophy, architecture (look in example architectures), as well as a computational substrate. Neural networks can be put into this category

(mathematically, this is true only if they are recurrent). They are the native substrate for connectionist, and for many bio-inspired approaches. Another implementation ‘tool’ that fits this category and that is used in control of locomotion are Central Pattern Generators (CPGs) (see Ijspeert, 2008 for a review). The CPGs themselves can be implemented on different levels of abstraction (from detailed biophysical to greatly abstracted oscillator models). While the dynamical systems substrate is typically used in a decentralized and non-hierarchical fashion, hierarchies can also be built (see Yamashita and Tani, 2008). The important feature of this substrate – as opposed to symbolic or finite state machines approaches – is that it is continuous.

Computation in the body

Up until now, all the substrates were classical computational substrates in the sense that computation is performed in the brain (i.e. typically in a computer). Passive dynamic walkers (Figure 4.3), on the other hand, demonstrate that simple walking can be achieved with no brain at all.

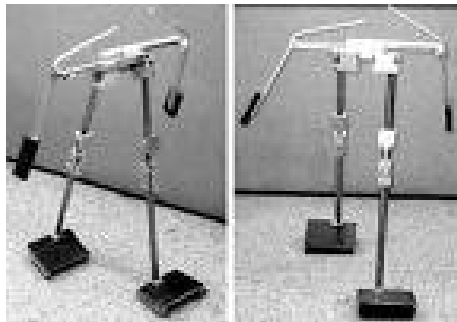


Figure 4.3 Passive Dynamic Walkers.

The work by McGeer (1990) stimulated a body of work in the last two decades that can be also named ‘intelligence by mechanics’ (see e.g. Blickhan et al. 2007). In these systems, the perception-action loop is integrated in the mechanics. Mechanics alone can even react to disturbances and stabilize locomotion patterns. This became known as self-stabilization. While such mechanisms are widespread in nature, their potential has not been fully exploited in robotics yet. Reactive or subsumption control architectures can be built on top of these. Architectures have to take the physical systems dynamics into account which is best achieved by mechanisms of embodiment, or using artificial evolution.

4.4. Examples of architectures

In this section we discuss a few representative architectures that have been designed to have a certain degree of biological plausibility.

4.4.1. Extended Braitenberg Architecture

The Braitenberg architecture is comprised of simple sensors, processing elements, unidirectional wires to connect elements, and motors to move animats which can convey robust and complex, both in space and time, behaviors. The core concept in this architecture is that simple components can produce complicated, emergent behaviors. What is important to note about this approach is the fact that behavior is not programmed explicitly but emerges from interactions between internal elements through both internal connections (if present) and through interaction with the external environment. Figure 4.4 shows two of the simplest Braitenberg vehicles, one named 'Hate', the other 'Love'. The two vehicles are formed by the same components. Two photodetectors (yellow), set at slightly divergent angles from the centerline, provide semi-directional sensing of light sources. Each sensor provides an excitatory signal that is propagated through a unidirectional wire (black) or, more generally, through a processing element or 'neuron' (light blue). The excitatory signal excites a motor element (red) which turns a drive wheel (dark blue). If one motor turns more rapidly than the other, then the vehicle will turn in the opposite direction. By simply connecting the two motors and two neurons in different way, the two vehicles express different behaviors: Hate avoids light while Love seeks light from the observers perspective.

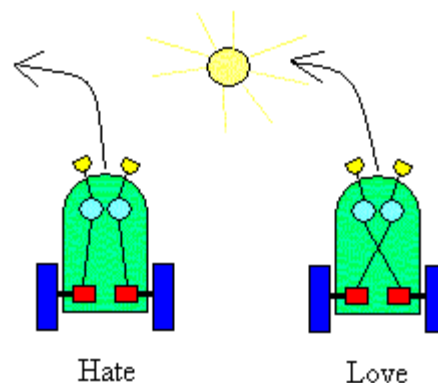


Figure 4.4 Two Braitenberg vehicles

The extended Braitenberg Architecture (EBA) follows the basic architecture of the Braitenberg vehicle while increasing the number and kinds of sensory detectors, associative networks and motor outputs. One example robot system, among many, that adapted the extended Braitenberg architecture is the MAVRIC (Mobile, Autonomous Vehicle for Research in Intelligent Control)(1994), illustrated in Figure 4.5 It was used to test various aspects of foraging search in an autonomous agent.

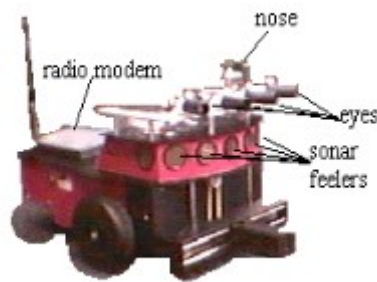


Figure 4.5 MAVRIC - an embodied EBA agent

Note that in the EBA, all process are continuously working and having an influence on the Behaviour. This is therefore, sometimes called a cooperative control architecture. This is in contrast to the Subsumption Architecture.

4.4.2. Subsumption architecture and behavior based methods

Brooks' original work (1986) advocated the use of a layered control system, embodied by the subsumption architecture but layered along a different dimension than what traditional research was pursuing. He argued persuasively that the traditional Sense-Think-Act approach of building world models and reasoning using explicit symbolic representational knowledge at best was an impediment to timely robotic response and at worst actually led robotics researchers in the wrong direction.

The Subsumption architecture is built in layers. Each layer gives the system a set of pre-wired behaviors. The higher levels build upon the lower levels to create more complex behaviors. The behavior of the system as a whole is the result of many interacting simple behaviors. The layers operate asynchronously. The layers of the Subsumption architecture are composed of networks of finite state machines augmented with timers (AFSMs). The timers enable state changes after preprogrammed periods of time. The inputs of AFSMs come from sensors or other AFSMs. The outputs of an AFSM are sent to the agent's actuators or to the inputs of other AFSMs.

Each AFSM also accepts a suppression signal and an inhibition signal. A suppression signal overrides the normal input signal. An inhibition signal causes output to be completely inhibited. These signals allow behaviors to override each other so that the system can produce coherent behavior .

The use of AFSMs results in a tight coupling of perception and action, producing the highly reactive response characteristic of subsumption systems. However, all patterns of behavior in these systems are pre-wired. AFSMs are the only units of processing in the architecture. Thus, there are no symbols.

Action selection schemes such as the Subsumption require an “arbitration” of which behavior becomes active and controls the agents behavior. This is an instance of a competitive scheme whereas extended Braitenberg is an instance of a cooperative scheme.

Pfeifer and Scheier (1999) note that, Subsumption has been sometimes been criticised as an engineering principle that bears little relationship to designing intelligent systems. However it brings a change in focus from the brain and higher level process to to interaction with environment, which is the focal point of the field of embodied artificial intelligence. One way of looking at it is as a particular design methodology while the other is a synonym for the whole field of behavior based robotics. This means that formalism of augmented finite state machines is not really important rather, more general ideas may be utilised like neural networks being used in the Cog robot (1998) for motor control.

Some work has also been done with a Planning and Learning Extension to the basic subsumption architecture. For instance, Mataric (1992) proposed extensions to pure reactive subsumption systems. These extensions are known as behavior-based architectures. Capabilities of behavior-based systems include landmark detection and map building, learning to walk, collective behaviors with homogeneous agents, group learning with homogeneous agents, and heterogeneous agents.

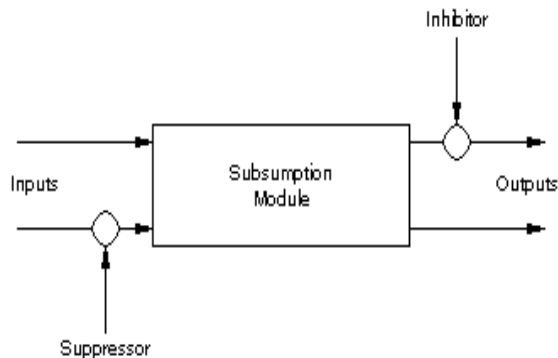


Figure 4.6 A simple layer in the subsumption architecture

4.4.3. Dynamical systems

Dynamical systems can be viewed as behavioral architecture. However, they can also constitute a whole paradigm and they are also used as a means of implementation. In the paradigmatical sense to explain cognition, they have been put forward by Thelen and Smith (1994) or Beer (1995), for instance. The advantage is that this approach is immune to the symbol-grounding problem, and not only the brain but also the body can be

characterized by using the dynamical systems language. Within the classifications we have mentioned, dynamical systems as an architecture would be a reactive (where representations - or models – can emerge from bottom up) or hybrid architecture that can be used to describe biological systems, but is increasingly being used in robotics. On the last axis, it would fit the enactive/embodied cognitive science approach.

Dynamical Systems are used by, Kuniyoshi and Sangawa (2006), where early motor development of humans is addressed in remarkable complexity, or the work of Jun Tani (e.g. Yamashita and Tani, 2008), where hierarchies emerge from a neural network. The iCub architecture (Degallier et al., 2008) is another example. For a relationship of dynamical systems and optimal control see (Schaal et al., 2007). Typically, fixed-point or periodic attractors of the dynamical systems are exploited to generate behavior patterns. However, some pioneer work is also demonstrating the potential of chaotic dynamics (e.g. Kuniyoshi and Suzuki, 2004).

4.4.4. MOSAIC

Wolpert and Kawato (1998) proposed a new modular architecture, the modular selection and identification for control (MOSAIC) model, for motor learning and control based on multiple pairs of forward (predictor) and inverse (controller) models. The architecture simultaneously learns the multiple inverse models necessary for control as well as how to select the set of inverse models appropriate for a given environment.

It combines both feedforward and feedback sensorimotor information so that the controllers can be selected both prior to movement and subsequently during movement. In their subsequent work in Haruno et al (2001), they then explored learning in the architecture using the expectation-maximization (EM) algorithm.

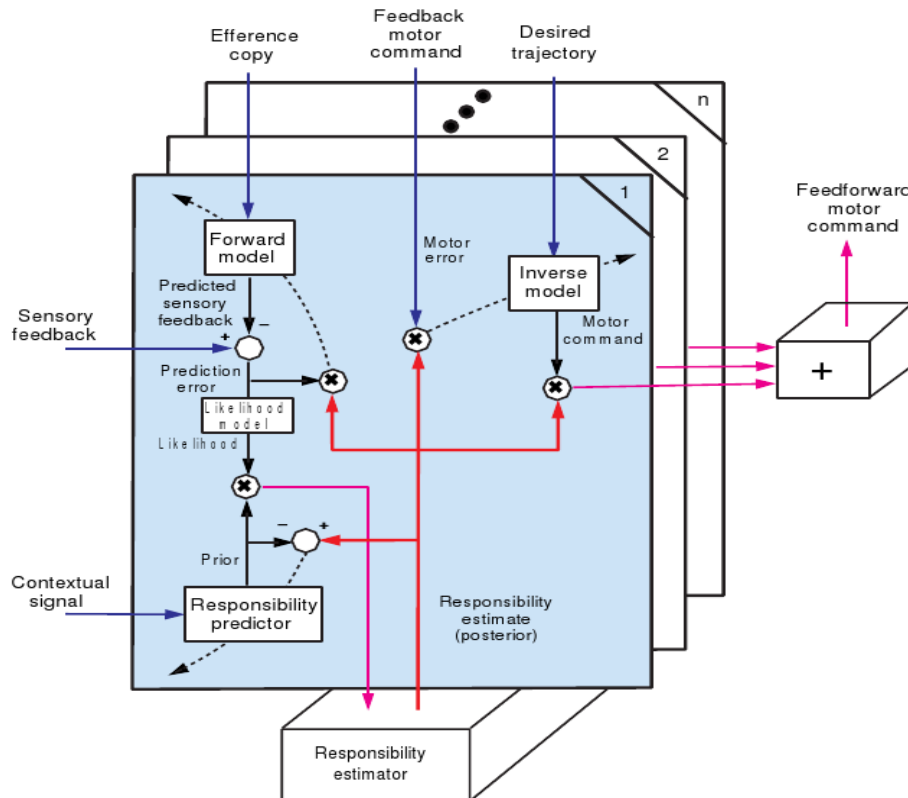


Figure 4.7 An Illustration of the MOSAIC control architecture showing the multiple forward and inverse models necessary for Control

Simulations of an object manipulation task showed that the architecture can learn to manipulate multiple objects and switch between them appropriately. The interesting aspect was that the model shows generalization to novel objects under certain conditions. Finally, when each of the dynamics is associated with a particular object shape, the model is able to select the appropriate controller before movement execution. When presented with a novel shape-dynamic pairing, inappropriate activation of modules is observed followed by on-line correction.

4.4.5 Probabilistic Models

Wolpert (2007) presented a probabilistic view of the models in sensori-motor control. The essence is from Bayesian statistics, wherein two important quantities are used, i.e., unobserved parameters (θ) and observed data (s). For example, in Vision, the Parameters are the object identity (eg . Apples or oranges). The observed data is then activity of ganglion cells taking information from the retina. In the alternate example of Localizing our hand in space, the Parameters are the hand's actual location , while the Observed data is Relevant sensory input from proprioception and vision. Wolpert observed that the Brain never has direct access to the true parameter values but must make inferences from other data. Essential question he thus addressed was the Relation between unobserved parameters and observed data, and thus a Generative model is

required. Techniques such as Maximum Likelihood Estimator, Bayesian Inference, etc. were employed to demonstrate the learning models.

4.4.6. iCub modular bio-inspired motor architecture

The iCub, Figure 4.8, is an open-systems cognitive humanoid robot comprising of 53 DOFs and with a height of 94cm. It is designed to be able to crawl on floors and sit up, with the motor and cognitive abilities of a 2 years old child. Videos, pictures and detailed introductions about this robot can be found its official website (<http://www.robotcub.org/>).

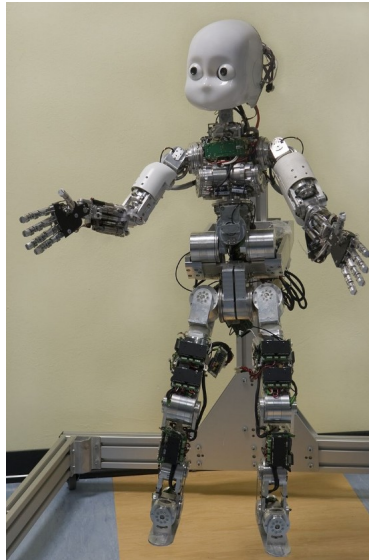


Figure 4.8 The iCub robot

The iCub's movement generation architecture is defined as a three-layered architecture whose layers are referred as the planner, the manager and the generator. The planner, corresponding to motor cortex in humans, creates the mental representation of the task. The manager (the brain stem, the basal ganglia, and the cerebellum) is involved in the selection, timing and coordination of the behaviors. And the generator, the spinal cord, generates trajectories through central pattern generators (CPGs). Each layer corresponds to a different level of abstraction in the representation of movement and reflecting the different processes involved in low-level movement generation(2008). This architecture is suitable for the online motor behaviors generation and the switch between motor tasks.

Modularity has proven to be a successful approach for generating fast, complex movement as it reduce remarkably the dimensionality of the control problem(1996). The trajectory generation module in this architecture uses Central Pattern Generator (CPG) and requires low computational needs, so it can be implemented in a Digital Signal Process (DSP) controller with fast feedback loops. The advantage of this approach is that the motion generation does not need optimization and planning at higher levels. The

complex joint movements are generated through the sequencing and superimposition of simple motor primitives generated by discrete and rhythmic unit generators.

This modular and discrete approach of motion generation is capable of reducing the control parameters drastically. This advantage is highly useful in the control of octopus arm which has a infinite number of DOFs.

4.4.7. Exploiting Body Dynamics

There is a body of work where the focus rather than on forcing prescribed trajectories on a robot, the goal is that the robot learns to exploit the dynamics of its interaction with the environment. Thus, rather than overriding its body dynamics, it can exploit it and only cheaply channel it in desired directions. For instance, a quadruped robot can be steered with a truly minimalistic controller as in Iida et al. (2005). This principle is also discussed in further detail in Pfeifer and Scheier (1999) and in Pfeifer and Bongard (2007) with the Puppy Robot example described.

4.4.8. WalkNET

The complex problem of coordination and control of hexapod insect-like walking was tackled in a novel mechanism proposed by Cruse(1991) and Dean et al (1999). They observed that the gait of the slow-walking stick insect apparently emerges from an extremely decentralized architecture with separate step pattern generators for each leg, a strong dependence on sensory feedback, and multiple, in part redundant, primarily local interactions among the step pattern generators. This is because insects have no internal process for global communication among legs and only locally communicate among each other.

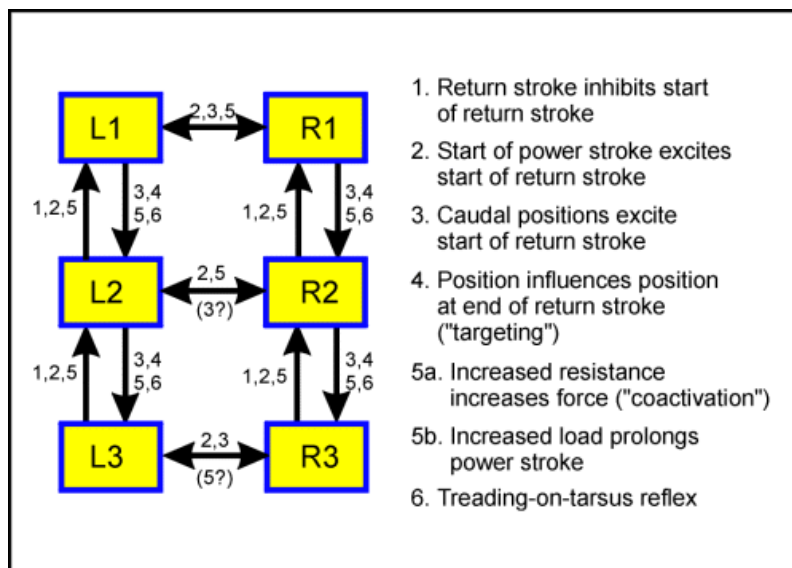


Figure 4.9: Inhibitions and Exitations of adjacent modules in WalkNet

Thus, stepping and step coordination do not reflect an explicit specification based on a global optimization using a representation of the system and its environment, instead they emerge from a distributed system and from the complex interaction with the environment. Cruse et al (1998) proposed Walknet, a decentralized control at the level of single leg joints to explain the control of leg dynamics. Through simulations they show that negative feedback for control of body height and walking direction combined with positive feedback for generation of propulsion produce a simple, extremely decentralized system that can handle a wide variety of changes in the walking system and its environment without requiring a central controller implementing global optimization. The extension of this work is to demonstrate its effectiveness in a real robot platform Tarry.



Figure 4.10 Tarry the Hexapod to demonstrate Walknet

5. Survey of Bio-inspired Soft Materials

(UREAD)

5.1 Introduction

The octopus artefact requires an external covering to provide multiple functions. First, it must provide an impermeable barrier against the aquatic environment. Second, it should provide tactile and proprioceptive sensory capabilities. Finally, it must provide a high degree of mechanical functionality, including the ability to deform under high strains and strain rates, mechanical protection from, and interaction with, substrates and additionally, some degree of mechanical actuation.

The purpose of this review is to identify existing biomimetic technologies, that may be appropriate in fulfilling the criteria detailed above. Additionally, we need to consider other technologies having the potential to contribute to the requirements of the compliant skin of the octopus artefact. We consider technologies that may be appropriate in adding sensing and actuation capabilities to the octopus skin.

At this stage in the project, we need to be mindful that the outputs of WP4 will include an analysis of the mechanical functionality of the skin of the octopus. These data, and the knowledge we gain from them, will refine our selection of appropriate material characteristics needed in the design of the prototype skin (WP 12).

In the following sections, we describe candidate technologies to provide actuation, review the role of fibres in biology, consider technologies for fibrous skins with sensors and, finally, review relevant biomimetic skin technologies.

5.2 Artificial Muscle

Natural muscles are both compliant and exhibit linear behavior (Full & Meijer, 2004). Making lifelike robots requires emulating these capabilities and the closest material systems with similar characteristics are the electroactive polymers (EAP) (Bar-Cohen, 2008]. For this property, EAP materials gained the name “artificial muscles” (Bar-Cohen, 2004).

Bar-Cohen (2004) divided EAP materials into two major groups based on their activation mechanism: ionic and electronic.

According to Bar-Cohen (2008), the electro-activity of ionic EAP materials involves transport or diffusion of ions. They consist of two electrodes, a polymer film and electrolyte and examples of these materials include conductive polymers, ionic polymer gels, polymer-metal composites, and carbon nanotubes. Their advantages are the need for low activation voltage (1-2 Volts) and generating large bending displacement. Their disadvantages are the need to maintain hydration, the relatively low force generation and they don't sustain constant displacement under activation of a DC voltage (except for conductive polymers).

In contrast to the ionic EAP, the electronic EAP are driven by Coulomb forces and they are activated by high voltages that can be as high as 200-V/ μm . Examples of these materials are electrostrictive, electrostatic, piezoelectric, and ferroelectric. This type of EAP materials can be made to hold the induced displacement while operated under a DC voltage, allowing them to be considered for robotic applications. These materials have a greater mechanical energy density and they can be activated in air with no major constraints. However, the electronic EAP require high activation field that may be higher than the electric breakdown level. EAP materials are still custom made mostly by researchers and they are not available in commercial quantities. To help in making these materials widely available, Bar-Cohen established a website that provides fabrication procedures for the leading types of EAP materials as well as website about sources for purchasing of custom made materials and samples [<http://eap.jpl.nasa.gov>] (Bar-Cohen, 2008).

There are two requirements: fast response, large strain (at force levels to be determined)

One of the key factors to obtain large displacements and high efficiency with dielectric electroactive polymer actuators is to have compliant electrodes (Duboid, Rosset, Nikius, Dadras & Shea, 2004). Most macrosized DEAs have electrodes made of conducting grease or powder (metal or graphite) (Carpi & Rossi, 2004). These techniques work well for devices whose area is greater than 1 cm² (Duboid, et. al., 2004).

Sommer-Larsen, Hanse & Benslimane (2008) have proposed a design of smart compliant electrodes. One design is with a sinusoidal corrugated profile.

Gong, Katsuyama, Jurokawa & Osada (2003) have developed double network hydrogel with mechanical strength exceeding 17 MPa (Furukawa & Gong, 2008).

Kaneto, Suematsu & Yamato (2008) studied the training effect of conducting polymer soft actuators based on polypyrrole and found that a training of an artificial muscle fabricated

with conducting polymers is feasible. Training effect was observed as the increased strain after an experience of heavier tensile stress.

5.3 Fibre orientation in soft materials from Nature

Fibres are the most frequent motives in the design of natural materials. They can be based on very different chemical substances, such as sugars, for example. Indeed the polysaccharides cellulose and chitin are the most abundant polymers on earth. The first reinforces most plant cell walls and the second is found for example, in the carapaces of insects. Other types of strong fibres are based on proteins, such as collagen, keratin and silk. The first can be found in skin, tendons, ligaments and bones; The second in hair and horn. Spider silk is among the toughest polymer filaments known to date (Fratzl & Weinkamer, 2007).

Without accurate control of fibre architecture, many animals and plants would collapse (Neville, 1993). Constructing with fibres requires a special design and it will be very helpful to see how nature designs fibre reinforced composite materials.

Figure 1 shows nine types of structures linked together by arrows (Neville, 1993).

Each has different mechanical consequences. There are

Parallel fibres arrays;

crossed fibrillar arrays/crossed helical arrays;

felt-works in which the fibres are more randomly arranged with some fibres going through the thickness of the materials.

In each arrangement, there are two distinguished systems: continuous and discontinuous fibre systems. Indeed, in multilayered fibre systems several fibre orientations can be combined to produce desirable effects in relation to structural deformability.

The term continuous as is used in (Fratzl & Weinkamer, 2007) does not necessarily imply that individual fibres extend through the entire material. It means that there is mechanical continuity within the fibre system, such that at some point in the extension of the material, the load will be applied directly to the fibre component. This continuity can be achieved either by having long fibres with traverse the full extent of the tissue or by having shorter fibres linked together at junction points by strong cross links. In a discontinuous fibre system the fibres may become aligned in the direction of stretch during extension, but the load is transferred from fibre to fibre through the matrix and not applied directly to the fibres alone.

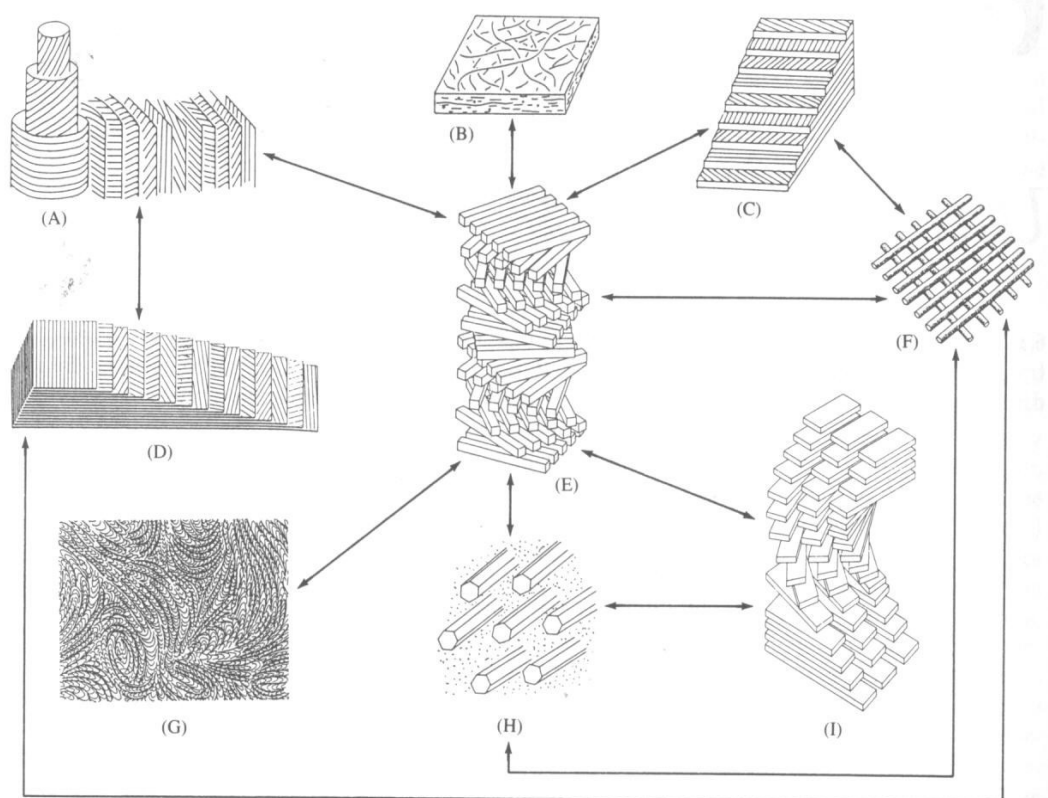


Figure 1. Evidence for a common Origin of the diversity of fibrous composite architectures. (A)

Cylindrical helical (double twist) grading into planar helical (single) twist). Example: bone, haversian system. This is the analogue equivalent of blue-phase liquid crystals. Bone can change from helical to orthogonal within an individual cylindrical osteon. (B) Planar random layer. Example: parts of some plant cell walls. (C) 45° helical. Example: dogfish eggcase (*Scyliorhinus*). Other systems are arranged at other angles (e.g. 60° in *Polynoe* scale worm). (D) Twisted orthogonal. Examples: fish scales, vertebrate cornea (fish, frog, turtle, birds). (E) Monodomain helical (small rotation angle). Examples: insect cuticles, some plant cell walls, many cysts and eggshells. This is the analogue equivalent of cholesteric liquid crystals. (F) Orthogonal. Examples: basement lamella in vertebrates and a flatworm; cuticles of cylindrical animals. (G) polydomain helical. Example: mentis eggcase proteins. (H) Parallel (unidirectional). Examples: tendons in arthropods and vertebrates, daytime layers in insect cuticle. This is the analogue equivalent of nematic liquid crystals. (I) Pseudoorthogonal. Examples: wood tracheids, endocuticle in some parts of adult beetles, bugs, stick insects, and dragonflies. Layers only appear to change abruptly through a large rotation angle; there is actually an intervening thin sandwich of helical. After Neville [11].

Parallel arrays of continuous collagen fibres are materials like tendon and are purely tensile in nature. Parallel arrays of discontinuous fibres, are important in pliant composites, as this arrangement provides a means of reinforcing the material in one particular direction. In fact any concentration of parallel or preferentially oriented,

discontinuous fibres will result in mechanically anisotropic material (Fratxl & Weinkamer, 2007).

5.3.1 Hydrostats of Fixed Fibre Length

Figure 2 shows two ways of fibre arrangements for a cylindrical surface (Vogel, 2003). The arrangement with longitudinal and circumferential fibre reinforcement does not deform in response to pushes or pulls-compression or tension- on the whole cylinder. It also has higher bending stiffness. Conversely, the arrangement shown in (b) can change shape smoothly as it is pulled and pushed. The driving force for deformation can be, for example, a swelling polymer system. It bends more easily as well. With few exceptions, nature uses the second arrangement of fibres for her internally pressurised, water-filled cylinders.

Crossed fibrillar or crossed helical arrays of continuous fibres provide the structural basis of the body wall connective tissues and cuticles of most of the worm-like animals and a number of vertebrates as well (Nadol, Gibbins & Porter, 1969, Olsson, 1964).

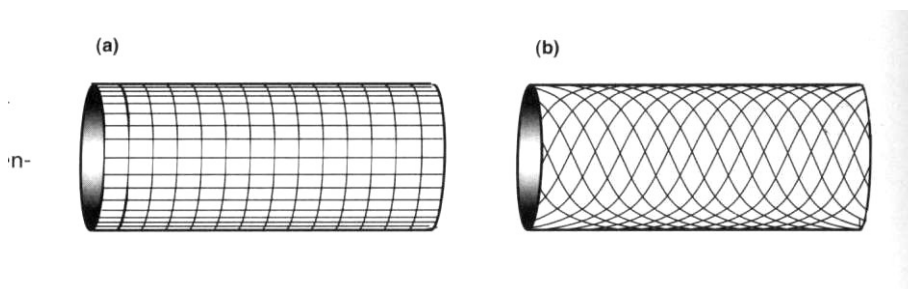


Figure 2. Two contrasting ways to arrange fibrous reinforcement in the membrane of an internally pressurised cylinder. A. fibres run lengthwise and circumferentially, b. fibres run in right- and left-hand helices (After Vogel, 2003).

Figure 3 shows the effect of fibre angle relative to the axle of the cylinder on the volume change of the structure.

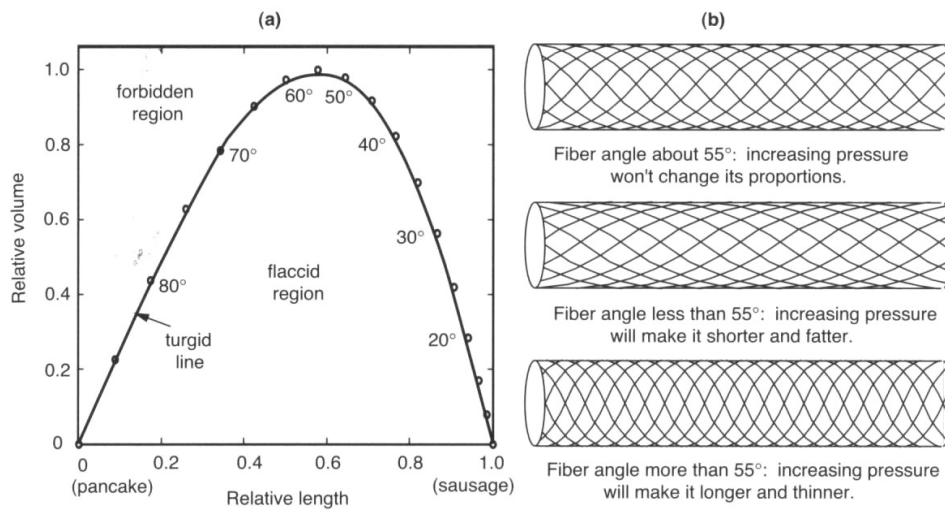


Figure 3. (a) the changes in volume and fibre angle as the length of the helically wound cylinder varies. The length of each fibre (and thus of the fully extended cylinder) has been arbitrarily set at 1.0. Beneath the curve the cylinder isn't fully inflated and so isn't circular in section; above the curve it would be impossibly overinflated. (b) The appearance of representative cylinders, and the practical consequences of their different fibre angles.

Figures 4 and 5 shows some examples of fibre arrangement in animals. After Vogel (2003).

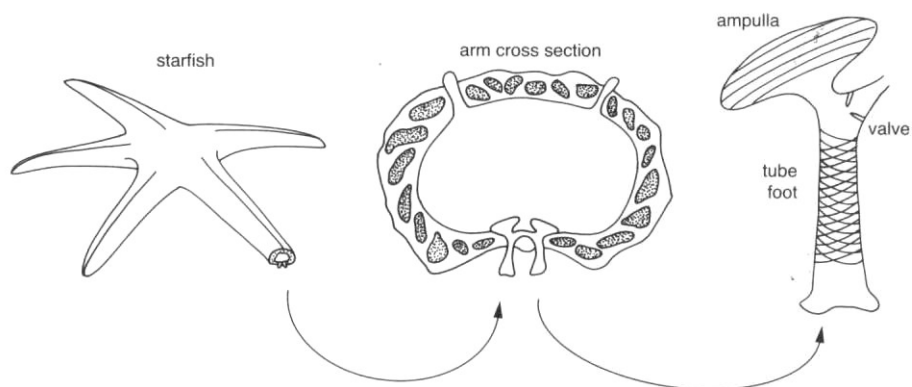


Figure 4. the layout of the tube foot and ancillary gear of a starfish or other echinoderm. After Vogel (2003).

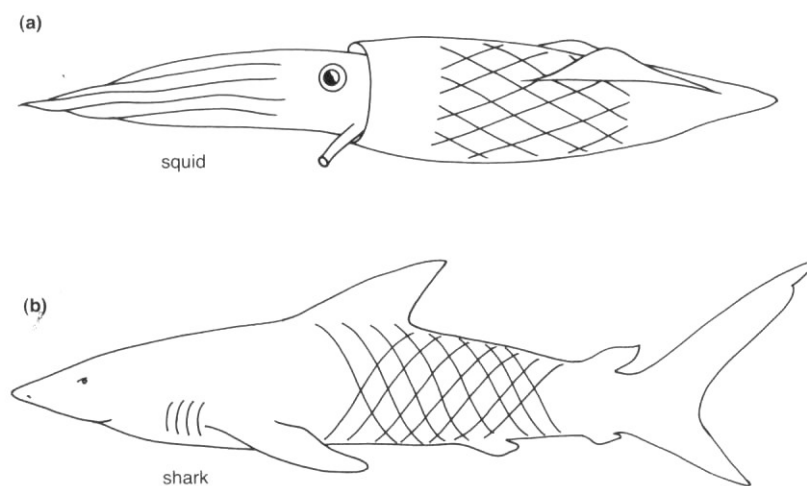


Figure 5. Fibre arrangements. (a) A squid and its outer mantle. (b) A shark. After Vogel (2003).

5.3.2 Pennate Muscles

A short, wide muscle produces relatively more force but shortens less far than does a long narrow one of the same volume and work output (Vogel, 2003).

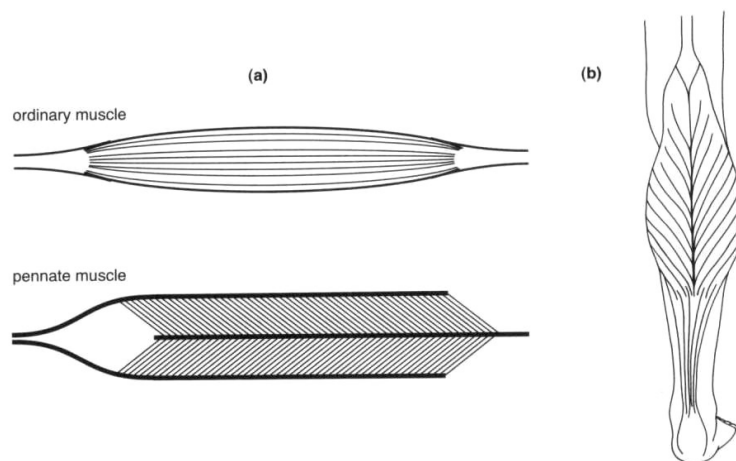


Figure 6. (a) The arrangement of fibres in ordinary and pinnate muscles. (b) The human gastrocnemius, a pinnate muscle, in situ. After Vogel (2003).

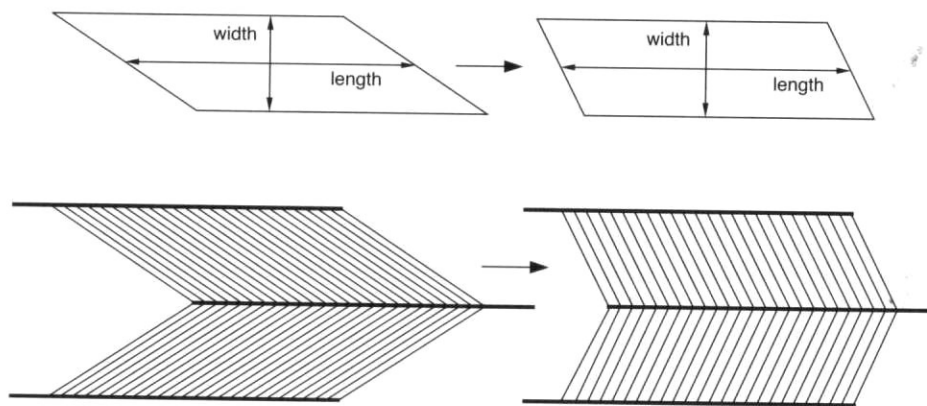


Figure 7. How pinnate muscle works as a constant-volume system: contraction leaves width and length- and hence area and volume unchanged. After Vogel (2003).

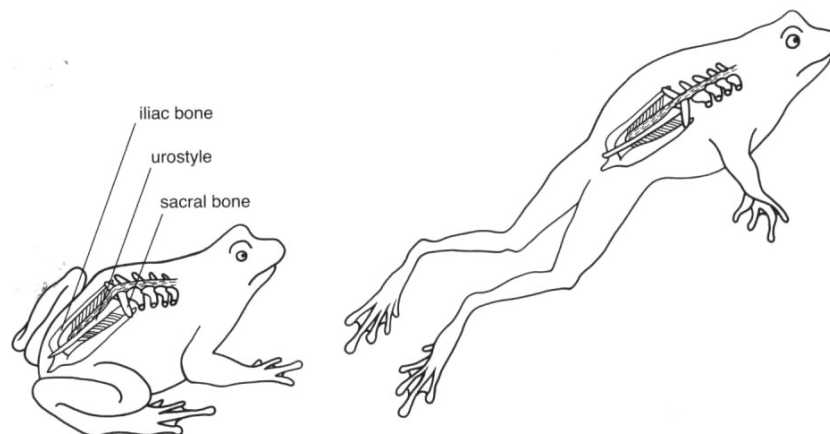


Figure 8. (a) the arrangement of iliac bones, sacral bones, and urostyle, in a frog. (b) When it jumps, contraction of the diagonal muscles between urostyle and ilia straightens out the frog's back and thus adds additional extension to what the legs provide. After Vogel (2003).

5.3.3 Muscular Hydrostats as Antagonists and levers

The structure of tongues, octopus tentacles and elephant trunks are mostly muscle systems. Muscle systems operate at constant volume. One characteristic of muscle fibres is that they actively shorten, but don't lengthen except as pulled upon by some external forces.

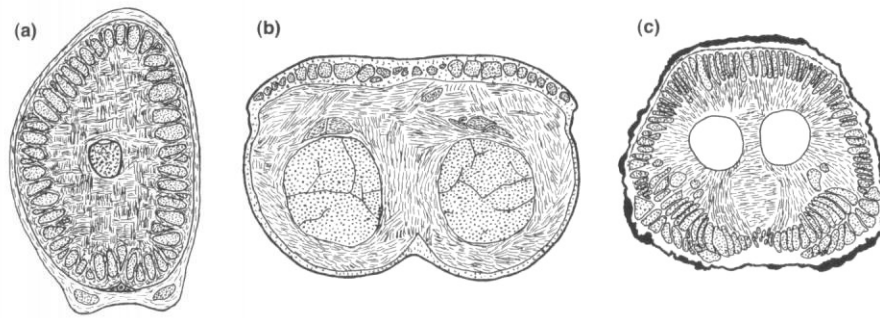


Figure 9. Cross sections of (a) squid tentacle, (b) lizard tongue, and (c) elephant trunk. After Kier and Smith (1985).

Kier and Stella (2007) studied the structure of Octopus arm and found that there are three kind of muscle fibre:

transverse muscle fibres oriented in planes perpendicular to the long axis of the arm;

2) longitudinal muscle fibres oriented parallel to the long axis; and

3) oblique muscle fibres arranged in helixes around the arm. The proportion of the arm cross section occupied by each of these muscle fibre groups (relative to the total cross sectional area of the musculature) remains constant along the length of the arm, even though the arm tapers from base to tip. A thin circular muscle layer wraps the arm musculature on the aboral side only.

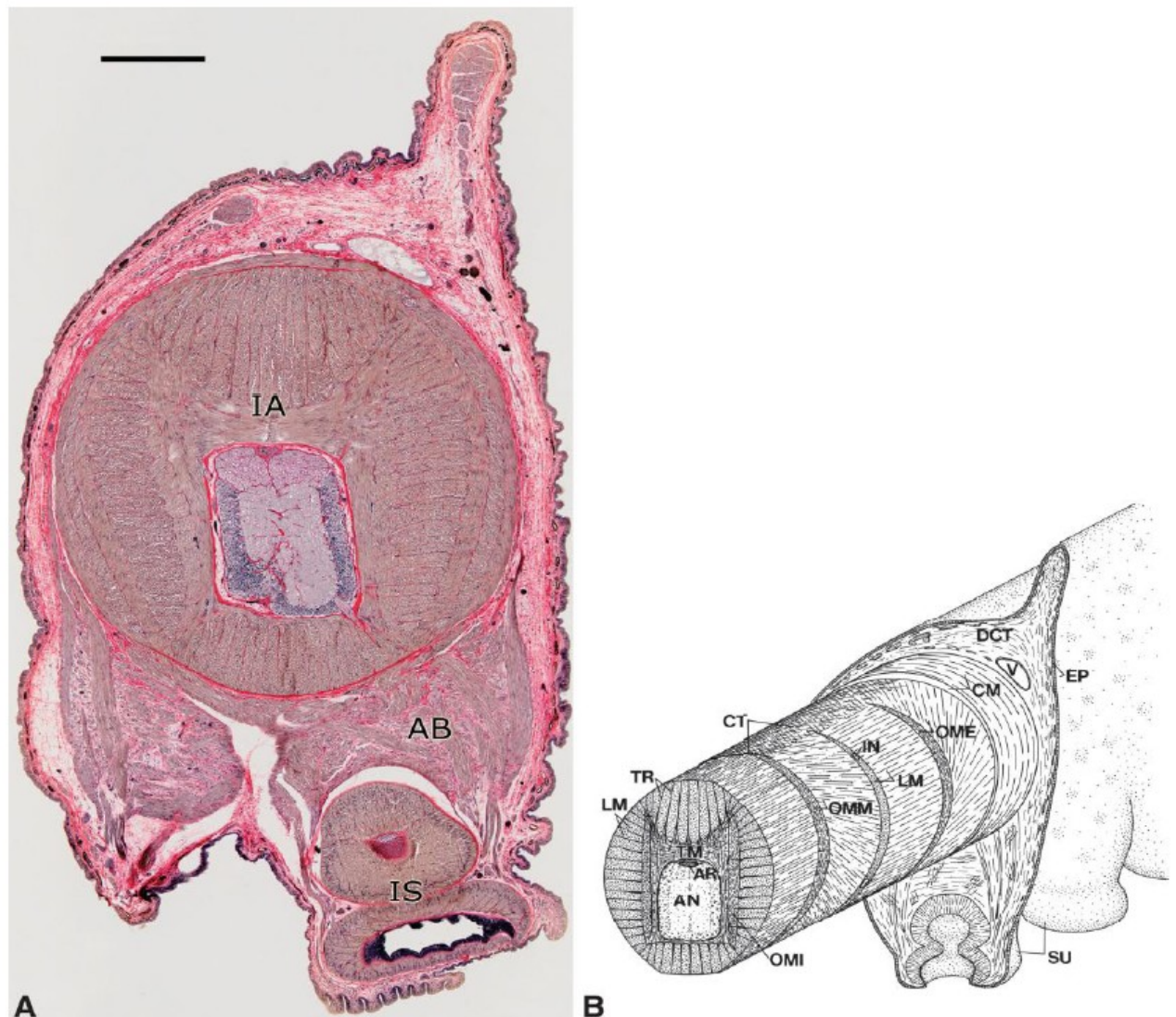


Fig.10 A: Transverse section of the arm of *Octopus bimaculoides* showing the three major subdivisions of the arm musculature: the intrinsic arm musculature (IA); the intrinsic sucker musculature (IS); and the acetabulo-brachial musculature (AB) connecting the arm and sucker musculature. Scale bar: 0.5 mm. Brightfield microscopy of 10- μ m-thick paraffin section stained with Picro- Ponceau and hematoxylin. B: Diagram of the arm of *Octopus* showing three-dimensional arrangement of muscle fibres and connective tissue fibres. AN, axial nerve cord; AR, artery; CM, circumferential muscle layer; CT, connective tissue; DCT, dermal connective tissue; EP, epidermis; IN, intramuscular nerve; LM, longitudinal muscle fibres; OME; external oblique muscle layer; OMI, internal oblique muscle layer; OMM, median oblique muscle layer; SU, sucker; TM, transverse muscle fibres; TR, trabeculae; V, vein. After Kier and Stalla (2007).

Analysis of arm morphology from the standpoint of biomechanics suggests that the transverse musculature is responsible for elongation of the arms, the longitudinal

musculature is responsible for shortening, and the oblique muscle layers and associated connective tissues create torsion. Arm bending may involve unilateral contraction of longitudinal muscle bundles in combination with resistance to arm diameter increase due to contraction of the transverse musculature or passive stiffness of the arm tissues. The arms may also be bent by a combination of decrease in diameter due to contraction of the transverse musculature and maintenance of constant length on one side of the arm by unilateral activity of longitudinal muscle bundles. An increase in flexural stiffness of the arm may be achieved by contraction of the transverse and longitudinal muscle. Torsional stiffness may be increased by simultaneous contraction of both the right- and left-handed oblique muscle layers.

5.4 Smart textile and tissue engineering

Method of fibre arrangement used in the architecture of soft biomimetic materials can be hardly found in the literature. But technologies could be used in the design of octopus skin are available.

5.4.1 Carbon nanotube yarns

Carbon nanotubes are of great technical interest because of their high stiffness and strength, good electrical conductivity, excellent thermal conductivity, and good thermal stability at both low and high temperatures. A difficulty has been absence of reliable methods of controlling assembly of the large number of carbon nanotubes required for practical application (Atkinson, Skourtis & Hutton, 2008, Mirfakhrai, Oh, Kozlov, Fang, Zhang, Baughman & Madden, 2008). Atkinson, et.al (2008) at the University of Texas developed a method of dry-spinning of twisted yarns of CNTs directly for a forest of CNTs (Zhang, Artkinson & Baughman, 2004, Atkinson, et.al, 2008). The yarn strength changes with the twisting angle of the nanotubes and reaches the maximum of 600MPa when the twisting angle is around 45°.

The best chance of success applications will be based on the electrical properties of the yarns; in particular, those that exploit the unique structure associated with the CNTs, until yarn strength are substantially increased.

Mirfakhrai, et al (2008) used twist-spun yarns of multi-walled carbon nanotubes to make eletromechanical actuators and force sensors. Strains of up to 0.6% at stresses of up to 200MPa have been achieved in actuation mode. While sharp and easily detectable current spikes of up to 75 nA are generated in the sensory mode.

5.4.2 Textile as sensors and monitors

Stylios and Wan (2008) investigated smart membranes and coatings by in situ synthesis of iron oxide nanoparticles in PVA hydrogels. They found that the combination of magnetic properties of iron nanoparticles with the biocompatibility of PVA suggests that these materials have a great potential to be used as drug delivery system. Ferrogels at

an optimal mixture of PVA and Fe₃O₄ display magnetic-sensitive behavior that permits them to be applied as microdevices for delivery of drugs in a highly controllable manner.

Textile can be used as sensing and measuring devices of body parameters by coating textile surfaces with metal. Schwarz, Hakuzimana, Gasana, Westbroek & Langehove (2008) successfully coated gold on PPy-copper coated polyester yarns. The application of metal coated textile can be health monitoring, heatable textile for garments, interior and technical textiles and environmental sensing and communication technologies for security personnel and workers at risk (Paradiso & Rossi, 2006, Carpi & De Rossi, 2005, Hertleer, Van Langgenhove & Puers, 2006, Mattila, Talvenmaa & Maekinen, 2006, Lymberis & Olsson, 2003, Proetex Project, 2008).

A research group at the University of Manchester have been working on the development of electrically active textiles using knitted structures. Knitted structures have good tensile recovery properties, superior drapability, which would provide excellent skin contact, and good breathability, as well as the potential for large deformations (depending on knitting pattern) (Wijeyesiriwardana, Dias, Mukhopadhyay, 2003, Dias, Hurley, Monaragala & Wijeyesiriwardana, 2008). They used the latest knitting technology to develop knitted heating structures using electro conductive fibres of different conductivity levels and non conductive yarns, DC equivalent Circuit of stitched textiles, and knitted finger touch sensitive switches using modern flat-bed knitting technology. The electronically functional chips are integrated with textile fibres by either inserting the chip into a textile fibre or encapsulating the chip within a bundle of fibres (Dias, et.al, 2008).

Recently, products enhancing electronics with textile functions and textiles with functions rely on electronics have emerged. Examples of these products include Polar's breast strap heart rate monitor, the MET5 jackets by The North Face, an electrical heating for the wearer's body, and the music playing jackets by Interactive Wear. But the reliability of the conductive embroidery around the transfer mold packages needs to be improved (Linz, Vieroeth, Diles, Koch, Braun, Becker, Kallmayer & Hong, 2008).

Narbonneau, Kinet, Paquet, Dapre, Jonckheere, Logier, Zinke, Witt & Krebber, (2008) have embedded optical fibre sensors in to textile for healthcare monitoring during magnetic Resonance Imaging.

5.4.3 Other Smart textiles

Polyvinylidene fluoride (PVDF) based electrospun nanoweb fibres with outstanding piezo-, pyro- and ferroelectric behavior are being intensely studied by many researchers, especially for touch-sensor applications. The properties of the synthetic fibres tend to

improve significantly with decreasing diameter toward nanoscale thickness (Yoon, prabgu, Ramasundaram & Kim, 2008).

Jimenez, Rocha, Aranherrri, Covas & Catarino (2008) studied the conductive polymer composites filaments of PP (polypropylene) with carbon black, carbon black with high conductivity and carbon fibres. They found that the electrical conductivity of the mono-filaments developed is not satisfactory due to the structure homogeneity problems and the possible aggregation of conductive materials. The mixing step, necessary to facilitate the filaments production, was no as efficient as improving the conductive filler dispersion (Jimenez, et.al. 2008).

Touching behavior of textile is an extremely important sense for human (Meinander, 2008). The HAPTEX project funded by European Commission is to develop a multimodal virtual reality system able to render the behavior of textiles haptically and visually.

5.4.4 Technologies for biomimetic skins

A key challenge in the development of soft-bodied robots is the development of functional skins. Skins may be expected to fulfil a variety of functions; physical protection, sensing and mechanical containment. Broadly speaking, given the requirement for working strains up to 130%, there are two main approaches to fabrication, either by use of a continuous elastomeric film or by use of woven textiles. There is also the possibility of using elastomeric fibres in woven, knitted or braided structures. Both classes of materials can be manufactured so as to function at both the high strains and strain rates observed in cephalopod tentacles (Kier & Leeuwen, 1997).

A comprehensive search of literature (conducted by using the ISI Web of Knowledge databases) has revealed a paucity of literature concerned with the design and manufacture of smart biomimetic skins. Most attempts to mimic functionality of skins have been based on research in the biomedical field. Broadly, these artificial skins are characterised as either acellular (manufactured from polymers) or cellular (composed of cultured skin cells on a biocompatible scaffold). Acellular graft materials frequently use collagen (of animal origin), polymeric fibres and silicone membranes (Supp & Boyce, 2005). Their function is markedly different than that required for the Octopus robotic tentacle, in that their role is to control moisture loss from the wound site and an impede microbial contamination. These materials also form a scaffold for subsequent regeneration of skin cells.

A team at Kyoto University, Japan, developed a method which employs water present in swollen hydrogels as a porogen for shape template and was suggested for preparing porous materials (Kang, Tabata & Ikada, 1999). Biodegradable hydrogels were prepared

through crosslinking of gelatin with glutaraldehyde in aqueous solution, followed by rinsing and washing. After freezing the swollen hydrogels, the ice formed within the hydrogel network was sublimated by freeze-drying. This simple method produced porous hydrogels. Results suggest that the porosity of dried hydrogels can be controlled by the size of ice crystals formed during freezing. Figure 10 show two pictures of gelatine hydrogels freeze-dried following freezing at two different conditions (Kang, et. al, 1999).

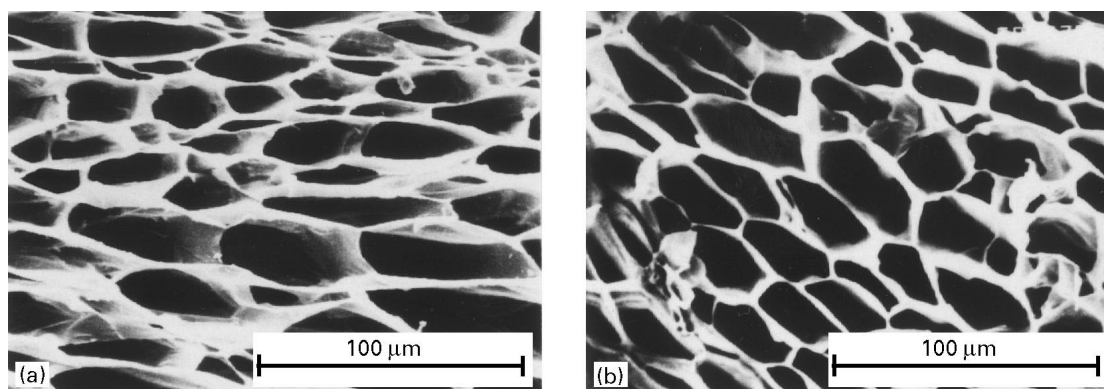


Figure 11. SEM micrographs of horizontal cross-sections of gelatin hydrogels freeze-dried following freezing (a) at -80°C and (b) in N₂(l). After Kang, et. al. [1999]

Lee, Jeon, Leea, Lee, Song, park, Nam & Ahn (2003) also used this method to produce porous scaffolds composed of gelatin and β -glucan.

A Group of researchers in Germany creating scaffolds with vascular structures using acellular porcine jejunum (Mertsching, Walles, Hofmann, Schanz & Knapp, 2005). This scaffold may answer the problem of bioartificial graft vascularization, which is an inalienable prerequisite for the generation of clinically applicable bioartificial tissues and organs of sufficient strength and size. This method is briefly illustrated in Figure 12

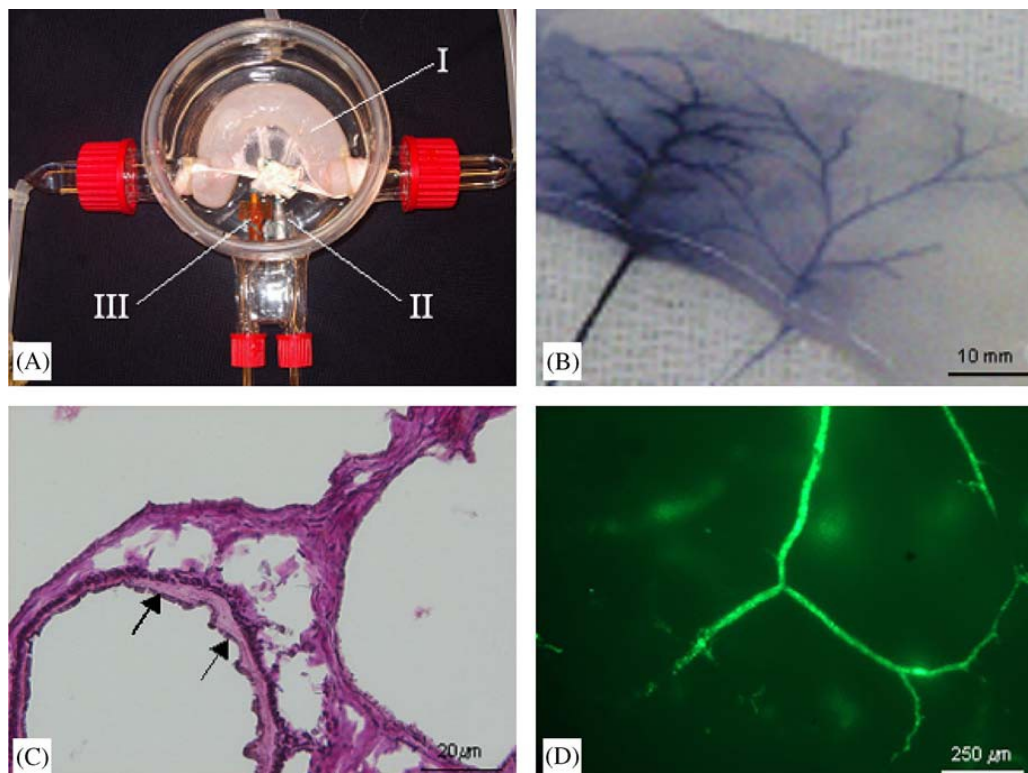


Figure. 12. Biological vascularized scaffold (BioVaMs). (A) The decellularized porcine small segment (I) is transferred into the bioreactor perfusion setup. Cell culture medium is infused via the cannulated arterial pedicle (II) and recovered from the venous pedicle (III). (B) Blue dye injected into the decellularized arterial pedicle stains tubular capillary structures in the acellular matrix. (C) Preserved vascular basal membrane (arrow) stained by Elastica van Gieson staining. (D) Reseeded, CDSFE labeled bmEPC forming capillary tubular structures within the matrix (Mertsching, et.al, 2005).

Integra™ artificial skin (Integra LifeSciences Corp., Plainsboro, NJ, USA) is a dermal template consisting of bovine collagen, chondroitin-6-sulphate and a silastic membrane manufactured as Integra™. This product has gained widespread use in the clinical treatment of third degree burn wounds and full thickness skin defects of different aetiologies. The product was designed to significantly reduce the time needed to achieve final wound closure in the treatment of major burn wounds, to optimise the sparse autologous donor skin resources and to improve the durable mechanical quality of the skin substitute (Kremer, Lang & Berger, 2000).

Young, Wu & Tsou in Taiwan (1998) developed pHEMA artificial skins reinforced with different fibre material and fibre arrangement, as shown in Figure 13. Results of their research show that knitted elastic spandex fibre reinforced pHEMA membranes have low Young's modulus of (16 Nm^{-2}) and higher strengths (13.98 MPa) and elongation at break (about 500%) (Young, et.al. 1998).

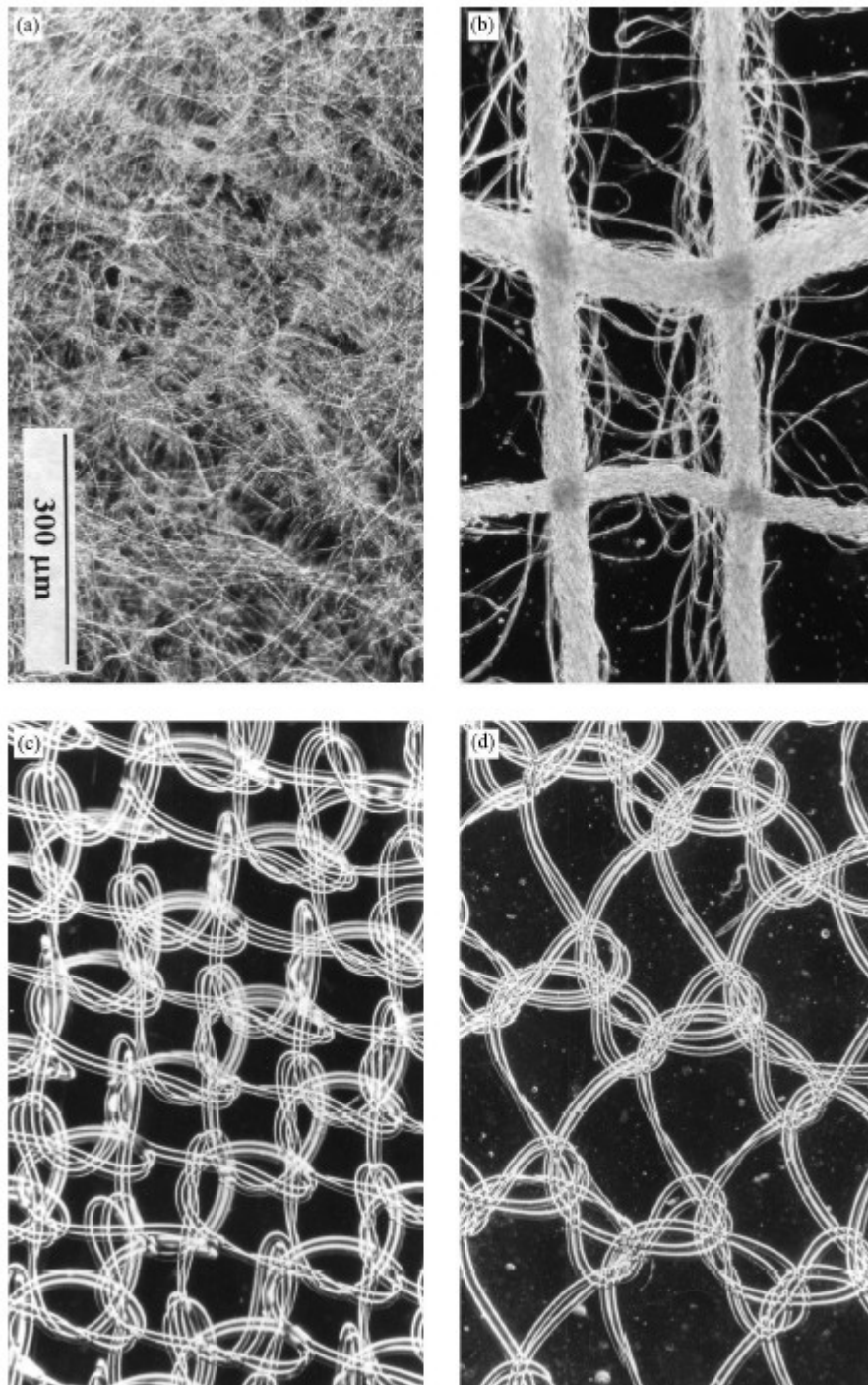


Figure 13 Microscopic morphologies of the fibre-reinforced pHEMA membranes(Young, et.al. 1998).

5.4.5 Application of Silk in Stem cell-based Tissue engineering

Silks are naturally occurring polymers that have been used clinically as sutures for centuries. When naturally extruded from insects or worms, silk is composed of a filament core protein, termed fibroin, and a glue-like coating consisting of sericin proteins. In

recent years, silk fibroin has been increasingly studied for new biomedical applications due to the biocompatibility, slow degradability and remarkable mechanical properties of the material (Wang, Kima, Vunjak-novakovicb & Kaplana, 2006) Wang and coworkers (2006) reviewed research in this area and concluded that the wide range of molecular structures, remarkable mechanical properties, morphology control, versatile processability and surface modification options make silk fibroin an attractive polymeric biomaterial for design, engineering and processing into scaffolds for applications in controlled drug delivery, guided tissue repair and functional tissue engineering. 3D porous or fibre silk fibroin scaffolds with surface morphology, useful mechanical features, biocompatibility, and ability to support cell adhesion, proliferation, and differentiation have expanded silk-based biomaterials as promising scaffolds for engineering a range of skeletal tissues like bone, ligament, and cartilage as well as connective tissues like skin. The generally slow rates of degradation of silk fibroin in vivo, coupled with the versatile control of structure, morphology and surface chemistry, offer a range of utility for this family of protein polymers in many needs in biomaterials and tissue engineering (Wang, et.al, 2006).

5.5 Examples of Biomimetic Sensors

5.5.1 Biomimetic fin

A research in China have successful developed biomimetic fin for cuttlefish (Wang, Hang, Wang, Li & Du, 2008). Figure 14 show the muscular structure of the cuttlefish fin and Figure 14 show the biomimetic substitute of the structure. The biomimetic fin mimics the structure of the cuttlefish fin segment, and Shape Memory Alloy (SMA) wires act as biomimetic muscle fibres. The biomimetic fin consists of a holder, SMA wires made of TiNi alloy, skins made of silicone, elastic substrate made of PVC and conducting wires. As well as SMA wires (actuated by temperature), there are now piezoceramic material available in fibre form, using electrical actuation.

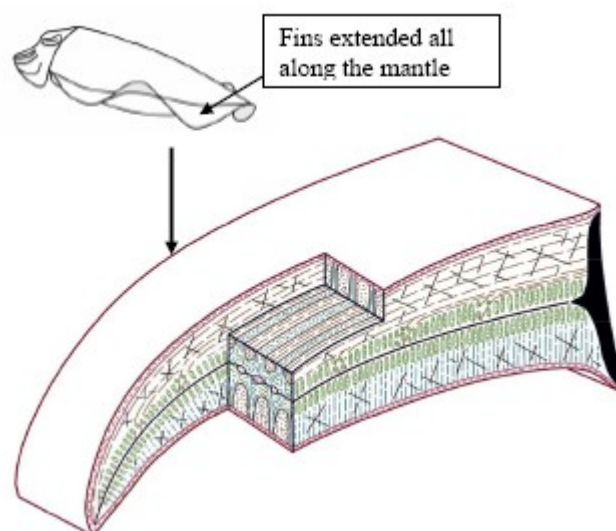


Figure 14. Schematic diagram of cuttlefish and the musculature of the cuttlefish fin, After Wang, et.al, 2008.

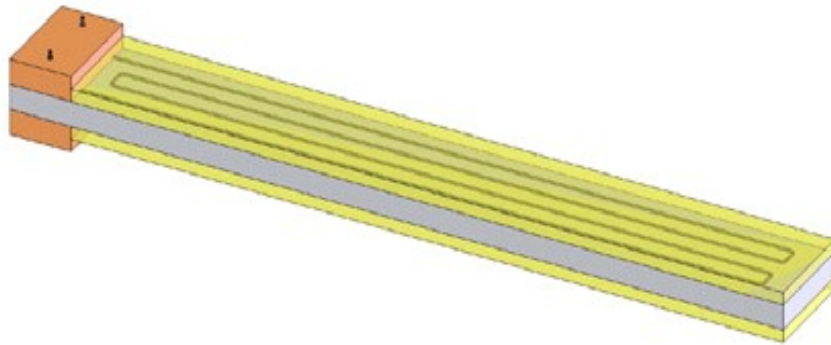


Figure 15. Structure of a dual-face biomimetic fin. After Wang et.al. (2008).

5.5.2 Biomimetic Fingerprinted Sensors

Scheibert, leurent, Prevost & Debregeas (2009) studied the process of the tactile perception of fine textures of human hands and the function of the fingerprints in this process by measuring the vibration frequencies and contact forces between fingertip and the receptor. They then developed a biomimetic finger with straight ridges (Scheibert, 2009) The sensing element consists of a microelectro mechanical system (MEMS) device that provides force measurements in a region of millimetre extension. The skin of the sensor is made of cross-linked poly(dimethylsiloxane) (PDMS) and has a maximum thickness of 2mm.. They found that the orientation of the fingerprints also plays an important role in the tactile perception of textures. MEMS-based hair-arrays sensor devices are also been developed as part of the EU CILIA project published at the internet address: <http://www.cilia-bionics.org> and could be adapted as touch sensors.

5.5.3 Biomimetic Sensor for a Crawling Minirobot

A research team at Pisa Centre for research in microengineering, have developed “a biomimetic sensor with the ability to imitate exteroceptor and proprioceptor functions of invertebrate, such as earthworms. A polyvinylidene fluoride (PVDF) film was selected as the sensing element because it is flexible, highly sensitive and easy to be integrated in different shapes. Perforated PVDF strips are embedded in a segmented silicone shell of a crawling earthworm minirobot with the ability to elongate and contract. The actuator is smartly configured using shape memory alloy. A 4-segment minirobot with a sensorised

skin has been fabricated. Experiment results show that the biomimetic PVDF-based sensors can detect both the external contact and the internal actions, thus imitating the exteroceptive and proprioceptive sensing capabilities of real earthworms (Liu, Menciassi, Scapellato, Dario & Chen, 2006).

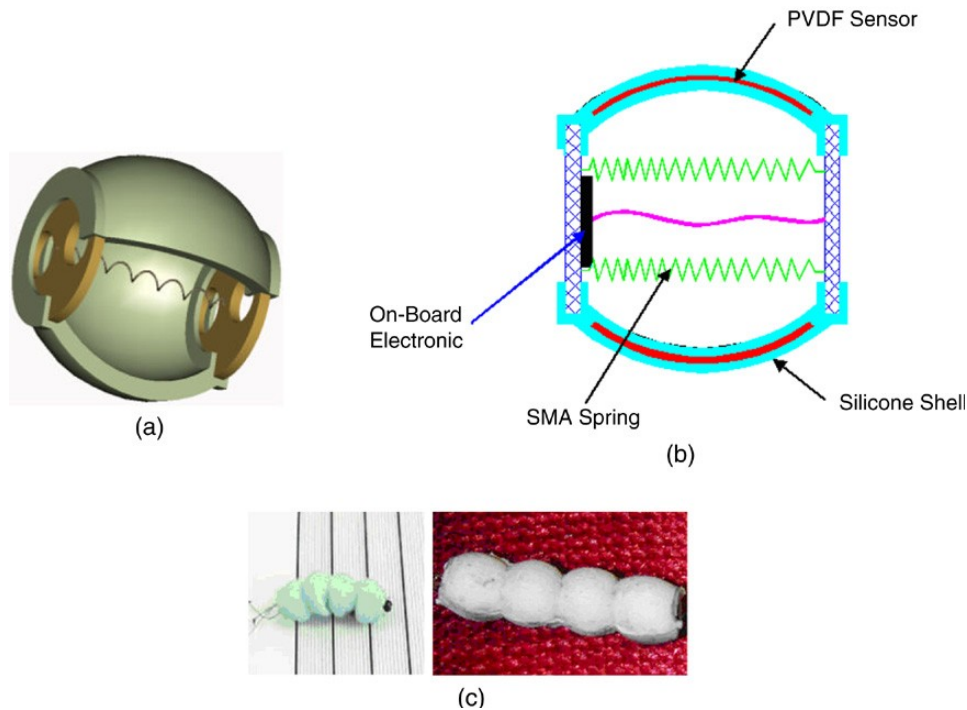


Figure16. (a) Artificial earthworm segment. (b) sensor layout and (c) crawling earthworm minirobot prototypes, (Liu, et. al, 2006)..

5.6 Conclusions

Our review of published literature indicates a paucity of biomimetic compliant skin technologies. The nearest equivalent technologies are found in biomedicine, specifically in artificial skins for wound healing. These technologies do have limitations when considering the octopus application, primarily due to the functions for which they have been designed. Biomedical artificial skins are designed with the purpose of preventing microbial contamination, tissue fluid loss from the site of injury and a scaffold for repopulation by skin cells. They cannot, therefore, be regarded as offering a similar mechanical performance to skin, as this is provided by regenerated skin cells.

The knowledge that epidermal tissues contain fibres of fine-tuned orientations allows us to consider how fibres can be best used to optimise both mechanical and sensing functionality. Advances in coating technologies and carbon nanotube fabrication provide the opportunity to incorporate strain sensing functionality, within fibrous layers, by exploiting the variable resistance properties these materials exhibit. This offers the opportunity to use fibres having both mechanical functionality and sensory feedback.

Finally, we describe three biomimetic technologies which have potential application to the skin of the artefact. The use of SMA wires has been demonstrated to provide a useful actuation technology in another project involving the manufacture of biomimetic actuated structures in a cephalopod-inspired robotic system, namely a fin for a cuttlefish robot. The flapping motion this generates may not be applicable to the locomotory and manipulative tasks required in the octopus, but at least demonstrates the feasibility of incorporating SMAs in thin, polymeric structures. Regarding sensing, the two technologies identified (fingerprints and PVDF sensors) may have applications in the tactile sensors of the octopus.

This review identifies some starting points for the design of the sensorised skin, however, there are further issues, to be addressed in WP8, which will inform our design. Most important is the question of the degree of actuation required in the flexible skin, particularly whether will it be required to provide a mechanical constraint for dimensional changes in the actuators within the arm. This really concerns whether the functionality of oblique muscles found in the arm of the octopus needs to be mimicked in the skin, or beneath it.

One final, and important, future consideration is the means by which the limbs of the artefact will adhere to target objects. It is possible that the fabrication of analogues of suckers may prove difficult, in which case the design considerations of the skin may additionally include a requirement for tailored frictional/adhesive properties in contact areas of the limb, so as to allow manipulation of objects.

In summary, our reviews of the literature have identified only limited reference to biomimetic technologies addressing the technical problems faced in the fabrication of the skin for the octopus artefact. Whilst this means there is no 'off-the-shelf' solution giving the desired performance characteristics, it does give the opportunity for the OCTOPUS consortium partners the exciting opportunity to develop a new class of biomimetic, compliant skin-like materials.

6. References

SURVEY OF SENSORS AND ACTUATION TECHNOLOGY

1. Analog VLSI Implementation of Neural Systems, Mead, C. & Ismail, M. (ed.) Norwell: Kluwer Academic Publ, 1989.
2. Attneave, F., "Some informational aspects of visual perception", *Psychological Review*, 1954, Vol. 61(3), pp. 183-193.
3. B. Morten, G. De Cicco, and M. Prudenziati, "Resonant pressure sensor based on piezoelectric properties of ferroelectric thick films", *Sensors and Actuators A*, 31:153–158, 1992.
4. B.L. Gray and R.S. Fearing "A surface micromachined microtactile sensor array" In *Proc. of the 1996 IEEE Int. Conf. On Robotics and Automation*, 1996.
5. Bandera, C., "Foveal Machine Vision Systems", PhD Dissertation, SUNY Buffalo, New York, 1990.
6. Brusca, R. & Brusca, G. "Invertebrates", Sinauer Associates, 1990
7. Burschka, D., Geiman, J. & Hager, G. "Optimal landmark configuration for vision-based control of mobile robots", *Proceedings of the IEEE International Conference on Robotics and Automation*, 2003, Vol. 3, pp. 3917-3922.
8. C. Domenici and D. De Rossi, "A stress-component-selective tactile sensor array", *Sensors and Actuators A*, 31:97–100, 1992.
9. D. Grant, V. Hayward. "Constrained Force Control of Shape Memory Alloy Actuators". *International Conference on Robotics and Automation*. San Francisco, CA, USA. April 2000.
10. D.T. Pawluck, J.S. Son, P.S. Wellman, W.J. Peine, and R.D. Howe, "A distributed pressure sensor for biomechanical measurements", *Journal of Biomechanical Engineering*, 1996.
11. E. Cheung and V. Lumelsky, "Development of sensitive skin for a 3rd robot arm operating in an uncertain environment" In *Proc. of the 1989 IEEE Int. Conf. on Robotics and Automation*, pages 1056–1061, 1989.
12. Etienne-Cummings, R., "Biologically Inspired Visual Motion Detection in VLSI", *Int. J. Comput. Vision*, Kluwer Academic Publishers, 2001, Vol. 44(3), pp. 175-198.
13. Etienne-Cummings, R., Van der Spiegel, J., Mueller, P. & Zhang, M., "A Foveated Visual Tracking Chip Proceedings - Solid-State Circuits Conference", 1997, pp. 38-39.
14. Etienne-Cummings, R., Van Spiegel, J., Mueller, P. & Zhang, M.-Z., "A foveated silicon retina for two-dimensional tracking", *IEEE Transactions on Circuits and Systems II: Analog and Digital Signal Processing*, 2000, Vol. 47(6), pp. 504-517.
15. F. Nobuyuki, Y. Takashi, and I. Shimoyama, "Micromachined planar coil tactile sensor implantable in soft structure". In *Proc. of the 2000 ASME Int. Mech. Eng. Congress and Exposition*, pages 51–56, 2000.
16. Fernald, R.D., "Evolution of Eyes", *Current Opinion in Neurobiology*, 10:444-450, 2000.

17. Fossum, E., "CMOS image sensors: electronic camera-on-a-chip", IEEE Transactions on Electron Devices, 1997, Vol. 44(10), pp. 1689-1698.
18. Fukushima, K. & Miyake, S., "Neocognitron: A new algorithm for pattern recognition tolerant of deformations and shifts in position", Pattern Recognition, 1982, Vol. 15(6), pp. 455-469.
19. Fukushima, K., Yamaguchi, Y., Yasuda, M. & Nagata, S., "An Electronic Model of the Retina", Proc. IEEE, 1970, Vol. 58, pp. 1950-1951
20. Gopalan, A., Kulkarni, P., and Titus, A.H. An algorithm for the AVLSI implementation of the cephalopod retina and visual system Proc. Int. Joint Conf. Neural Networks, vol. 2, Washington, DC, Jul. 15–19, pp. 832–836, 2001
21. H F Schulte. "The Characteristics of the McKibben Artificial Muscle", In the Application of External Power in Prosthetics and Orthotics. Pp 94-115. 1962.
22. <http://www.actuatorweb.org/index.php?page=main>
23. http://www.mide.com/products/qp/qp45n/qp45n_faq.php Last retrieved on 10 April 2009
24. <http://www.technohands.co.jp/products/um-tula.html> Last retrieved on 10 April 2009
25. J. D. W. Madden, N. A. Vandesteeg, P. A. Anquetil, P. G. A. Madden, A. Takashi, R. Z. Pytel, S. R. Lafontaine, P. A. Wieringa, I. W. Hunter, Artificial Muscle Technology: Physical Principles and Naval Prospects, IEEE Journal of oceanic engineering, Vol. 29, No. 3, 2004.
26. J. Franden, "Handbook of modern sensors : Physics, Designs and Applications", Springer-Verlag USA, 2003.
27. J. L. Pons, Emerging Actuator Technologies: A Micromechatronic Approach, John Wiley & Sons, Ltd, England, 2005.
28. J.B.C. Davies, D.M. Lane, G.C. Robinson, D.J. O'Brien, M. Pickett, M. Sfakiotakis, B. Deacon. "Subsea Applications of Continuum Robots". IEEE/OES Underwater Technology Tokyo, Japan. 1998.
29. Jeong, K.-H., Kim, J. & Lee, L., "Biologically inspired artificial compound eyes", Science, 2006, Vol. 312(5773), pp. 557-561.
30. Jin-hao Qiu, Hong-li Ji, Jian Liu, Kong-Jun Zhu(2008) Piezoelectric devices and their application in smart structures. Piezoelectricity, Acoustic Waves, and Device Applications, 2008. SPAWDA 2008. Symposium on , vol., no., pp.416-422, 5-8 Dec. 2008
31. K Inoue. "Rubbertuators and Applications for Robots", 4th Int. Symp. On Robotics Research, pp 57-64. 1987. Santa Cruz, USA.
32. K.J. De Laurentis , A. Fisch, J. Nikitczuk, C. Mavroidis. "Optimal Design of Shape Memory Alloy Wire Bundle Actuators". International Conference on Robotics and Automation. Washington, USA. May 2002.
33. Kenji Uchino (1997). Piezoelectric actuators and ultrasonic motors. Springer
34. Kentaro Noda, Kazunori Hoshino, Kiyoshi Matsumoto, Isao Shimoyama, "A shear stress sensor for tactile sensing with the piezoresistive cantilever standing in elastic material", Sensors and Actuators A 127, pp.295–301, 2006.
35. Kreider, G., A Treatise on Log-Polar Imaging Using a Custom Computational Sensor PhD Dissertation, Dept. Electr. Eng., Univ. of Pennsylvania, Philadelphia, PA, 1993.

36. L.D. Harmon, "Automated tactile sensing", *Int. Journal of Robotics Research*, 2(1):3–31, 1982.
37. Land, M., "Visual acuity in insects", *Annual Review of Entomology*, 1997, Vol. 42, pp. 147–177.
38. Land, M.F., "Optics and Vision in Invertebrates", In *Handbook of Sensory Physiology*, Ed. H.-J. Austrum, VII/6B, pp. 471-592, Springer, Berlin, 1981.
39. M. Shimojo, M. Ishikawa, and K. Kanaya "A flexible high resolution tactile imager with video signal output", In *Proc. Of the 1991 IEEE Int. Conf. on Robotics and Automation*, pages 384–391, 1991.
40. Manzotti, R., Gasteratos, A., Metta, G. & Sandini, G., "Disparity estimation on log-polar images and vergence control", *Computer Vision and Image Understanding*, 2001, Vol. 83(2), pp. 97-117.
41. Massoud Momeni, and Albert H. Titus, *An Analog VLSI Chip Emulating Polarization Vision of Octopus Retina*, *IEEE Transactions On Neural Networks*, Vol. 17, No. 1, pp. 222-232, 2006
42. Mead, C., "Analog VLSI and Neural Systems", Reading: Addison Wesley Publ, 1989.
43. Meneses, Y.L. d. & Michel, O. "Vision Sensors on the Webots Simulator", *VW '98: Proceedings of the First International Conference on Virtual Worlds Springer-Verlag*, 1998, pp. 264-273.
44. Metta, G., "An attentional system for a humanoid robot exploiting space variant vision", *IEEE-RAS International Conference on Humanoid Robots 2001*, pp. 359-366.
45. Moini, A. "Vision Chips", New York and Oxford: Oxford University Press., Norwell: Kluwer Academic Publ., 1999.
46. Möller, R., Lambrinos, D., Pfeifer, R., Labhart, T. & Wehner, "R.Modeling ant navigation with an autonomous agent", *From Animals to Animals 5, Proc. of the 5th International Conf. on Simulation of Adaptive Behavior*, 1998, pp. 185-194
47. Nishimura, M., "A VLSI Computational Sensor for the Detection of Image Features", PhD Dissertation, Dept. Electr. Eng., Univ. of Pennsylvania, Philadelphia, PA, 2001.
48. P. Dario, "Tactile sensing: Technology and applications", *Sensors and Actuators A*, pages 25–27, 1991.
49. P. Li and Y. Wen, "An arbitrarily distributed tactile piezoelectric sensor array", *Sensors and Actuators A*, (65):141–146, 1998.
50. Pardo, F., Boluda, J.A. & Ves, E.D., "Feature Extraction and Correlation for Time-to-Impact Segmentation Using Log-Polar Images", *Computational Science and Its Applications - ICCSA 2004*, 2004, pp. 887-895.
51. Piezo Actuator Selection Guides.
http://www.physikinstrumente.com/en/products/piezo/piezo_selection.php?table=all
Last retrieved on 15 April 2009
52. R. Bonser, W. Harwin, W. Hayes, G. Jeronimidis, G. Mitchell, C. Santulli, Final Report, *EAP-Based Artificial Muscles as an Alternative to Space Mechanisms ESA/ESTEC Contract No. 18151/04/NL/MV*, 2004.
53. R. Kageyama, S. Kagami, M. Inaba, and H. Inoue, "Development of soft and distributed tactile sensors and the application to a humanoid robot", In *Proc. of the*

- 1999 IEEE Int. Conf. on Systems, Man, and Cybernetics, volume 2, pages 981–986, 1999.
54. R.S. Fearing, "Tactile sensing mechanisms", *Int. Journal of Robotics Research*, 9(3):3–23, 1990.
 55. Reichardt, W. "Autocorrelation, a principle for the evaluation of sensory information by the central nervous system", Rosenblith, W. (ed.), *Sensory Communication*, New York: J. Wiley, 1961, pp. 303-317.
 56. Ruffier, F. & Franceschini, N., "Optic flow regulation: The key to aircraft automatic guidance", *Robotics and Autonomous Systems*, 2005, Vol. 50(4), pp. 177-194.
 57. S. hirai, K. Shimizu, S. Kawamura. "Vision-Base Motion Control of Pneumatic Group Actuators". *International Conference on Robotics and Actuation*. Washengton, USA. May 2002
 58. Sandini, G. & Tagliasco, V. "An anthropomorphic retina-like structure for scene analysis", *Computer Graphics and Image Processing*, 1980, Vol. 14(4), pp. 365-372.
 59. Shaoze Yan, Fuxing Zhang et al(2006). A 3-DOFs Mobile Robot Driven by Piezoelectric Actuator. *Smart Materials and Structures*. 15
 60. Shen, W., Polymorphic Robotics Laboratory, University of Southern California, Marina del Ray, <http://www.isi.edu/robots/>
 61. T. Mirfakrai, J. D. W. Madden, R. H. Baughman, *Ploymer artificial Muscles*, *Materials today*, Vol. 10, No. 4, 2007.
 62. Thakoor, S., Chahl, J., Srinivasan, M., Young, L., Werblin, F., Hine, B. & Zornetzer, S., "Bioinspired engineering of exploration systems for NASA and DoD.", *Artificial life*, 2002, Vol. 8(4), pp. 357-369.
 63. Tistarelli, M. & Sandini, G., "On the advantages of polar and log-polar mapping for direct estimation of time-to-impact from optical flow", *IEEE Transactions on Pattern Analysis and Machine Intelligence*, 1993, Vol. 15(4), pp. 401-410.
 64. Ude, A., Atkeson, C. & Cheng, G., "Combining peripheral and foveal humanoid vision to detect, pursue, recognize and act", *IEEE International Conference on Intelligent Robots and Systems*, 2003, Vol. 3, pp. 2173-2178.
 65. Van der Spiegel, J., Etienne-Cummings, R. & Nishimura, M., "Smart Sensors and Biologically Inspired Algorithms", *Tech. Dig. 15th Sensor Symp*, Kawasaki, 1997, pp. 7-17
 66. Viollet, S. & Franceschini, N. "Aerial Minirobot that stabilizes and tracks with a bio-inspired visual scanning sensor", *Biorobotics*, 2001, pp. 67-83.
 67. *Vision Chips: Implementing Vision Algorithms With Analog VLSI Circuits* Koch, C. & Li, H. (ed.) Piscataway: IEEE Computer Press, 1995
 68. W. Hunter, S. Lafontaine, A comparison of muscle with artificial actuators, *IEEE Solid-State Sensor and Actuator Workshop*, pp. 178-165, 1992.
 69. Waram, T., 1993, *Actuator Design Using Shape Memory Alloys*, 2nd Edition.
 70. Y. Bar-Cohen, *Electroactive Polymer (EAP) Actuators as Artificial Muscles*, Second edition, SPIE Press, Bellingham, Washington USA, 2004.
 71. Y. Hayakawa, S. Kawamura. "Sensing Actuators Using a Pneumatic Bellows System and Its Application to a Soft Gripper". *International Conference on Robotics and Automation*. Atlanta, Georgia, USA. May 1993.

72. Yoshikawa, Shoko; Shrouf Thomas(1993) Multilayer piezoelectric actuators - Structures and reliability. Structures, Structural Dynamics, and Materials Conference, 34th and AIAA/ASME Adaptive Structures Forum, La Jolla, CA, Technical Papers. Pt. 6 (A93-33876 13-39), p. 3581-3586.
73. Zanker, J.M. & Zeil, J., "Motion Vision", Springer-Verlag, Berlin, 2001.

SURVEY OF BIO-INSPIRED SOFT ROBOTS AND CONTROL SCHEMES

74. Alba, E. & Chicano, J. (2004), Training neural networks with GA hybrid algorithms Lecture Notes in Computer Science, Vol. 3102, pp. 852-863.
75. Arena, P., Fortuna, L., Frasca, M. & Vagliasindi, G. (2006), A wave-based cnn generator for the control and actuation of a lamprey-like robot. International Journal of Bifurcation and Chaos, 2006, Vol. 16(1), pp. 39-46.
76. Ayers, J., Wilbur, C. & Olcott, C. (2000), Lamprey Robots. Proc. Int. Symposium on Aqua Biomechanisms.
77. Baldassarre, G., Parisi, D. & Nolfi, S. (2004), Coordination and behavior integration in cooperating simulated robots From Animals to Animats 8: Proceedings of the VIII International Conference on Simulation of Adaptive Behavior.
78. Bayraktaroglu, Z.Y., Kilicarslan, A. & Kuzucu, A. (2006) Design and Control of Biologically Inspired Wheel-less Snake-like Robot. Proc. 1st IEEE/RAS-EMBS Int. Conference on Biomedical Robotics and Biomechatronics (BIROB'06), pp. 1001-1006.
79. Beer, R.D. & Gallagher, J.C. (1992), Evolving dynamical neural networks for adaptive behavior Adaptive Behavior, MIT Press, 1992, Vol. 1(1), pp. 91-122.
80. Bianco, R. & Nolfi, S. (2004), Toward open-ended evolutionary robotics: Evolving elementary robotic units able to self-assemble and self-reproduce Connection Science, Vol. 16(4), pp. 227-248.
81. Bloch, A. M., Krishnaprasad, P. S., Marsden, J. E., and Murray, R. M. (1996) Nonholonomic mechanical systems with symmetry Arch. Ration. Mech.Anal., vol. 136, no. 1, pp. 21-99.
82. Bongard, J. & Lipson, H. (2005), Nonlinear system identification using coevolution of models and tests. IEEE Transactions on Evolutionary Computation, 2005, Vol. 9(4), pp. 361-384.
83. Bongard, J. (2002), Evolving modular genetic regulatory networks Proceedings of the IEEE 2002 Congress on Evolutionary Computation (CEC2002), pp. 1872-1877.
84. Borrett, D., Jin, F. & Kwan, H. (2005), Evolutionary autonomous agents and the nature of apraxia. BioMedical Engineering Online, Vol. 4.
85. Braganza D, Dawson DM, Walker ID, Nath, N. (2006), Neural network grasping controller for continuum robots. In: 45th IEEE Conference on Decision and Control. San Diego: IEEE, 6445-6449.
86. Burdick, J.W., Radford, J. & Chirikjian, G.S. (1993) A 'sidewinding' locomotion gait for hyper-redundant robots Proc. IEEE International Conference on Robotics and Automation, pp. 101-106.

87. Chalmers, D.J. (1990), The Evolution of learning: an experiment in genetic connectionism Proceedings of the 1990 Connectionist Models Summer School Morgan Kaufmann, pp. 81-90.
88. Chandra, A. & Yao, X. (2006), Ensemble learning using multi-objective evolutionary algorithms Journal of Mathematical Modelling and Algorithms, 2006, Vol. 5(4), pp. 417-445.
89. Chellapilla, K. & Fogel, D. (2001), Evolving an expert checkers playing program without using human expertise IEEE Transactions on Evolutionary Computation, Vol. 5(4), pp. 422-428.
90. Chen, T. L. T.; Liu, S.-H. & Yen, J.-Y. (2008), A biomimetic snake-like robot: Sensor based gait control Proc. IEEE Workshop on Advanced robotics and Its Social Impacts (ARSO '08), pp. 1-6
91. Chiaverini, S., Oriolo, G. & Walker, I.D. (2008), Kinematically Redundant Manipulators Siciliano, B. & Khatib, O. (ed.) Handbook of Robotics, Springer.
92. Chirikjian, G.S. & Burdick, J.W. (1991), Kinematics of hyper-redundant robot locomotion with applications to grasping. Proc. IEEE International Conference on Robotics and Automation, pp. 720-725.
93. Chirikjian, G.S. & Burdick, J.W. (1990), Kinematics of hyper-redundant manipulators American Society of Mechanical Engineers, Design Engineering Division (Publication) DE, Vol. 25, pp. 391-396.
94. Chirikjian, G.S. & Burdick, J.W. (1994), Modal approach to hyper-redundant manipulator kinematics IEEE Transactions on Robotics and Automation, Vol. 10(3), pp. 343-354.
95. Chirikjian, G.S. & Burdick, J.W. (1995), Kinematics of hyper-redundant robot locomotion IEEE. Transactions on Robotics and Automation, Vol. 11(6), pp. 781-793.
96. Chirikjian, G.S. & Burdick, J.W. (1995), Kinematically optimal hyper-redundant manipulator configurations. Robotics and Automation, IEEE Transactions on , vol.11, no.6, pp.794-806
97. Chitrakaran VK, Behal A, Dawson DM, Walker ID. (2007), Setpoint regulation of continuum robots using a fixed camera. Robotica. 25:581–586.
98. Cho, S.-B. (2001), Cooperative Co-evolution of Multi-agents Proceedings of the Joint JSAI 2001 Workshop on New Frontiers in Artificial Intelligence Springer-Verlag, pp. 185-194.
99. Clark, R.B. (1976), Undulatory swimming in polychaetes, Davis, P. (ed.) Perspectives in Experimental Biology, Proc. 15th Anniv. Meeting of the Society for Experimental Biology, Pergamon Press, Vol. 1, pp. 437-446.
100. Cliff, D., Harvey, I. & Husbands, P. (1993), Explorations in evolutionary robotics Adaptive Behavior, 1993, Vol. 2(1), pp. 73-110.
101. Crespi, A., Badertscher, A., Guignard, A. & Ijspeert, A.J. (2005), Amphibot I: an amphibious snake-like robot Robotics and Autonomous Systems, Vol. 50(4), pp. 163-175.

102. Darwen, P. & Yao, X. (2002), Co-evolution in iterated prisoner's dilemma with intermediate levels of cooperation: application to missile defense *International Journal of Computational Intelligence and Applications*, 2002, Vol. 2, pp. 2002.
103. Dayan, P. (2001), *Encyclopedia of cognitive science* Wilson, R. A. & Keil, F. C. (ed.) Chapter Levels of analysis in neural modeling London: Macmillan.
104. Di Paolo, E. (2003). Evolving spike-timing-dependent plasticity for single-trial learning in robots *Philosophical Transactions of the Royal Society A: Mathematical, Physical and Engineering Sciences*, 2003, Vol. 361(1811), pp. 2299-2319.
105. Eggenberger, P. & Gomez, G. (2004), The transfer problem from simulation to the real world in artificial evolution *Proc. 9th Int. Conference on the Simulation and Synthesis of Living Systems (Alife IX)*, pp. 17-20.
106. Eggenberger, P. (1997), Evolving morphologies of simulated 3D organisms based on differential gene expression *Proceedings of the Fourth European Conference on Artificial Life*, pp. 205-213.
107. Eskiizmirli S, Forestier N, Tondu B, Darlot C. (2002), A model of the cerebellar pathways applied to the control of a single joint robot arm actuated by McKibben artificial muscles. *Biol Cybernet.* 86(5):379–394.
108. Floreano, D. & Mondada, F. (1994), Automatic creation of an autonomous agent: genetic evolution of a neural-network driven robot SAB94: *Proceedings of the third international conference on Simulation of adaptive behavior : from animals to animats 3*, MIT Press, pp. 421-430.
109. Floreano, D. & Mondada, F. (1998), Evolutionary neurocontrollers for autonomous mobile robots *Neural Networks*, Vol. 11(7-8), pp. 1461-1478.
110. Floreano, D. & Urzelai, J. (2001), Evolution of plastic control networks *Autonomous Robots*, Vol. 11(3), pp. 311-317.
111. Floreano, D., Dorr, P. & Mattiussi, C. (2008), Neuroevolution: from architectures to learning *Evolutionary Intelligence*, Vol. 1(1), pp. 47-62.
112. Floreano, D., Husbands, P. & Nolfi, S. (2008), *Evolutionary Robotics* Siciliano, B. & Khatib, O. (ed.) *Handbook of Robotics* Springer.
113. Floreano, D., Kato, T., Marocco, D. & Sauser, E. (2004), Coevolution of active vision and feature selection *Biological Cybernetics*, Vol. 90(3), pp. 218-228.
114. Floreano, D., Schoeni, N., Caprari, G. & Blynell, J. (2003), Evolutionary bits'n'spikes *ICAL 2003: Proceedings of the eighth international conference on Artificial life* MIT Press, pp. 335-344.
115. Funes, P. & Pollack, J. (1998), Evolutionary body building: Adaptive physical designs for robots *Artificial Life*, Vol. 4(4), pp. 337-357.
116. Gravagne I.A., Walker I.D. (2002), Manipulability, Force, and Compliance Analysis for Planar Continuum Manipulators, in *IEEE Transactions on Robotics and Automation*, Vol.18, N 3.
117. Gravagne IA, Rahn CD, Walker ID. (2001). Good vibrations: a vibration damping setpoint controller for continuum robots. In: *Proceedings of the 2001 IEEE International Conference on Robotics & Automation*; Seoul, Korea: IEEE, 21–26, pp 3877–3884.

118. Gravagne IA, Walker ID. (2002), Uniform regulation of a multisection continuum manipulator. In: IEEE International Conference on Intelligent Robots and Systems; San Francisco, CA, USA: IEEE, p. 1519–1524.
119. Gravagne IA, Walker ID. (2000a). Kinematic transformations for remotely actuated planar continuum robots. IEEE International Conference on Intelligent Robots and Systems; San Francisco, CA, USA: IEEE, p. 19–26.
120. Gray, J. & Hancock, G.J. (1955), Propulsion of Sea-Urchin Spermatozoa *Journal of Experimental Biology*, 1955, Vol. 32(4), pp. 802-814.
121. Gray, J. & Lissmann, H. (1950), The kinetics of locomotion of the grass snakes *Journal of Experimental Biology*, 1950(26), pp. 354-367.
122. Gray, J. (1968), *Annelids Animal Locomotion* Weidenfeld & Nicolson, 1968, pp. 377-410.
123. Gruau, F. (1994), Automatic definition of modular neural networks *Adaptive Behavior*, MIT Press, 1994, Vol. 3(2), pp. 151-183.
124. Gutfreund Y, Flash T, Yarom Y, Fiorito G, Segev I, Hochner B. (1996). Organization of octopus arm movements: a model system for studying the control of flexible arms. *J Neurosci*.16:7297–7307.
125. H. Mochiyama, E. Shimemura, and H. Kobayashi, (1999), Control of manipulators with hyper degrees of freedom: Shape tracking using only joint angle information, *Int. J. Syst. Sci.*, vol. 30, no. 1, pp. 77–85.
126. Hagaras, H., Pounds-Cornish, A., Colley, M., Callaghan, V. & Clarke, G. (2004). Evolving spiking neural network controllers for autonomous robots *Proceedings - IEEE International Conference on Robotics and Automation*, Vol. 2004(5), pp. 4620-4626.
127. Hallinan, J. & Wiles, J. (2004), Evolving genetic regulatory networks using an artificial genome *Proc. 2nd Asia-Pacific Bioinformatics Conf*, Vol. 29, pp. 291-296.
128. Hannan M, Walker ID. (2005). Real-time shape estimation for continuum robots using vision. *Robotica* 23:645–651.
129. Hinton, G.E. & Nowlan, S.J. (1987), How learning can guide evolution *Complex Systems*, Addison-Wesley Longman Publishing Co., Inc., Vol. 1, pp. 495-502.
130. Hirose, S. & Fukushima, E. (2004), Snakes and strings: New robotic components for rescue operations *International Journal of Robotics Research*, Vol. 23(4/5), pp. 341-349.
131. Hirose, S. (1993), *Biologically Inspired Robots: Snake-Like Locomotors and Manipulators* Oxford University Press.
132. Hochner B, Gutfreund Y, Fiorito G, Flash T, Segev I, Yarom Y (1995), Arm electromyograms in freely moving octopus (*Octopus vulgaris*). *Isr J Med Sci* 31.12:745.
133. Hodgkin, A. & Huxley, A. (1990), A quantitative description of membrane current and its application to conduction and excitation in nerve *Bulletin of Mathematical Biology*, Vol. 52(1-2), pp. 25-71.
134. Holwill, M.E.J. & Sleight, M.A. (1967), Propulsion by Hispid Flagella *Journal of Experimental Biology*, Vol. 47(2), pp. 267-276.

135. Hornby, G. & Pollack, J. (2001), Body-brain coevolution using L-systems as a generative encoding Genetic and Evolutionary Computation Conference, pp. 868-875.
136. Hornby, G., Takamura, S., Yokono, J., Hanagata, O., Yamamoto, T. & Fujita, M. (2000), Evolving robust gaits with AIBO Proceedings - IEEE International Conference on Robotics and Automation, Vol. 3, pp. 3040-3045.
137. Husbands, P., Smith, T., Jakobi, N. & O'Shea, M. (1998), Better Living Through Chemistry: Evolving GasNets for Robot Control Connection Science, Vol. 10(3-4), pp. 185-210..
138. Inoue, K., Sumi, T., Sato, N. & Ma, S. (2007) CPG-based adaptable control of a snake-like robot Proc. Annual Conference SICE, pp. 2161-2164
139. Ivanescu M, Popescu N, Popescu D, (2005). A Variable length Hyperredundant Arm control system. IEEE Mechatronics and Automation, p. 1998-2003.
140. Ivanescu M. (2002). Position dynamic control for a tentacle manipulator . IEEE Robotics and Automation, p. 1531-1538.
141. Jacobi, N., Husbands, P. & Harvey, I. (1995), Noise and the reality gap: The use of simulation in evolutionary robotics Advances in Artificial Life: Proceedings of the Third European Conference on Artificial Life, pp. 353-367.
142. Jakobi, N. (1993), Half-baked, Ad-hoc and Noisy: Minimal Simulations for Evolutionary Robotics Fourth European Conference on Artificial Life MIT Press, pp. 348-357.
143. Keymeulen, D., Iwata, M., Kuniyoshi, Y. & Higuchi, T. (1998), Online Evolution for a Self-Adapting Robotic Navigation System Using Evolvable Hardware Artificial Life, MIT Press, Vol. 4(4), pp. 359-393
144. Kicinger, R., Arciszewski, T. & De Jong, K. (2005), Evolutionary computation and structural design: A survey of the state-of-the-art Computers and Structures, Vol. 83(23-24), pp. 1943-1978.
145. Kier WM, Smith KK, (1985), Tongues, tentacles and trunks: the biomechanics of movement in muscular-hydrostats. Zool J Linn Soc 83:307–324.
146. Kim B, Ryu J, Jeong Y, Tak Y, Kim B, Park JO. (2003). A ciliary based 8-legged walking micro robot using cast ipmc actuators. Proceedings of the 2003 IEEE International Conference on Robotics and Automation, September 2003, Taipei, Taiwan: IEEE.
147. Kolesnik, M. & Streich, H. (2002). Visual Orientation and Motion Control of MAKRO - Adaptation to the Sewer Environment Proc. 7th Int. Conference on Simulation of Adaptive Behavior (SAB'02), pp. 62-69.
148. Komosinski, M. & Rotaru-Varga, A. (2001), of different genotype encodings for simulated three-dimensional agents Artificial Life, Vol. 7(4), pp. 395-418.
149. Krishnaprasad, P.S. & Tsakiris, D.P. (1994) G-snakes: nonholonomic kinematic chains on Lie groups Proc. 33rd IEEE Conference on Decision and Control, Vol. 3, pp. 2955-2960.
150. Krishnaprasad, P.S. & Tsakiris, D.P. (2001), Oscillations, SE(2)-Snakes and Motion Control: The Roller Racer Dynamical Systems, Vol. 16, No. 4, pp. 347-397.

151. La Spina, G., Sfakiotakis, M., Tsakiris, D.P., Menciassi, A. & Dario, P., (2007), Polychaete-like undulatory robotic locomotion in unstructured substrates, IEEE Transactions on Robotics, 2007, Vol. 6, pp. 1200-1212
152. Lapierre, L. & Jouvencel, B. (2005) Path following control for an eel-like robot Proc. IEEE Int. Conference OCEANS'05 Europe, pp. 460-465.
153. Li, B., Ma, S., Wang, Y., Iv, Y. & Chen, L. (2004). Environment-Adaptable Locomotion of a Snake-Like Robot Proc. IEEE Int. Conference on Robotics and Biomimetics (ROBIO'04), pp. 584-588.
154. Lighthill, (1975) J. Mathematical Biofluidynamics SIAM.
155. Lipkin, K., Brown, I., Peck, A., Choset, H., Rembisz, J., Gianfortoni, P. & Naaktgeboren, (2007), A. Differentiable and piecewise differentiable gaits for snake robots Proc. IEEE/RSJ International Conference on Intelligent Robots and Systems IROS 2007, 2007, pp. 1864-1869.
156. Lipson, H. & Pollack, J. (2000), Automatic design and manufacture of robotic lifeforms Nature, Vol. 406(6799), pp. 974-978.
157. Lopez-Nicolas, G., Sfakiotakis, M., Tsakiris, D., Argyros, A.A., Sagues, C. & Guerrero, J. (2009), Visual Homing for Undulatory Robotic Locomotion Proc. IEEE International Conference on Robotics and Automation ICRA, 2009
158. Lund, H.H., Hallam, J. & Lee, W.-P. (1997), Evolving robot morphology Proc. IEEE International Conference on Evolutionary Computation 1997, pp. 197-202.
159. Ma, S. (2002), Development of a creeping locomotion snake-robot International Journal of Robotics and Automation, Vol. 17(4), pp. 146-153.
160. Ma, S., Ohmameuda, Y., Inoue, K. & Li, B. (2003), Control of a 3-dimensional snake-like robot Proc. IEEE Conference on Robotics and Automation (ICRA'03), pp. 2067-2072.
161. Magg, S. & Philippides, A. (2006), GasNets and CTRNNs - A comparison in terms of evolvability Lecture Notes in Computer Science, Vol. 4095 LNAI, pp. 461-472.
162. Maniadakis, M. & Trahanias, P. (2008), Hierarchical CoEvolution of Cooperating Agents Acting in the Brain-Arena Adaptive Behavior, Vol. 16, pp. 221-245.
163. Maniadakis, M., Hourdakis, M. & Trahanias, P. (2007). Modeling overlapping execution/observation brain pathways IEEE International Conference on Neural Networks - Conference Proceedings, pp. 1255-1260.
164. Marbach, D. & Ijspeert, A. (2004), Co-evolution of configuration and control for homogenous modular robots Proceedings of the Eighth Conference on Intelligent Autonomous Systems (IAS8), pp. 712-719.
165. Mattiussi, C. & Floreano, D. (2007). Analog genetic encoding for the evolution of circuits and networks IEEE Transactions on Evolutionary Computation, Vol. 11(5), pp. 596-607.
166. Mattiussi, C., Marbach, D., Dórr, P. & Floreano, D. (2008), The age of analog networks AI Magazine, Vol. 29(3), pp. 63-76.
167. Mayley, G. (1996). Landscapes, learning costs, and genetic assimilation Evolutionary Computation, Vol. 4(3), pp. 213-234.

168. Mclsaac, K.A. & Ostrowski, (2002), J.P. Experimental Verification of Open-loop Control for an Underwater Eel-like Robot International Journal of Robotics Research, Vol. 21, pp. 849-860.
169. Mondada, F., Pettinaro, G., Guignard, A., Kwee, I., Floreano, D., Deneubourg, J.-L., Nolfi, S., Gambardella, L. & Dorigo, M. (2004), Swarm-bot: A new distributed robotic concept Autonomous Robots, Vol. 17(2-3), pp. 193-221.
170. Mori, M. & Hirose, S. (2002), Three-dimensional serpentine motion and lateral rolling by active cord mechanism ACM-R3 Proc. IEEE/RSJ International Conference on Intelligent Robots and System, Vol. 1, pp. 829-834.
171. Ng, S.-C., Leung, S.-H. & Luk, A. (1999), Hybrid algorithm of weight evolution and generalized back-propagation for finding global minimum Proceedings of the International Joint Conference on Neural Networks, Vol. 6, pp. 4037-4042.
172. Nolfi, S., Miglino, O. & Parisi, D. (1994), Phenotypic plasticity in evolving neural networks From Perception to Action Conference, 1994., Proceedings, pp. 146-157.
173. Olsson, B. (2001), Co-evolutionary search in asymmetric spaces Information Sciences, Vol. 133(3-4), pp. 103-125.
174. Ostrowski, J. & Burdick, J. (1996), Gait kinematics for a serpentine robot Proc. IEEE International Conference on Robotics and Automation, Vol. 2, pp. 1294-1299.
175. Ostrowski, J.P. & Burdick, J. (1998), The geometric mechanics of undulatory robotic locomotion International Journal of Robotics Research, Vol. 17(7), pp. 683-701.
176. Otake M, Kagami Y, Kuniyoshi Y, Inaba M, Inoue H. (2003). Inverse dynamics of gel robots made of electro-active polymer gel. In: IEEE International Conference on Robotics and Automation; Taipei, Taiwan. Pisa, Italy: IEEE, p. 2299–2304.
177. Pfeifer, R., Iida, F. & Bongard, J. (2005), New robotics: Design principles for intelligent systems Artificial Life, Vol. 11(1-2), pp. 99-120.
178. Poi, G., Scarabeo, C. & Allotta, B. (1998), Traveling wave locomotion hyper-redundant mobile robot Proc. IEEE International Conference on Robotics and Automation, Vol. 1, pp. 418-423.
179. Potter, M. & De Jong, K. (2000), Cooperative coevolution: an architecture for evolving coadapted subcomponents. Evolutionary computation, Vol. 8(1), pp. 1-29.
180. Quick, T., Nehaniv, C., Dautenhahn, K. & Roberts, G. (2003), Evolving embodied genetic regulatory network-driven control systems Lecture Notes in Artificial Intelligence (Subseries of Lecture Notes in Computer Science), Vol. 2801, pp. 266-277.
181. Quinn, M. (2001), Evolving Communication without Dedicated Communication Channels ECAL '01: Proceedings of the 6th European Conference on Advances in Artificial Life Springer-Verlag, pp. 357-366
182. Robinson, G. & Davies, J. (1999), Continuum robots - a state of the art Proceedings - IEEE International Conference on Robotics and Automation, Vol. 4, pp. 2849-2854.
183. Roggen, D., Thoma, Y. & Sanchez, E. (2004), An evolving and developing cellular electronic circuit ALife9: Proceedings of the Ninth International Conference on Artificial Life, pp. 33-38.
184. Ruppin, E. (2002), Evolutionary autonomous agents: A neuroscience perspective Nature Reviews Neuroscience, Vol. 3(2), pp. 132-141.

185. Salemi, B., Moll, M. & Shen, W.-M. (2006), SUPERBOT: A Deployable, Multi-Functional, and Modular Self-Reconfigurable Robotic System Proc. IEEE/RSJ International Conference on Intelligent Robots and Systems, pp. 3636-3641.
186. Sato, M., Fukaya, M. & Iwasaki, T. (2002), Serpentine locomotion with robotic snakes IEEE Control Systems Magazine, Vol. 22(1), pp. 64-81.
187. Sfakiotakis, M. & Tsakiris, D. (2008), Pedundulatory Robotic Locomotion: Centipede and Polychaete Modes in Unstructured Substrates Proc. IEEE Int. Conference on Robotics and Biomimetics (ROBIO'08).
188. Sfakiotakis, M. & Tsakiris, D. (2009), Undulatory and Pedundulatory Robotic Locomotion via Direct and Retrograde Body Waves Proc. IEEE Int. Conference on Robotics and Automation (ICRA'09) (to appear).
189. Sfakiotakis, M. & Tsakiris, D.P. (2006) SIMUUN: A Simulation Environment for Undulatory Locomotion International Journal of Modelling and Simulation, Vol. 26(4), pp. 4430-4464.
190. Sfakiotakis, M. & Tsakiris, D.P. (2007), A Biomimetic Centering Behavior for Undulatory Robots International Journal of Robotics Research, Vol. 26(11-12), pp. 1267-1282.
191. Sfakiotakis, M. & Tsakiris, D.P. (2007), Neuromuscular Control of Reactive Behaviors for Undulatory Robots Neurocomputing, Vol. 70(10-12), pp. 1907-1913.
192. Sfakiotakis, M., Tsakiris, D.P. & Karakasiliotis, K. (2007), Polychaete-like Pedundulatory Robotic Locomotion Proc. IEEE International Conference on Robotics and Automation, pp. 269-274.
193. Sims, K. (1994), Evolving 3D morphology and behavior by competition Proceedings of Fourth Conference on Artificial Life.
194. Smith, J. (1987), When learning guides evolution Nature, Vol. 329(6142), pp. 761-762.
195. Soltoggio, A., Dórr, P., Mattiussi, C. & Floreano, D. (2007), Evolving neuromodulatory topologies for reinforcement learning-like problems, IEEE Congress on Evolutionary Computation, CEC, pp. 2471-2478.
196. Stanley, K. & Miikkulainen, R. (2002), Evolving neural networks through augmenting topologies Evolutionary Computation, Vol. 10(2), pp. 99-127.
197. Sumbre G, Fiorito G, Flash T, Hochner B. (2005). Octopuses use a human-like strategy to control precise point-to-point arm movements. *Curr Biol.* 16:767–772.
198. Sumbre G, Fiorito G, Flash T, Hochner B. (2005). Precise motor control of flexible arms. *Nature* 433:595–596.
199. Suzuki T, Shintani K, and Mochiyama H, (2002), Control methods of hyperflexible manipulators using their dynamical features, in Proc. 41st SICE Annu. Conf., Osaka, Japan, pp. 1511–1516.
200. Suzuki, M., Floreano, D. & Di Paolo, E. (2005), The contribution of active body movement to visual development in evolutionary robots Neural Networks, Vol. 18(5-6), pp. 656-665.
201. Tamburrini, G. & Datteri, E. (2005), Machine experiments and theoretical modelling: From cybernetic methodology to neuro-robotics Minds and Machines, Vol. 15(3-4), pp. 335-358.

-
202. Tanaka, M. & Matsuno, F. (2006), Cooperative control of two snake robots Proc. IEEE Int. Conf. on Robotics and Automation (ICRA'06), pp. 400-405.
 203. Tanaka, M. & Matsuno, F. (2008). Modeling and control of a snake robot with switching constraints Proc. SICE Annual Conference, pp. 3076-3079.
 204. Taylor, G. (1952), Analysis of the swimming of long and narrow animals Proceedings of the Royal Society (A), Vol. 214, pp. 158-183.
 205. Thompson, A. (1995), Evolving electronic robot controllers that exploit hardware resources Advances in Artificial Life: Proceedings of the Third European Conference on Artificial Life, Vol. 929, pp. 640-656.
 206. Transeth, A., Leine, R., Glocker, C., Pettersen, K. & Liljeback, P. (2008). Robot Obstacle-Aided Locomotion: Modeling, Simulations, and Experiments IEEE Transactions on Robotics, Vol. 24(1), pp. 88-104.
 207. Transeth, A.A. & Pettersen, K.Y. (2006), Developments in Snake Robot Modeling and Locomotion Proc. 9th International Conference on Control, Automation, Robotics and Vision ICARCV '06, pp. 1-8
 208. Transeth, A.A., Pettersen, K.Y. & Liljebeck, P. (2009), A survey on snake robot modeling and locomotion Robotica.
 209. Trivedi, D., Rahn, C., Kier, W. & Walker, I. (2008), Soft robotics: Biological inspiration, state of the art, and future research Applied Bionics and Biomechanics, 2008, Vol. 5(3), pp. 99-117.
 210. Tuci, E., Gross, R., Trianni, V., Mondada, F., Bonani, M. & Dorigo, M. (2006), Cooperation through self-assembly in multi-robot systems ACM Transactions on Autonomous and Adaptive Systems, Vol. 1(2), pp. 115-150.
 211. Tuci, E., Quinn, M. & Harvey, I. (2003), An evolutionary ecological approach to the study of learning behavior using a robot-based model Adaptive Behavior, Vol. 10(3-4), pp. 201-221.
 212. Urzelai, J. & Floreano, D. (2001), Evolution of adaptive synapses: robots with fast adaptive behavior in new environments. Evolutionary computation, Vol. 9(4), pp. 495-524.
 213. Walker, I., Dawson, D., Flash, T., Grasso, F., Hanlon, R., Hochner, B., Kier, W., Pagano, C., Rahn, C. & Zhang, Q. (2005), Continuum robot arms inspired by cephalopods Proceedings of SPIE - The International Society for Optical Engineering, Vol. 5804, pp. 303-314.
 214. Walker, J., Garrett, S. & Wilson, M. (2003), Evolution for Real Robots: A Structured Survey of the Literature. Adaptive Behavior, Vol. 11(3), pp. 179-203.
 215. Wiegand, R. (2003), An analysis of cooperative coevolutionary algorithms PhD Dissertation, Department of Computer Science, George Mason University, USA.
 216. Wiegand, R., Liles, W. & De Jong, K. (2001), An empirical analysis of collaboration methods in cooperative coevolutionary algorithms, Proceedings of the Genetic and Evolutionary Computation Conference (GECCO), pp. 1235-1242.
 217. Wilson, M.S., King, C.M. & Hunt, J.E. (1997), Evolving hierarchical robot behaviours Robotics and Autonomous Systems, Vol. 22(3-4), pp. 215-230.

218. Worst, R. & Linnemann, R. (1996), Construction and Operation of a Snake-like Robot Proc. IEEE Int. Joint Symp. on Intelligence and Systems (IJSIS'96), pp. 164-169.
219. Worst, R. & Linnemann, R. (1996), Construction and Operation of a Snake-like Robot Proc. IEEE Int. Joint Symp. on Intelligence and Systems (IJSIS'96), pp. 164-169.
220. Yamakita, M., Hashimoto, M. & Yamada, T. (2003), Control of locomotion and head configuration of 3D snake robot (SMA) Proc. IEEE Conference on Robotics and Automation (ICRA'03), pp. 2055-2060.
221. Ye, C., Ma, S., Li, B. & Wang, Y. (2004), Turning and side motion of a snake-like robot Proc. IEEE Conference on Robotics and Automation (ICRA'04), pp. 5075-5080
222. Yekutieli Y, Sagiv-Zohar R, Aharonov R, Engel Y, Hochner B, Flash T. (2005). Dynamic model of the octopus arm. I. Biomechanics of the octopus reaching movement. *J Neurophysiol* 94:1443–1458.
223. Yim, M., Shen, W.-M., Salemi, B., Rus, D., Moll, M., Lipson, H., Klavins, E. & Chirikjian, G.S. (2007), Modular Self-Reconfigurable Robot Systems, *IEEE Robotics & Automation Magazine*, Vol. 14(1), pp. 43-52.
224. Zykov, V., Mytilinaios, E., Desnoyer, M. & Lipson, H. (2007), Evolved and Designed Self-Reproducing Modular Robotics, *IEEE Transactions on Robotics*, Vol. 23(2), pp. 308-319

SURVEY OF BEHAVIORAL/SENSORY-MOTOR CONTROL ARCHITECTURES

225. Arkin, R. C. (1998), *Behavior-based Robotics*, MIT Press. Newell and H. A. Simon, *Computer Science as Empirical Inquiry: Symbol and Search*, Communication of the Association for Computing Machinery, vol. 19, pp. 113-126, Mar. 1976, tenth Turing award lecture, ACM, 1975
226. Beer, R. (1995), 'A dynamical systems perspective on agent-environment interaction', *Artificial Intelligence* 72, 173-215.
227. Braitenberg, V. (1984). *Vehicles: Experiments in synthetic psychology*. Cambridge, MA: MIT Press.
228. Brooks, R. A. (1991), "Intelligence Without Reason," *Proceedings of 12th Int. Joint Conf. on Artificial Intelligence*, Sydney, Australia, August 1991, pp. 569—595.
229. Brooks, R. A., Cynthia B., et. al., *The Cog Project: Building a Humanoid Robot*, in C. Nehaniv, ed., *Computation for Metaphors, Analogy and Agents*, Vol. 1562 of *Springer Lecture Notes in Artificial Intelligence*, Springer-Verlag, 1998.
230. D. Floreano and C. Mattiussi (2008), "Bio-Inspired Artificial Intelligence :Theories, Methods, and Technologies", MIT Press, Cambridge, Massachusetts, USA.
231. D. Lambrinos, R. Möller, T. Labhart, R. Pfeifer, R. Wehner, "A Mobile Robot Employing Insect Strategies for Navigation", *Robotics and Autonomous Systems*, vol. 30, 1999.
232. D. M. Wolpert, M. Kawato (1998): Multiple paired forward and inverse models for motor control. *Neural Networks* 11(7-8): 1317-1329 (1998)

233. D. Wolpert, "Probabilistic Models in Sensori-Motor Control", *Hum Mov Sci.* 2007 August; 26(4): 511–524.
234. Degallier, S.; Righetti, L.; Natale, L.; Nori, F.; Metta, G.; Ijspeert, A., "A modular bio-inspired architecture for movement generation for the infant-like robot iCub," *Biomedical Robotics and Biomechatronics, 2008. BioRob 2008. 2nd IEEE RAS & EMBS International Conference on*, vol., no., pp.795-800, 19-22 Oct. 2008
235. H. Cruse (1991), "Coordination of leg movement in walking animals", in *Proc of the first international conference on simulation of adaptive behavior on From animals to animats*, Paris, France
236. H. Cruse, T. Kindermann, M. Schumm, J. Dean, J. Schmitz (1998), "Walknet – a biologically inspired network to control six legged walking", *Neural Networks* 11, p1435-1447, April 1998.
237. H. Moravec, (1980), "Obstacle Avoidance and Navigation in the Real World by a Seeing Robot Rover", (PhD Thesis) Computer Science Dept., Stanford University, March 1980.
238. Hofstadter, D.R. (1985). Waking up from Boolean dream, or, subcognition as computation. In: Hofstadter, D.R. (1985): *Metamagical Themas: Questing for the Essence of Mind and Pattern*. Bantam Books, Toronto, 1985, pp. 631-665.
239. Iida, F.; Gómez, G. & Pfeifer, R. (2005), Exploiting Body Dynamics for Controlling a running quadruped robot, in 'Proceedings of the 12th Int. Conf. on Advanced Robotics (ICAR05).', pp. 229-235.
240. Ijspeert, A. (2008), 'Central pattern generators for locomotion control in animals and robots: a review', *Neural networks* 21, 642-653.
241. J. Dean, T. Kindermann, J. Schmitz, M. Schumm, H. Cruse (1999), "Control of Walking in the Stick Insect: From Behavior and Physiology to Modeling", *Autonomous Robots*, Volume 7, Issue 3 p 271-288 (November 1999).
242. J. Tani, M. Ito, Y. Sugita (2004): Self-organization of distributedly represented multiple behavior schemata in a mirror system: reviews of robot experiments using RNNPB, *Neural Networks*, Vol.17, pp.1273-1289
243. Kuniyoshi, Y. & Sangawa, S. (2006), 'Early motor development from partially ordered neural-body dynamics: experiments with a cortico-spinal-musculo-skeletal model', *Biological Cybernetics* 95, 589-605.
244. Kuniyoshi, Y. and Suzuki, (2004). Dynamic emergence and adaptation of behavior through embodiment as coupled chaotic field. *Proc. of the IEEE/RSJ Int. Conf. on Intelligent Robots and Systems*.
245. M. Haruno, D.M. Wolpert, W.W. Kawato (2001), "MOSAIC Model for Sensori-motor Learning and Control", *Neural Computation*, Volume 13, Issue 10 (October 2001).
246. M. Kawato. Learning internal models of the motor apparatus. In SP Wise JR Bloedel, TJ Ebner, editor, *The Acquisition of Motor Behavior in Vertebrates*, page 409-430. Cambridge MA: MIT Press, 1996.
247. M. Mataric (1992), "Behavior-Based Control: Main Properties and Implications", in *Proceedings, IEEE International Conference on Robotics and Automation, Workshop on Architectures for Intelligent Control Systems*.

-
248. Matijevic, J. (1996), Mars Pathfinder Microover - Implementing a Low Cost Planetary Mission Experiment, Proceedings of the Second IAA International Conference on Low-Cost Planetary Missions, John Hopkins University Applied Physics Laboratory, Laurel, Maryland.
249. Mobus, G.E. (1994), "Toward a theory of learning and representing causal inferences in neural networks", in Levine, D.S. and Aparicio, M (Eds.), Neural Networks for Knowledge Representation and Inference, Lawrence Erlbaum Associates
250. Nilsson, N., J. (1984), "Shakey The Robot, Technical Note 323". AI Center, SRI International, 333 Ravenswood Ave., Menlo Park, CA 94025, Apr 1984.
251. Pezzulo, G. (2007). Anticipation and Future-Oriented Capabilities in Natural and Artificial Cognition. In 50 Years of AI (Lungarella, Iida, Bongard, Pfeifer, eds.), Springer LNAI 4850, 2007, 258-271.
252. R. Blickhan, A. Seyfarth, H. Geyer, S. Grimmer, H. Wagner, M. Guenther: Intelligence by Mechanics. Phil Trans R. Soc A 365 (2007) 199-220.
253. R. Brooks (1986), A Robust Layered Control System for a Mobile Robot. IEEE Journal of Robotics and Automation, 2 (1), 1986.
254. R. Grush (2004), "The emulation theory of representation: Motor control, imagery, and perception", Behavioral and Brain Sciences, 27, 377-442
255. R. Pfeifer, C. Scheier (1999), "Understanding Intelligence", MIT Press, Cambridge, Massachusetts, USA.
256. R. Pfeifer, M. Lungarella, F. Iida, "Self-organization, embodiment, and biologically inspired robotics", Science 318, November 2007.
257. Russel, S. and Norvig, P. (1995). Artificial Intelligence. A modern approach. Prentice hall.
258. S. Russel, and P. Norvig (2003), "Artificial Intelligence : A Modern Approach", 2nd Edition, Prentice Hall Series in Artificial Intelligence, USA.
259. S. Thrun, M. Montemerlo, H. Dahlkamp, D. Stavens, A. Aron, J. Diebel, P. Fong, J. Gale, M. Halpenny, G. Hoffmann, K. Lau, C. Oakley, M. Palatucci, V. Pratt, P. Stang, S. Strohband, C. Dupont, L.-E. Jendrossek, C. Koelen, C. Markey, C. Rummel, J. van Niekerk, E. Jensen, P. Alessandrini, G. Bradski, B. Davies, S. Ettinger, A. Kaehler, A. Nefian, and P. Mahoney, "Stanley, the robot that won the DARPA Grand Challenge", Journal of Field Robotics, 2006.
260. S. Degallier, L. Righetti, L. Natale, F. Nori, G. Metta, and A.J. Ijspeert (2008). A modular bio-inspired architecture for movement generation for the infant-like robot icub. In Proceedings of the second IEEE RAS / EMBS International Conference on Biomedical Robotics and Biomechatronics, BioRob
261. S. Schaal, P. Mohajjerian, and A.J. Ijspeert. Dynamics systems vs. optimal control a unifying view. Progress in Brain Research, 165:425-445, 2007.
262. T. McGeer: Passive dynamic walking. Int. J. Robot. Res. 9 (1990) 62-82.
263. Thelen, E. & Smith, L. (1994), A Dynamic systems approach to the development of cognition and action, MIT Press.
264. Thelen, E. & Smith, L. (1994), A Dynamic systems approach to the development of cognition and action, MIT Press.

265. Varela, F. J., Thompson E., Rosch, E.: *The Embodied Mind*. The MIT Press, Cambridge, Massachusetts, London, England (1991)
266. Vernon, D.; Metta, G. & Sandini, G. (2007a), 'A survey of artificial cognitive systems: Implications for the autonomous development of mental capabilities in computational agents', *IEEE Transaction on Evolutionary Computation* 11, 151-180.
267. Vernon, D.; Metta, G. & Sandini, G. (2007b), *The iCub Cognitive Architecture: Interactive Development in a Humanoid Robot*, in 'Proc. IEEE International Conference on Development and Learning'.
268. W.G. Walter, (1967), "The Living Brain", Penguin, London
269. Webb, B. (1994) *Robotic experiments in cricket phonotaxis*, Proceedings of the third international conference on Simulation of adaptive behavior : from animals to animats 3: from animals to animats 3, pp. 45-54, Cambridge, MA: MIT Press
270. Yamashita, Y. & Tani, J. (2008), 'Emergence of Functional Hierarchy in a Multiple Timescale Neural Network Model: A Humanoid Robot Experiment', *PLoS Comput Biol.* 4 (11).

SURVEY OF BIO-INSPIRED SOFT MATERIALS

271. Atkinson, K.R., Skourtis, C. and Hutton, S.R., "Properties and Applications of Dry-Spun Carbon Nanotube Yarns", *Advances in Science and Technology*, Vol. 60, Trans Tech Publications Ltd, Switzerland, pp. 11-20, 2008.
272. Bar-Cohen, Y., "EAP actuators for biomimetic technologies with humanlike robots as one of the ultimate challenges", *Advances in Science and Technology*, Vol. 61, pp. 1-7, 2008.
273. Bar-Cohen, Y., Edited, *Electroactive Polymer (EAP) Actuators as Artificial Muscles – Reality, Potential and Challenges*, 2nd Edition, SPIE-The International Society for Optical Engineering, 2004.
274. Carpi, F. and De Rossi, D., "Dielectric Elastomer Cylindrical Actuators: Electromechanical Modelling and Experimental Evaluation", *Materials Science and Engineering*, Vol. C24 (4), pp. 555-562., 2004
275. Carpi, F. and De Rossi, D., "Electroactive Polymer-Based Devices for e-textiles in Biomedicine", *IEEE Trans Info Tech in Biomed*, 9(3), pp 295-318, 2005
276. Dias, T., Hurley, W., Monaragala, R. and Wijeyesiriwardana, R., "Development of electrically Active Textiles". *Advances in Science and Technology*, Vol. 60, Trans Tech Publications Ltd, Switzerland, pp. 74-84, 2008.
277. Duboid, P., Rosset, S., Nikiaus, M., Dadras, M. and Shea, H., "Metal ion Implanted Compliant Electrodes in Dielectric Electroactive Polymer (EAP) Membranes", edited by Y. Bar-Cohen, 2nd Edition, SPIE-The International Society for Optical Engineering, pp. 18-25, 2004.
278. Fratzl, P. and Weinkamer, R., "Nature's hierarchical materials", *Progress in material science*, 52, pp 1263-1334, 2007.
279. Full, R.J. and Meijir, K., "Metrics of Natural Muscle Function", *Electroactive Polymer (EAP) Actuators as Artificial Muscles – Reality, Potential and Challenges*, edited by

- Y. Bar-Cohen, 2nd Edition, SPIE-The International Society for Optical Engineering, pp. 73-89, 2004.
280. Furukawa, H. and Gong, J.P., "Tough Hydrogel – Learn from Nature", *Advances in Science and Technology*, Vol. 61, ed. by P. Vincenzini, Y. Bar-Cohen and F. Carpi, pp. 40-45, 2008.
281. Gong, J.P., Katsuyama, Y., Jurokawa, T. and Osada, Y., "Double-network hydrogels with extremely high mechanical strength", *Advanced materials*, Vol. 15(14), p.1155, 2003.
282. Hertleer, C., Van Langgenhove, L. and Puers, R., "Intelligent Textiles for Children", Published in *Intelligent textiles and clothing*, Woodhead Publishing, 2006.
283. <http://www.cilia-bionics.org>.
284. Kaneto, K., Suematsu, H. and Yamato, K., "Conducting Polymer Soft Actuators based on Polypyrrole – Training Effect and Fatigue", *Advances in Science and Technology*, Vol. 61, ed. by P. Vincenzini, Y. Bar-Cohen and F. Carpi, pp. 122-130, 2008.
285. Kang, H.W., Tabata, Y. and Ikada, Y., "Fabrication of porous gelatine scaffolds for tissue engineering", *Biomaterials*, Vol.20, 1339-1344, 1999.
286. Kier, W.K. and Smith, K.K., "Tongues, tentacles and trunks: the biomechanics of movement in muscular-hydrostats", *Zoological Journal of the Linnean Society*, Vol.83pp. 307-327, 1985,.
287. Kier, W. M. and Stella, M. P., "The Arrangement and Function of Octopus Arm Musculature and Connective Tissue", *J. Morphol.* Vol.268, pp. 831–843, 2007.
288. Kier, W.M. and Leeuwen, J.L.V., "A Kinematic Analysis of Tentacle Extension in the Squid *Loligo Pealei*", *The Journal of experimental biology*, Vol.200, pp. 41-53, 1997.
289. Kremer, M., Lang, E. and Berger, A.C., "Evaluation of dermal-epidermal skin equivalents ('composite-skin') of human keratinocytes in a collagen-glycosaminoglycan matrix (Integra TM Artificial Skin)", *British Journal of Plastic Surgery*, Vol. 53, pp. 459-465, 2000.
290. Jimenez, L., Rocha, A.M., Aranherri, L., JCovas, .A. and Catarino, A.P., "Electrically conductive monofilaments for smart textiles", *Advances in Science and Technology*, Vol. 60, Trans Tech Publications Ltd, Switzerland, pp. 58-63, 2008.
291. Lee, S. B., Jeon, H. W., Leea, Y. W., Lee, Y. M., Song, K. W., Park, M. H., Nam, Y. S. and Ahn, H.C., "Bio-artificial skin composed of gelatin and (1-3), (1-6)- β -glucan" *Biomaterials*, Vol.24, pp. 2503–2511, 2003.
292. Linz, T., Vieroth, R., Dils, C., Koch, M., Braun, T., Becker, K.F., Kallmayer, C. and Hong, S.M., "Embroidered Interconnections and Encapsulation for Electronics in Textiles for Wearable Electronics Applications." *Advances in Science and Technology*, Vol. 60, Trans Tech Publications Ltd, Switzerland, pp. 85-94, 2008.
293. Liu, W., Menciassi, A., Scapellato, S., Dario, P. and Chen, Y., "A Biomimetic sensor for a crawling minirobot", *Robotics and Autonomous systems*, 54, pp. 513-528, 2006.
294. Lymberis A. and Olsson, S., "Intelligent biomedical clothing for personal health and disease management : Stat of the art and future vision", *Telemed. J. e-Health*, Vol. 9, pp.379-386, 2003.

-
295. H. Mattila, P. Talvenmaa and M. Maekinen, "WearCare – Usability of intelligent materials in workwear", Published in Intelligent textiles and Clothing, Woodhead Publishing, 2006.
 296. Meinander, H., "Haptic Sensing in Intelligent Textile Development", Advances in Science and Technology, Vol. 60, Trans Tech Publications Ltd, Switzerland, 2008, pp.123-127.
 297. Mertsching, H., Walles, T., Hofmann, M., Schanz, J. and Knapp, W. H., "Engineering of a vascularized scaffold for artificial tissue and organ generation", Biomaterials, Vol.26, pp.6610–6617, 2005.
 298. Mirfakhrai, T., Oh, J., Kozlov, M., Fang, S., Zhang, M., Baughman R.H. and Madden, J.D., "Carbon Nanotube Yarns as High Load Actuators and Sensors", Advances in Science and Technology, Vol. 61, ed. by P. Vincenzini, Y. Bar-Cohen and F. Carpi, pp. 65-74, 2008.
 299. Narbonneau, F., Kinet, D., Paquet, B., Dapre, A., de jonckheere, J., Logier, R., Zinke, J., Witt, J. and Krebber, K., "Smart textile Embedding Optical Fibre Sensors for Healthcare." Advances in Science and Technology, Vol. 60, Trans Tech Publications Ltd, Switzerland, pp. 134-143, 2008.
 300. Neville, A.C., Biology of Fibrous Composites - Development beyond the Cell Membrane, Cambridge University Press, 1993.
 301. Nadol, J.B. Gibbins, J.R. and Porter, K.R., "Collagen texture in basal lamella of fish skin", Devel. Biol. 20, pp. 304-331, 1969.
 302. Olsson, R., "Skin of amphioxus", Z. ellforsch, 54, pp.90-104, 1964.
 303. R. Paradiso and D. De. Rossi, "Advances in textile technologies for unobtrusive monitoring of vital parameters and movements", Proceedings of the 28th IEEE EMBS ~Annual International Conference, New York City, USA August 2006.
 304. Proetex project, <http://www.proetex.org/>, April 17th, 2008.
 305. Scheibert, J., Leurent, S., Prevost, A. and Debregeas, G., "The Role fo Fingerprints in the Coding of Tactile Information Probed with a Biomimetic Sensor", Science, Vol. 323, pp. 1503-1506, 2009.
 306. Schwarz, A., Hakuzimana, J., Gasana, E., Westbroek, P. and Langehove, L.V., "Gold coated polyester yarn", Advances in Science and Technology, Vol. 60, Trans Tech Publications Ltd, Switzerland, 2008, pp. 47-51, 2008.
 307. Sommer-Larsen, P., Hansen, K. and Benslimane, M., "Multilayer actuator and sensor sheets with smart compliant electrodes", Advances in Science and Technology, Vol. 61, ed. by P. Vincenzini, Y. Bar-Cohen and F. Carpi, pp. 169-179, 2008.
 308. Stylios, G.K. and Wan, T., "Investigating SMART Membranes and Coatings by in situ Synthesis of Iron Oxide Nanoparticles in PVA Hydrogels", Advances in Science and Technology, Vol. 60, Trans Tech Publications Ltd, Switzerland, 2008, pp. 32-37, 2008.
 309. Supp, D.M. and Boyce, S.T., "Engineered skin substitutes: practices and potentials" Clinics in Dermatology, Vol.23. pp 403 – 412, 2005.
 310. Vogel, S., Comparative Biomechanics- Life's physical world, Princeton University Press, 2003.

-
311. Wainwright, S.A., Biggs, W.D., Currey, J.D. and Gosline, J.M., "Mechanical Design in Organisms", Published by Edward Arnold, 1976.
312. Wang, J.Z., Hang, G., Wang, Y., Li, J. and Du, W., "Embedded SMA wire Actuated biomimetic Fin: a Module for biomimetic Underwater Propulsion". *Smart Mater. Struct.* 17, 025039, 2008.
313. Wang, Y., Kima, H.J., Vunjak-Novakovic, G., and Kaplana, D. L., "Review Stem cell-based tissue engineering with silk biomaterials" *Biomaterials*, 27, pp 6064–6082, 2006.
314. Wijeyesiriwardana, R., Dias, T., and Mukhopadhyay, S., "Resistive fibre-meshed transducers", 7th International symposium on wearable computer proceedings, pp. 200-209, 2003.
315. Yoon, S., Prabhu, A.A., Ramasundaram, S. and Kim, K.J., "PVDF Nanoweb touch sensors prepared using electro-spinning process for smart apparels applications", *Advances in Science and Technology*, Vol. 60, Trans Tech Publications Ltd, Switzerland, pp. 52-57, 2008
316. Young, C.D., Wu, J.R. and Tsou, T.L., "High-strength ultra-thin and fibre-reinforced pHEMA artificial skin", *Biomaterials*, Vol.19, pp. 1745-1752, 1998.
317. Zhang, M., Artkinson, K.R., and Baughman, R.H., "[Multifunctional carbon nanotube yarns by downsizing an ancient technology](#)," *Science*, Vo